A SPECTROSCOPIC AND PHOTOMETRIC INVESTIGATION OF THE EXTREME HELIUM-RICH STAR HD 168476

Helen Joan Walker

A Thesis Submitted for the Degree of PhD
at the
University of St Andrews

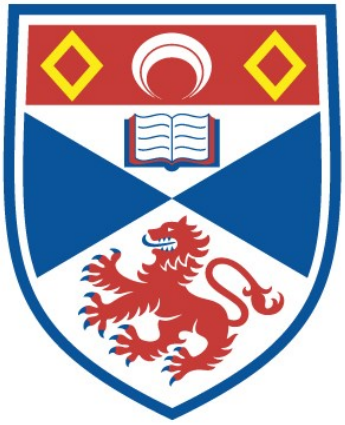

1979

A SPECTROSCOPIC AND PHOTOMETRIC INVESTIGATION OF THE EXTREME HELIUM-RICH STAR HD 168476

by

Helen Joan Walker

A dissertation submitted for the degree of Doctor of Philosophy at the University of St. Andrews

St. Andrews May 1979

ProQuest LLC.
789 East Eisenhower Parkway
P.O. Box 1346
Ann Arbor, MI 48106 – 1346

CERTIFICATE

I certify that Helen Joan Walker has spent nine terms in research work at the University Observatory, St. Andrews, that she has fulfilled the conditions of Ordinance General No. 12 and Senate Regulations under Resolution of the University Court, 1967, No. 1, and that she is qualified to submit the accompanying dissertation in application for the degree of Ph.D..

DECLARATION

Except where reference is made to the work of others, the research described in this thesis and the composition of the thesis are my own work. No part of this work has been submitted for another degree at this or any other University. Under Ordinance General No. 12, I was admitted to the Faculty of Science of the University of St. Andrews as a research student on 1st. October 1975, to carry out an investigation of the atmosphere of the helium-rich star HD 168476. I was accepted as a candidate for the degree of Ph.D. on 1st. October 1976, under Resolution of the University Court, 1967, No. 1.

ABSTRACT

Spectra were obtained from several sources for a fine abundance analysis of the extreme helium-rich star HD 168476. The atmospheric parameters are found using theoretical models and abundances determined for the ions identified in the spectra. The star is found to have an effective temperature of 14000°K, log(surface gravity) of 1.5 and a microturbulent velocity of 10 km/s. Over 1400 lines are identified on the spectra ranging in wavelength from 3100A to 4925A and 5490A to 6585A, and about 530 lines are suitable for the abundance analysis. It is confirmed that helium, carbon, nitrogen and neon are overabundant, with hydrogen and oxygen underabundant.

An ultraviolet spectrum of the star is also obtained and lines identified. In addition to the ions found in the visible region of the spectrum, neutral ions are also present, indicating the possibility of a cool outer shell to the star. Photometric and spectroscopic observations are made to study the light and radial velocity of the star, to determine if it is variable. Statistical tests showed that the star is variable in its V magnitude, and most probably in its colours, as well as being variable in its radial velocity. No period is found and it is suspected that the variability may be complex. Several theories for the causes of the variability are discussed and a possible origin for the extreme helium-rich nature of the star mentioned.

Acknowledgements

I am indebted to my supervisor, Dr. P. W. Hill, for his guidance, help and discussions at all stages of my work. I am extremely grateful to Prof. K. Hunger for his assistance and to Prof. D. W. N. Stibbs for all his help, especially with the statistical analysis of the observations. I am most grateful to Dr. D. Schönberner for his help with the stellar models needed for this project. I am also grateful to Dr. D. Kilkenny and Dr. A. E. Lynas-Gray for all the help and advice they have given me, and for the comments made on the draft of this thesis. My thanks also go to Dr. J. P. Kaufmann and Dr. R. W. Hilditch for their assistance, to the staff and research students of the University Observatory of St. Andrews, the computing laboratory staff, St. Andrews, the staff of S.A.A.O. (especially Mr. R. Catchpole, Dr. W. Martin), R.G.O., A.A.O. (especially Dr. Louise Webster), the staff of the Institut für Astrophysik, Technische Universität, West Berlin and Institut für Theoretische Physik, Neue Universität Kiel, and the staff of E.S.A. Villafranca satellite tracking station (especially Dr. D. J. Stickland and Dr. J. Clavel).

I would like to acknowledge the Panel for the Allocation of Telescope Time and the Science Research Council for the financial support, travelling expenses and subsistence, and the allocations of telescope time for observations.

This thesis was partly based on observations by the International Ultraviolet Explorer collected at the Villafranca satellite tracking station of E.S.A..

CONTENTS

Tables

Tables (cont.)

Tables (cont.)

Figures

Figures (cont.)

1 INTRODUCTION

1.1 History

1.1a Early work up to 1960

Plaskett (1927) found that the spectrum of ν Sagittarii, a close binary star, was best described as a strong helium absorption line spectrum superimposed on a metallic absorption line spectrum. Popper (1942) discovered the first extreme helium-rich star HD 124448 which he investigated further in 1946-7. He found that the lines originally attributed to hydrogen were due to neutral helium and that there were no lines of hydrogen visible in the spectrum. As well as strong lines of helium he found strong lines due to carbon and nitrogen, with weak oxygen lines. This discovery instituted a search by Thackeray & Wesselink (1952) for stars with similar properties. The criteria used were that the stars should be of spectral type B, fainter than a magnitude of 7.5 and with a galactic latitude $b > 10^{\circ}$. They reported that the first of the eight suitable stars chosen, HD 168476, had been found to have strong lines due to helium and no lines due to hydrogen in its spectrum. It was very similar to HD 124448, although slightly cooler, and both stars had high radial velocities. Although the search was extended to a further fifteen stars no more helium-rich stars were found. In the same year as the discovery of HD 168476, Bidelman (1952) found that HD 160641 had helium lines dominating its spectrum and no lines due to hydrogen present. Thackeray (1954) gave a list of 206 spectral lines for HD 168476 in the region 3700A to 6700A. No hydrogen or oxygen lines were found, but strong lines due to He I, C II, and Ne I were present.

The first subdwarf to be found overabundant in helium (Gould et

al., 1957) was BD+75°325, which had lines of ionised helium dominating the spectrum. A member of a multiple system, θ Ori. E, quite a distance away from the centre of the group, was discovered by Greenstein & Wallerstein (1958) to have very strong neutral helium lines, together with hydrogen lines, and this star is often regarded as a prototype of the intermediate helium-rich stars. One of the brightest intermediate helium-rich stars HD 96446 was discovered a year later by Jaschek & Jaschek (1959).

1.1b Coarse analyses 1954 - 1970

Aller (1954) used the technique of Unsöld to do a coarse analysis of HD 160641 and found abundances for helium, carbon, nitrogen, oxygen, neon, magnesium and silicon. He found that helium, carbon, nitrogen and neon were overabundant with respect to oxygen. Klemola (1961) analysed BD+10°2179 and gave the wavelengths of 116 lines between 3258A and 4713A. He found the Balmer series were weak, with oxygen and neon lines absent. Klemola gave abundances for hydrogen, helium, carbon, nitrogen, magnesium, aluminium, calcium and silicon, with a maximum possible abundance for oxygen. Hydrogen was underabundant by a factor of 10^2 to 10^3 and the carbon and nitrogen abundances were normal. HD 124448 and HD 168476 were analysed in detail by Hill (1965). He determined abundances for 16 elements in HD 124448 and 17 elements in HD 168476, and gave a maximum abundance for hydrogen and oxygen in both stars, determined by the lack of their lines visible in the spectrum. Hill found the stars were overabundant in helium, carbon, nitrogen and possibly neon. He also suspected that the iron peak elements in HD 168476 might be overabundant or formed in a cool outer shell. Hill (1970) gave an abundance for oxygen, determined in HD 168476

from the O I triplet at 7771 - 5 A. This confirmed that oxygen was underabundant in HD 168476.

1.1c Fine analyses 1967 - 1978

Hünger & Van Blerkom (1967) computed a model atmosphere for a pure helium star, to be used for BD+10°2179. (For further details of the technique see section 6.1.) The technique of fine analysis was first applied to BD+10°2179 by Hünger & Klinglesmith (1969). The same type of analysis was applied to several other stars, namely the intermediate helium-rich star, ϵ Ori. E (HD 37479), analysed by Klinglesmith et al. (1970), HD 144941 by Hünger & Kaufmann (1973) and others (see notes to table 1.1). Schönberner & Wolf (1974) performed a fine analysis upon HD 124448. They also did a differential analysis of HD 168476 relative to HD 124448 using Hill's (1964) equivalent widths. BD-9°4395 has also been analysed by Kaufmann & Schönberner (1977) using the technique of fine analysis.

1.1d Variability

Thackeray (1954) suspected that HD 168476 might have lines that varied slightly in intensity with a period of less than a day. He felt that although there was a large scatter in the measurements, the radial velocity was constant. Hill (1964) suspected that the radial velocity of HD 168476 might be variable. Hill (1969a) reported that the magnitude of HD 168476 and HD 160641 was variable, whilst that of HD 124448 was constant, and there were no variations in colour. Landolt (1973) made photoelectric UBV observations of several intermediate and extreme helium-rich stars. He found that HD 264111, BD+37°442 and HD 168476 were not variable (although he

noted there were only six observations made of HD 168476). Landolt found that BD+10°2179, HD 124448, BD+13°3224 and HD 160641 were variable in the V magnitude. He suspected that there might be a secular brightening in HD 168476 from a comparison of his observations with those of Hill (1969a). Landolt (1975) gave a period of 0.1 day for BD+13°3224 with an amplitude in V of 0.1 mag.. He found that the colours of BD+13°3224 also varied. Landolt (1975) also suspected that HD 160641 might have a period of about 0.6 day.

It was suspected by Gough (Trimble, 1972) that hot helium-rich stars would be in an instability strip. The calculations were made mainly for R CrB stars, and thus at lower temperatures than required for the extreme helium-rich stars. It appeared that there would be an instability region starting at around T_e = 7850°K for Z = 0.03. Lower metal abundances would bring the start of the region to higher temperatures. Wood (1976) found (in agreement with Gough) that the fundamental mode of radial pulsations was unstable below 7580°K. He also found that a region of overtone instability occurred between 8500°K and 13000°K depending upon L/M. There was also a tendency for overtone instability to occur around 16000°K. HD 124448, BD+10°2179, HD 160641 and BD+13°3224 are all very close to or hotter than 16000°K and HD 168476 has a temperature very close to the lower boundary at 13000°K.

1.1e Ultraviolet observations 1978

Snow & Linsky (1979) noted that ultraviolet spectroscopy would be valuable for determining the outer layers of a stellar atmosphere. Schönberner & Hunger (1978) discussed observations of BD-9°4395 and BD+10°2179 made with the International

Ultraviolet Explorer satellite. They found no emission lines in the spectra and there was no evidence of mass loss. Profiles were fitted to silicon and carbon lines and a model with the number fraction of carbon (n_C) as 0.01 was used for both stars.

1.2 General properties and outstanding problems

1.2a General properties

The extreme helium-rich stars, or extreme helium stars, usually have spectral type B or O and normally have no lines or very faint lines of hydrogen visible in their spectra. For convenience a limit is put upon the ratio of hydrogen to helium, expressed by number as $n_H/n_{He} < 0.1$ (Hunger, 1975). The intermediate helium-rich stars (spectral type B) have more hydrogen than this, usually approximately equal numbers of hydrogen and helium atoms, although some may have only a marginal overabundance of helium. There are also helium-rich subdwarfs (spectral type O) which again usually contain equal numbers of hydrogen and helium atoms. Often included with these three groups of helium-rich stars is another group, the helium-rich close binaries which, if hot, have strong helium lines in their spectra due to the overabundance of this element (Hack, 1967). In this case the overabundance of helium is presumed to be the result of mass exchange in the system.

Table 1.1 shows the known extreme and intermediate helium-rich stars, and the helium-rich subdwarfs and close binaries, arranged in order of right ascension. The galactic latitude, apparent visual magnitude, absolute magnitude and helium abundance with any known abundance analysis are shown. Johnson colours for the stars, galactic longitude, proper motions and some other details are

available from Hunger (1975), or for the close binaries, from Hack (1967).

Two stars were originally thought to be intermediate helium-rich stars but abundance analyses showed their true nature. HD 135485, it was discovered, had been analysed relative to a star deficient in helium, and is now known to have a normal helium abundance (Schönberner, 1973; Baschek, 1973), but Hunger (1975) suggested that due to the overabundance in metals it may be the first object of a new class. HD 120640 has recently been found to be a normal B star by Detz (1977). BD+13°3224 is suspected of being an extreme helium-rich star, not a subdwarf, since it may have a low gravity (see chapter 7), and it has a continuum similar to HD 160641 (Rosendhal & Schmidt, 1973). BD+37°1977 has been suspected of being a subdwarf by Wolff et al. (1974). MV Sgr. and V348 Sgr. are also classed as R CrB stars (e.g. Warner, 1967).

Drilling (1973, 1978) reported that SS 3378 and LSII+33°5 were extreme helium-rich stars. LSII is the 'Luminous Stars in the Northern Milky Way II' catalogue (Stock, Nassau & Stephenson, 1960), and SS is the 'Luminous Stars in the Southern Milky Way' catalogue (Stephenson & Sanduleak, 1971). In addition Drilling (1979) reported that BD+1°4381 and LSIV-14°109 were extreme helium-rich stars of spectral type A. LSIV is the 'Luminous Stars in the Northern Milky Way IV' catalogue (Nassau & Stephenson, 1963).

Table 1.1 List of helium-rich stars

Star	R.A.(1950) h m	Dec ° '	b °	rv km/s	m	M	n(He)	Anal
Extreme helium-rich stars								
BD+37°442	01 56	+38 19	-22	-156	10.0	-2		
BD+37°1977	09 21	+36 56	+44	-59	9.0	0		
BD+10°2179	10 36	+10 19	+56	+155	10.0	1.6	0.97	1,2
HD 124448	14 12	-46 03	+14	-68	10.0	-3	0.99	2,3
SS 3378	15 35	-48 26	+06	-1	10.5	-1.5 or -4		
BD-9°4395	16 27	-09 13	+26		10.6		0.99	4
HD 160641	17 39	-17 53	+08	+100	9.8	-3	0.99	2
BD-1°3438	18 01	-01 01	+10		10.4		0.99*	
HD 168476	18 19	-56 39	-19	-171	9.3	-1 to -2	0.99	2,3
V348 Sgr.	18 37	-22 59	+11	+174	11.8→>16.5			
MV Sgr.	18 42	-21 00	-10	-68	12.7→15.0	-1.6 to +2		
LSIV-14°109	18 57	-14 30	-08		11.2			
LSII+33°5	19 43	+33 51	+05		10.4			
BD+1°4381	20 49	+02 08	-25		9.6			
Intermediate helium-rich stars								
HD 37479	05 36	-02 37	-17	+27	6.7	-2.2	0.4	5
HD 37776	05 38	-01 32	-16	+29	7.0			
HDE 260858	06 35	+12 49	+02		9.0			
HD 264111	06 45	+04 43	+01	high	9.6		0.5*	
HD 60344	07 31	-23 50	-02	+30	7.8	-1.4	0.4	6
HD 64740	07 52	-49 29	-11		4.6		0.4*	
CPD-46°3093	08 48	-46 40	-02		10.0		0.3*	
HD 93030	10 41	-64 08	-05	+24	2.8			
HD 96446	11 04	-59 41	00	-12	6.7	-1.9	0.5	7
HD 133518	15 03	-51 50	+05	-5	6.4		0.55	8
HD 144941	16 06	-27 08	+18	-52	10.1	-1.8	0.94	9,10
CPD-69°2698	17 07	-70 02	-18	-65	9.3	-1.8	0.3	10
HD 168785	18 20	-30 10	-07	+5	8.5	-1.7	0.45	9
HD 184927	19 34	+31 10	+05		7.7	-3.2	0.5	11
HD 186205	19 40	+09 05	00		8.7		0.4	12
BD+39°4926	22 44	+39 51	-17	-17,-47	9.2	-3	0.6	13

Table 1.1 (cont.)

Star	R.A.(1950)	Dec	b	rv	m	M	n(He)	Anal
Helium-rich subdwarfs								
HD 49798	06 47	-44 16	-19	+14	8.3	-0.2 or 1.0	0.4	14
CPD-31°1701	07 35	-32 06	-05		10.5	+3	1.0*	
BD+75°325	08 05	+75 07	+31	-19	8.9	+5		
BD+48°1777	09 27	+48 29	+45	-29	10.7			
HD 113001B	12 58	+36 02	+81	-8	9.6	3.6	0.5	14,15
HZ 44	13 21	+36 52	+79		11.7	3.7	0.4	14
HD 127493	14 30	-22 25	+35	+13	9.5	3.6	0.5	14,15
HD 128220B	14 33	+19 26	+65	-8	8.5	0.0	0.4	14,15
BD+13°3224	16 46	+13 21	+34	+22	10.5			
BD+28°4211	21 49	+28 37	-19	+26	9.5			
BD+25°4655	21 57	+26 12	-22		9.8	+5 to +6	0.92	14
GS 259-8	22 46	+37 36	-19	-11	12.5	+3 or +4		
Helium-rich close binaries								
HD 30353	04 42	+43 06	00		7.8	-1.6	0.99	16
HD 37017	05 33	-04 32	-22		6.6		0.84	17
β Lyr.	18 48	+33 18	+13		3.4 to 4.3	-3.5	0.69	18
ν Sgr.	19 19	-16 03	-16		4.3 to 4.4	-5.5	0.94	19

Notes * in n(He) column denotes helium abundance taken from :-
BD-1°3438 : Schönberner (1978)
HD 264111 : Stephenson (1967)
HD 64740 : Kaufmann & Schacht (see Hunger, 1975)
CPD-46°3093: Osmer & Peterson (1974)
CPD-31°1701: Garrison & Hiltner (1973)

1. Hunger & Klinglesmith (1969)
2. Hill (1965)
3. Schönberner & Wolf (1974)
4. Kaufmann & Schönberner (1977)
5. Klinglesmith, Hunger, Bless & Millis (1970)
6. Kaufmann & Hunger (1975)
7. Wolf (1973)
8. Osmer & Peterson (1974)
9. Kaufmann & Schönberner (1974)
10. Hunger & Kaufmann (1973)
11. Higginbotham & Lee (1974)
12. Lee & O'Brien (1977)
13. Kodaira, Greenstein & Oke (1970)
14. Richter (1971)
15. Tomley (1970)
16. Nariai (1973)
17. Lester (1972)
18. Hack & Job (1965)
19. Hack (1967)

General - Hunger (1975)

As can be seen from table 1.1 the subdwarfs are found at high galactic latitudes, whereas the intermediate helium-rich stars are found in the galactic plane. About three-quarters of the extreme helium-rich stars are found at high galactic latitudes. In general, the extreme helium-rich stars have high radial velocities (apart from SS 3378), but Hunger (1975) shows that these stars follow the galactic rotation independent of galactic latitude, and so the stars are not necessarily population II objects as their high radial velocities suggest. The distribution of the stars in all groups appears to be independent of galactic longitude.

Mainly from the work of Pederen & Thomsen (1977) it appears that many intermediate helium-rich stars are variable with periods of days, from HD 37479 (σ Ori. E) at 1.19 days to BD+39°4926 at 775 days (Kodaira et al., 1970). Osmer & Peterson (1974) and Pedersen (1978) suggest that the intermediate helium-rich stars are related to the helium-weak stars and the Ap stars. Pedersen (1978) noted that magnetic fields had been found in some of the intermediate helium-rich stars. Osmer & Peterson (1974) suggest that these stars have enrichment of helium by diffusion.

1.2b Evolution

Due to the uncertainty in distances and hence absolute magnitudes the evolution of the helium-rich stars is usually desribed in terms of the log T_e - log g diagram (see figure 1.1), which is equivalent to a Hertzsprung-Russell diagram. Figure 1.1 is taken from Schönberner & Hunger (1978), with the positions of the intermediate helium-rich stars and helium-rich subdwarfs taken from Hunger (1975). Further details of the tracks are shown in figure 7.3 and Schönberner & Hunger (1978). The subdwarf below the main sequence

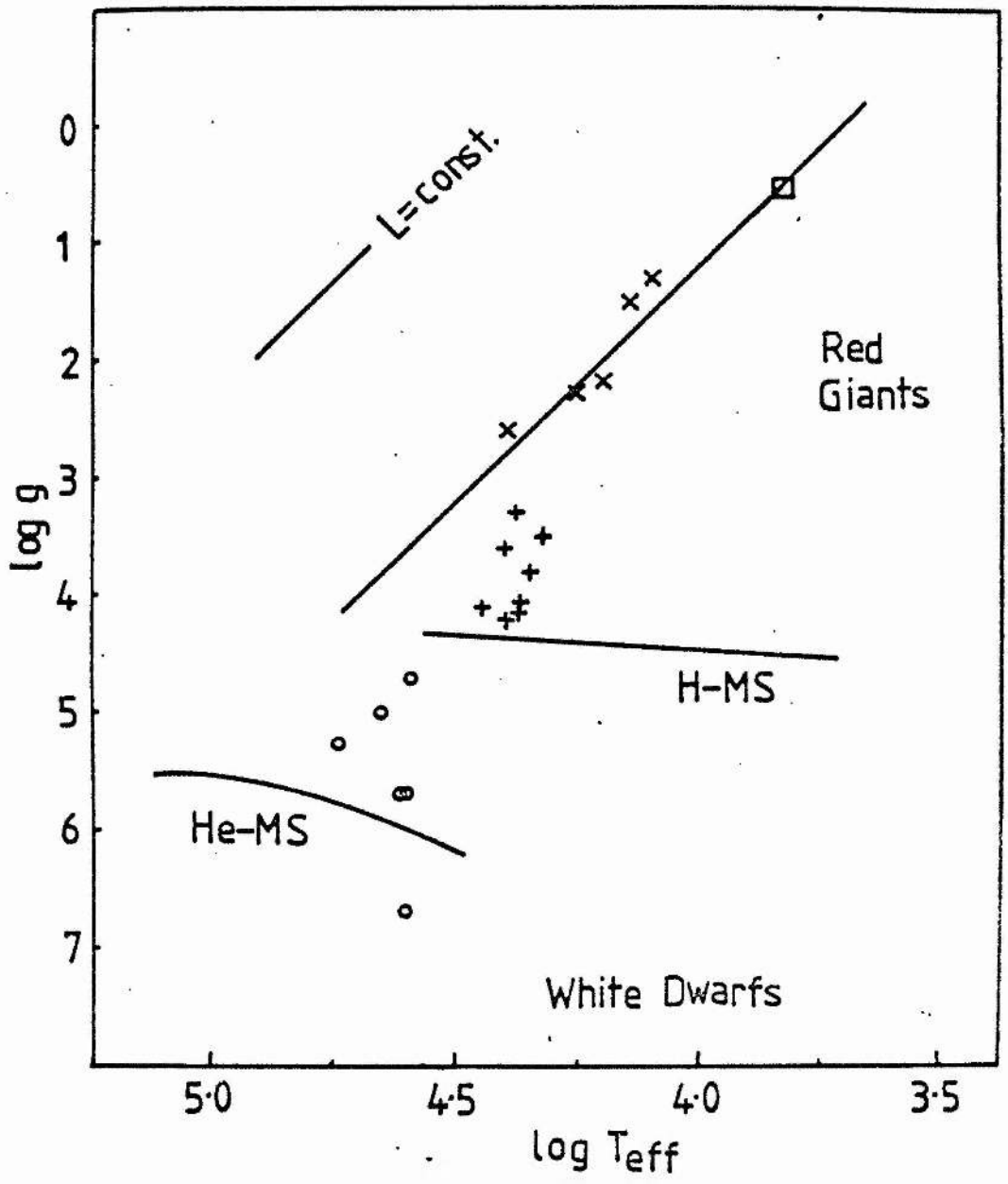

Figure 1·1 Log T_{eff} - log g diagram for helium-rich stars

□ R CrB stars

x extreme helium-rich stars

\+ intermediate helium-rich stars

o helium-rich subdwarfs

is BD+25°4655 which is extremely rich in helium (see table 1.1) with strong lines due to carbon, nitrogen and neon, whilst oxygen is slightly underabundant (Peterson, 1970).

Warner (1967) included the extreme helium-rich stars in his list of hydrogen deficient carbon (HdC) stars as non-variable members and put the R Corona Borealis (R CrB) stars including MV Sgr. and V348 Sgr. in the list of variable members. He suggested that the HdC stars and the extreme helium-rich stars were similarly distributed throughout the galaxy. Schönberner (1975) re-analysed three R CrB stars (R CrB, RY Sgr, XX Cam) and confirmed that hydrogen was very underabundant but that helium and carbon were overabundant. An oxygen abundance determined for RY Sgr. was similar to that estimated for the extreme helium-rich stars.

Schönberner (1977) suggested that remnants of red giants which have lost their hydrogen envelopes become R CrB stars and then contract towards higher temperatures, becoming extreme helium-rich stars and then helium-rich (DB) white dwarfs. Dinger (1972) and Schönberner (1977) suggest that the extreme helium-rich stars evolve through that phase in a few thousand years, which would explain why so few of them are seen. The DB white dwarfs (Weidemann, 1975) are classified as such by the lack or weakness of hydrogen lines in their spectra. He II is present which indicates a very high temperature. Bues (1970) examined models of white dwarfs with $11000^{\circ}K < T_e < 21000^{\circ}K$ and $7 < \log g < 8$. She found im addition to the depletion of hydrogen ($n_H/n_{He} < 10^{-4}$ to 10^{-5}) a metal deficiency of 10 to 100 in the DB white dwarfs, so that she felt they could not be related to the extreme helium-rich stars which have a much higher metal abundance. Schönberner (1977) suggested that the birth-rate of DB white dwarfs is not very different to the predicted death-rate

of extrem helium-rich stars, so that a large number of all low mass stars ($M \gtrsim 1.2 - 1.4\ M_\odot$) would pass through the extreme helium-rich star phase.

1.2c Problems

As Schönberner (1977) remarked "the mechanism of the creation of stars with helium envelopes is unknown yet". This has been a problem since the first discovery by Popper. Popper (1947) concluded that HD 124448 must either have been formed in the absence of hydrogen, or it must have evolved to that state. The known galactic distribution of the objects negates the former possibility, leaving only the latter. The stars must have evolved to that point either by converting all the hydrogen to helium by complete mixing or by removing the hydrogen-rich envelope, or by a combination of both. Schönberner & Hunger (1978) suggested that an extreme helium-rich star was the remainder of a binary system in which one component blew up as a supernova.

There are several problems in assuming that there is a simple transition between R CrB stars and extreme helium-rich stars based on effective temperature and surface gravity (e.g. figure 1.1). MV Sgr. is a hot R CrB star with a temperature similar to BD+10°2179 (Kaufmann & Schönberner, 1977) and they also noted that BD-9°4395 has the He I line at 3888A filled with emission, as in hot R CrB stars. The A stars discovered by Drilling (1979) to be extreme helium-rich stars may be very close to the R CrB star region of the log T_e - log g diagram, and LSIV-14°109, he noted, has very strong carbon lines.

As mentioned in section 1.1d Wood (1976) has investigated theoretical radial pulsations in extreme helium-rich stars. Most

of the known extreme helium-rich stars are hotter than 16000°K where the overtone instability occurs so that only stars cooler than that (but hotter than 13000°K) will have the overtone and fundamental modes stable. HD 168476 is very close to the lower temperature boundary. For only one extreme helium-rich star, BD+13°3224, has a period been found (Landolt, 1975). If the stars have evolved from R CrB stars there may be evidence of residual mass loss either as P Cygni profiles in the spectrum or as a shell around the star at some distance. Ultraviolet spectroscopy may be useful for this problem. The space density calculated for extreme helium-rich stars was estimated before the discovery of the stars by Drilling (1973, 1978, 1979) and the theoretical work by Schönberner (1977). It would be valuable to re-determine the space density and birth rate in the light of this work, and a new estimate is made in chapter 7.

I.3 Spectroscopic and photometric observations of HD 168476

Perek (1957, 1958) investigated the space motion of HD 168476 assuming a distance to the star of either 1kpc or 2kpc and found that the star was in a hyperbolic galactic orbit rather than a closed orbit. The errors in the proper motion and possibly the distance are large, so that this should be recalculated with more accurate data if possible. If the orbit is not closed, this may be evidence of a severe perturbation at some time in the star's history, lending credence to the supernova hypothesis.

Feast & Glass (1973) measured the infra-red colours of HD 168476 and noted that, in common with HD 124448, it did not show an infra-red excess, unlike the R CrB stars, including MV Sgr. and V348 Sgr.. This suggests that any shell around the star will be

cooler than 700°K. Ultraviolet spectroscopy will be very important in revealing the structure of the outer layers of the star, especially since there are many resonance lines in the ultraviolet. Also, evidence of mass loss from the outer layers might be seen in this region of the spectrum. Although, as noted in section 1.1e, there is no evidence of mass loss from either BD-9°4395 and BD+10°2179. HD 168476 is much closer to the R CrB stars and so may have some residual mass loss.

Hill (1969a) suspected HD 168476 of being variable in its V magnitude and Landolt (1973) noticed a secular brightening between his observations and those of Hill. Thackeray (1954) found the radial velocity constant, although there was a large range in the measurements noted, and Hill (1964) suspected that it might be variable. As mentioned in the previous section it is very close to the boundary for overtone stability in radial pulsation according to Wood (1976). Simultaneous photometry and spectroscopy (for radial velocities) will be valuable to determine if there is any variability in each, and if there is any correlation. This may then give valuable insight into the nature of any variation present.

To clarify the position of HD 168476 in respect to the boundary of Wood's instability region a new determination of the model using fine analysis techniques is important. There is a large difference in the surface gravity determined by Schönberner & Wolf (1974) and that found by Hill (1965). HD 168476 is the only extreme helium-rich star suitable for LTE analysis with neon lines observed in its spectrum. The star appears to occupy a position between the hot extreme helium-rich stars and the R CrB stars, so that the accurate abundance of carbon in this star is important. Detailed

atmospheric parameters and a complete fine analysis of HD 168476 should give valuable information for the study of extreme helium-rich stars, and perhaps shed light on their evolution.

2 PHOTOMETRY

2.1 Introduction

The Strömgren 'uvby' system (Strömgren, 1963) is an intermediate passband photometric system with central wavelengths and half-widths as shown in table 2.1. The 'u' filter is a glass filter and the other three are interference filters. Originally the filters were used for stars in the range A2 to G0 but the technique was extended towards the earlier spectral type stars (e.g. Strömgren, 1966). A set of parameters y, (b-y), c_1 and m_1 are used with normal stars. The Strömgren 'y' magnitude was chosen to be very similar to the Johnson system 'V' magnitude (Johnson & Morgan, 1953). The filter bandwidth is narrower than the Johnson 'V' filter and so a "force-fit" must be applied to make them identical. The 'b' filter was chosen to be in a region free from strong spectral features. The colour (b-y) is similar to (B-V) in the Johnson system, and is fairly insensitive to the number of lines in the spectrum, so it can be used as an indicator of effective temperature (Golay, 1974). The parameter 'c_1' is such that

$$c_1 = (u - v) - (v - b)$$

and is a measure of the Balmer discontinuity. The parameter 'm_1' is expressed as :-

$$m_1 = (v - b) - (b - y)$$

and is a measure of the line blanketing, i.e. the metal content in

the star. All the parameters are affected by interstellar extinction. It is possible to use the $(b-y) - m_1$ and $(b-y) - c_1$ diagrams, such as are displayed schematically in Kilkenny & Hill (1975) to classify objects that are peculiar, as well as those stars that are normal.

2.2 Observations

In the case of HD 168476 the Strömgren set of filters gives valuable information about the star, but it is not easy to interpret this due to the lack of hydrogen in the star. The c_1 index becomes a measure of the helium jumps, most affected by that at 3450A, instead of the Balmer jump, and m_1 is still an indicator of metallicity (see table 2.1).

Table 2.1 Stellar lines affecting Strömgren magnitudes

	y	b	v	u
Approx central λ	5500	4700	4100	3500
Approx half-width	200	180	200	380
lines affecting magnitude				
HD 168476	many weak metallic lines	4713 He I many weak metallic lines	4143 He I 4128/30 Si II 4120 He I 4026/09 He I	3725 He I j 3450 He I j
normal B star	many weak metallic lines	many weak metallic lines	4143 He I 4128/30 Si II 4101 H δ	3646 H j

Observations of HD 168476, other helium-rich stars and related objects, were made on the 0.5m South African Astronomical Observatory (SAAO) telescope at Sutherland South Africa. The

observations ~~made~~ in 1976 and 1977 were made as part of a programme of simultaneous photometry and spectroscopy. It was expected that a study of magnitude and radial velocity of HD 168476 would show any variations in each, and if possible any correlation between the two types of variability. Table 2.2 shows the time used for the observations and assistance given with the observing.

Table 2.2 Allocation of telescope time for photometric work

Date	1976 July	1977 June	1978 June
Allocation (nights)	7 + 2	7	7
Usable	4 whole	1 whole	4 whole
	1 ½-night		1 ⅔-night
	2 < 2hrs		1 ⅓-night
Observer	AB for 2 nights	AELG	HW
	HW		

Notes :- AB A. Brown
AELG A. E. Lynas-Gray
HW H. J. Walker

The Strömgren filters were used since they had a passband wide enough to allow sufficient light through in a reasonable length of time for accurate photometry, but were narrow enough not to have too many unusual lines (due to the nature of the star) affecting each filter.

The "Peoples'" photometer, a two channel photometer, (SAAO Facilities manual) was used on the telescope with thermoelectrically-cooled EMI photomultiplier tubes, having an S-11 response. Only

the 'straight-through' tube was used for this work. Stobie (1978) reported measurements of a halo around stars, independent of seeing, caused by scattering inside the telescope and/or dust on the surface of the mirror. A loss of about 0.01 mag. at 20" of arc and about 0.002 mag. at 30" of arc was found for two sizes of diaphragm, but the effect cancels out when programme and standard stars are observed with the same aperture. However, in the last year a 33 arc second aperture was used to observe the stars, so that more of the surrounding halo could be included. Prior to that a 22 arc second aperture was used.

The 1976 and 1977 observations were made by D.C. integration for 30 seconds, the result being recorded on a Brown recorder chart roll. A double D.C. electrometer amplifier was used (SAAO Facilities manual) which had two manually set gain controls, a coarse gain and a fine gain. The chart roll was later measured by hand and reduced using programs written by Dr. G. Hill (Dominion Astrophysical Observatory, DAO). In 1978 June a completely automatic system was used, including computer-controlled filter changes, which had been developed by Dr. L. Balona (SAAO). A Nova 3/12 computer was used with Nather board interface (SAAO Facilities manual). The system used pulse-counting via SSR amplifiers and the integration time could be varied. Standards taken from Crawford & Barnes (1970) and Crawford, Barnes & Golson (1970) were frequently observed. Between three and eighteen standard stars were observed in a night, depending on weather conditions. One or two standards were observed over a range of air mass to derive the extinction coefficients for the night.

2.3 Technique

In 1976, four-colour photometry of HD 168476 was obtained, with that of other related stars. For the programme stars a sequence of comparison, programme, check, programme, comparison (CO,P,CH,P,CO) or CO,P,CO was used to enable the search for variations in magnitude and/or colour to be carried out. The sequence was altered in 1977 to allow more observations of HD 168476 to be made in one night, to determine if there were any variations on the time-scale of a few hours. Each star was observed through the four filters y,b,v,u with a 30 second integration for each, and in poor conditions this was repeated after sky observations by the sequence u,v,b,y.

It was decided that the time resolution was too low with this method of observing each colour, so that in 1978 a new technique was employed following Kurtz (1977). This involved making observations through just one filter, which in the case of HD 168476 was the 'b' filter as the maximum number of counts were received through it and the best signal-to-noise ratio for a given integration time could be obtained. In order to remove any variation due to sky or interference in the equipment a batch of six 20 second integrations was made for each star. This proved essential since the computer was picking up spurious counts, and these could not be eliminated except by inspection of the output. The sequence of CO,P,CH,P,CO was again used, and this could be repeated, either immediately or after a measurement of the sky background had been made.

Since the operation was under computer-control several different sequences of observations could be used; a maximum of ten programs could be stored in the computer memory. The standard stars were

observed with a 20-second integration for each filter, and the computer paused while the star was moved from the aperture so that sky could be observed. Occasionally the programme stars were observed through all four filters too, in the sequence (ybvu)star, (uvby)sky, (ybvu)star, each integration for 30 seconds.

2.4 Reductions

The computer program used in the reductions was written by Dr. G. Hill (DAO). The program solved the colour equations for V, (b-y), (v-b) and (u-b), each involving the scale factor, extinction and zero point, using the standard stars observed. The equations were solved for each quantity simultaneously and the residuals (Obs. - Calc.) for the standard stars printed out so that the residuals could be checked for time, colour or orientation correlation. Since the scale factors will not change on a small time scale, average values for these were taken and the colour equations resolved for extinction and zero point. The extinction should not change very much during the observing run of several nights so that this was then fixed and a final solution made for the zero point. Different zero points were fixed for each night.

In addition colour corrections may have to be applied to the colour equations and an allowance made for a drift in the zero point through the night. Figures 2.1 and 2.2 show examples of a 'good' night and a 'poor' night for the drift in the V magnitude. The drift is probably caused by small variations in the transmission of the atmosphere during the night or instrument sensitivity. These can be removed by allowing the zero point for the night to change slightly. The programme star observations were then reduced using the values obtained for scale factor,

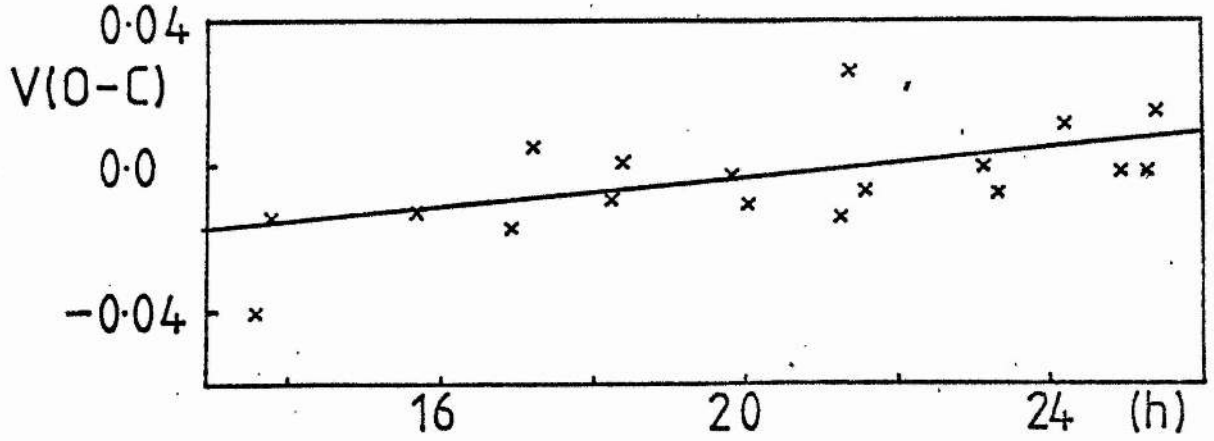

Local Sidereal Time 1976 July 13/14

Figure 2·1 Drift curve for V — Good night

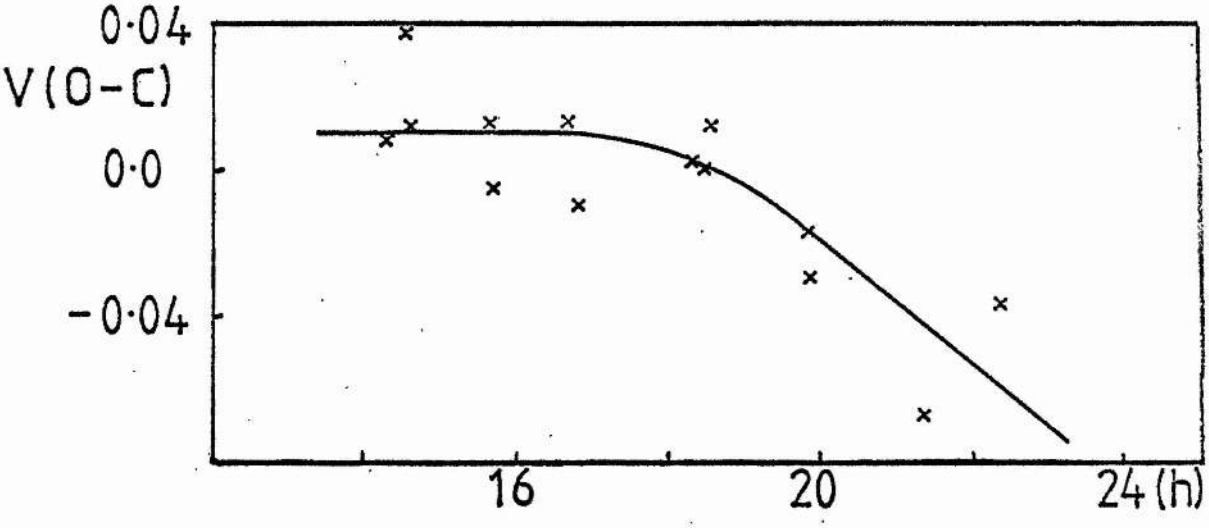

Local Sidereal Time 1976 July 21/22

Figure 2·2 Drift curve for V — Poor night

extinction and zero point, then corrected for the colour term and drift as necessary.

2.4a 1976 July data

Values for the scale factors and extinctions were compared with a set of values for the filters determined from many previous observing runs over several years by Dr. D. Kilkenny and Dr. R. W. Hilditch, and those values were used. The reduction of the data was hindered by the discovery that the 'v' filter had deteriorated and was giving rise to an error dependent upon the colour of the star. After this discovery by Dr. D. Kilkenny, the observations were re-reduced excluding the redder stars and corrections made by plotting the V magnitude against (b-y) and (v-b) against (b-y). This was done using all the nights so that the errors due to drifts would be minimised (see figure 2.3). There was no colour term in (u-b). The drifts were found to be quite serious on the last two nights of the run, due to increasing wind as dawn approached. On each of the last two nights the observing had to be curtailed due to the high wind speed.

2.4b 1977 June data

The first comparison star chosen for HD 168476, HD 168910, was suspected of being variable, since the residuals in the observations for the nights in 1976 were often larger than those for HD 168476. The check star HD 167918 was used as a comparison star in subsequent observational runs and a new check star found, CPD-56°8745, both stars proved to be constant in magnitude and colour. A new set of filters was used for this observing run replacing the old set which had deteriorated. Since only one

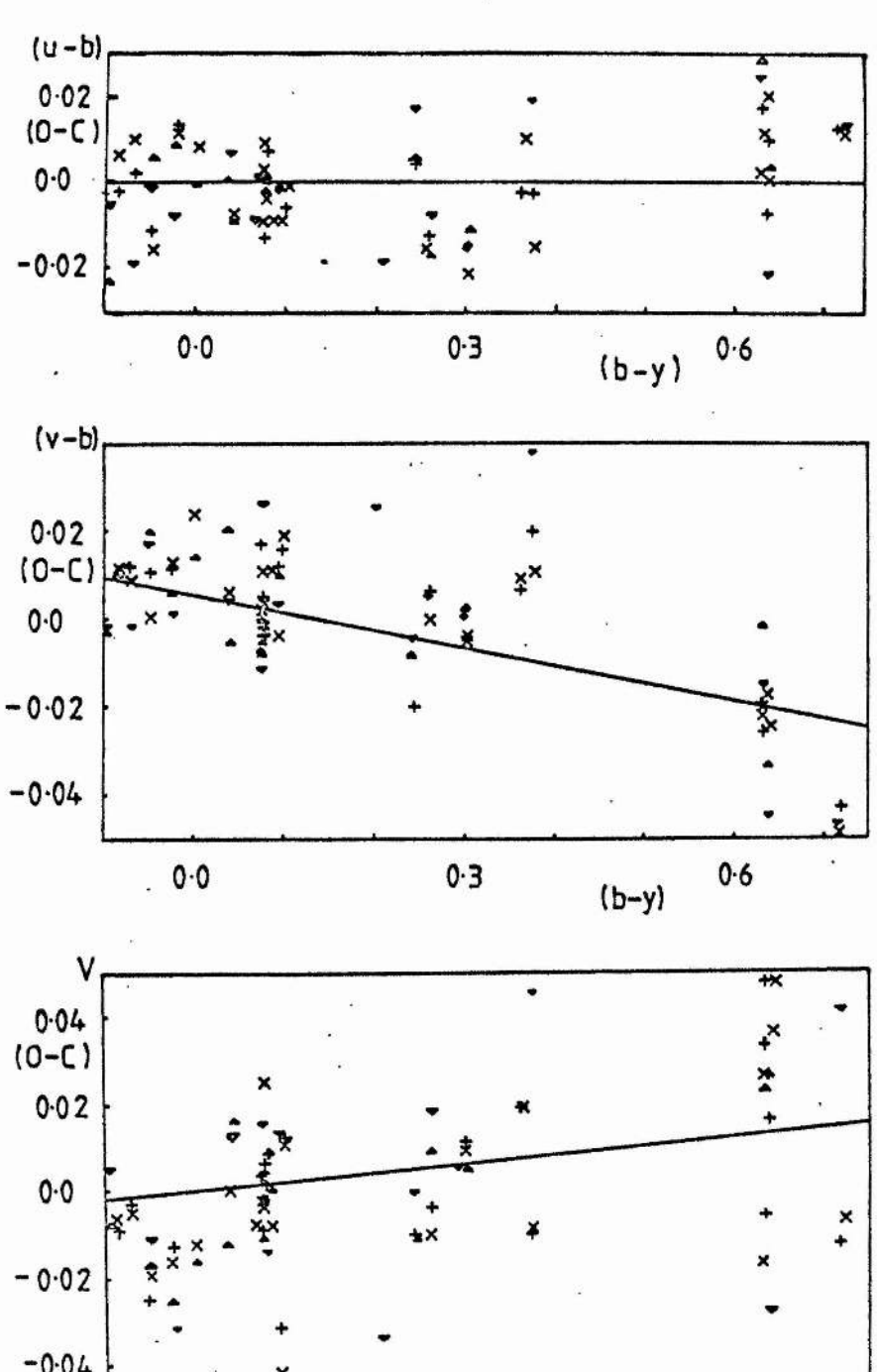

Figure 2·3 Colour terms for 1976

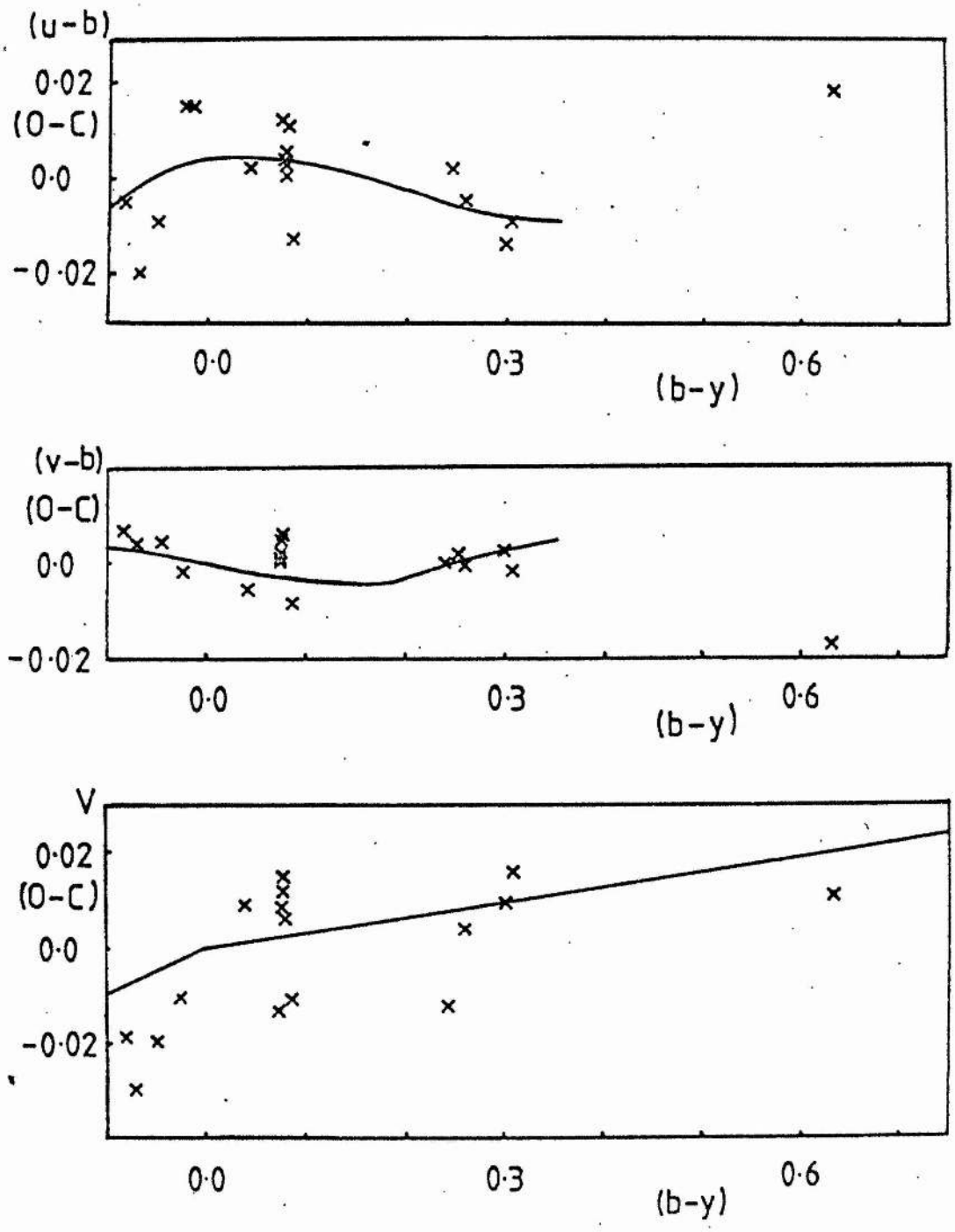

Figure 2·4 Colour terms for 1977

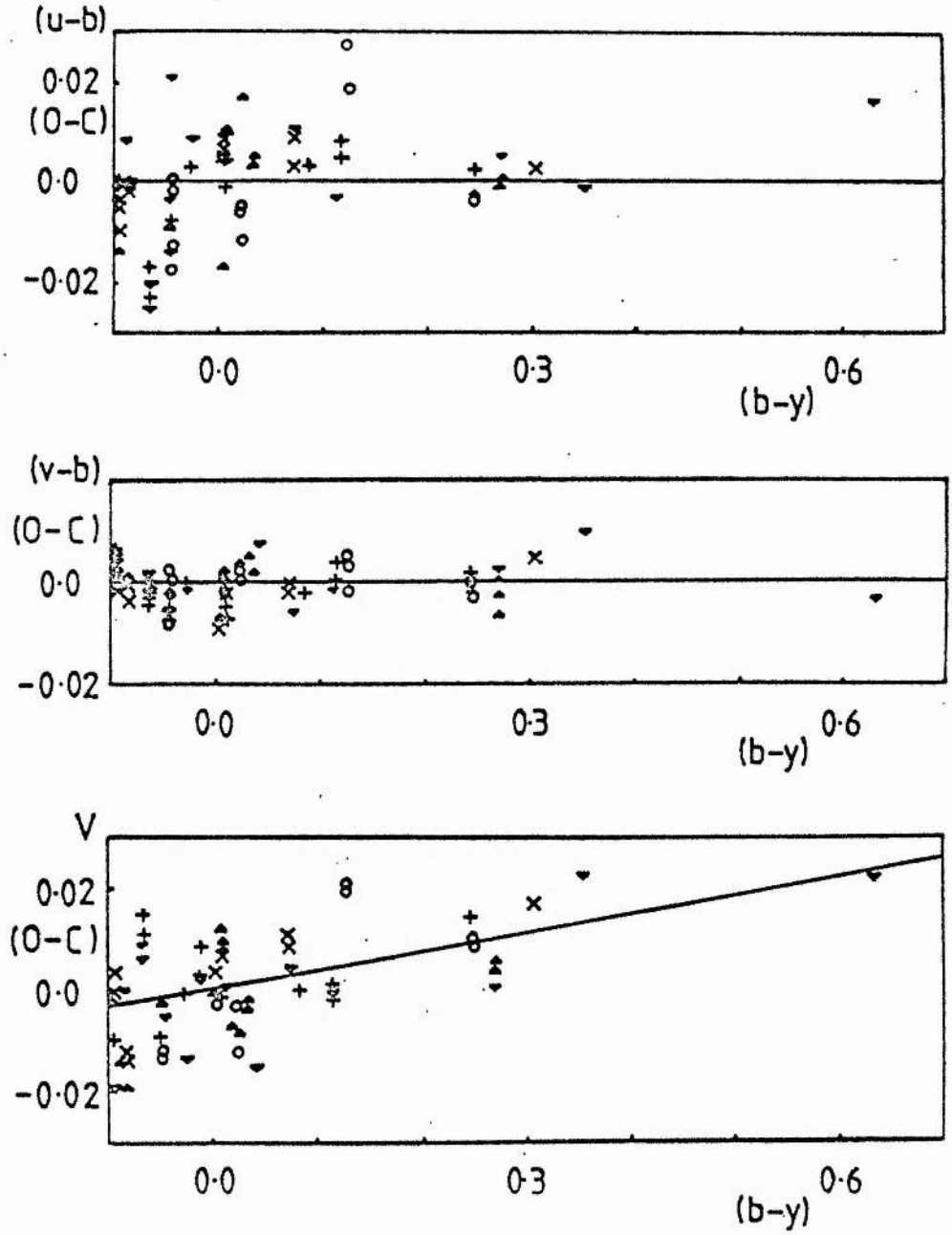

Figure 2·5 Colour terms for 1978

× May 30/31
○ May 31/1
+ June 2/3
△ June 3/4
▼ June 5/6

night out of the seven allocated was usable a set of standard scale factors and extinctions was used from observations by Dr. R. W. Hilditch and Dr. D. Kilkenny. The residuals (O-C) for the standard stars were plotted against colour (b-y) and agreed well with curves provided by Dr. D. Kilkenny from his observing data (see figure 2.4). The lines in figure 2.4 are taken from Kilkenny (1979).

2.4c 1978 June data

A new set of SAAO Strömgren filters was used for this run which concentrated upon observations through the 'b' filter using the Kurtz (1977) technique to monitor variability. Curves to correct for a colour term were plotted (see figure 2.5). No colour term correction was necessary for (u-b) or (v-b).

2.5 Results

Several tables follow showing the results obtained for the three observing runs. Table 2.3 shows the standard values for the scale factor and extinction x scale factor, together with the colour term for the 1976 and 1978 run. The errors quoted here are root-mean-square errors for all the standard stars used, calculated from the residuals (Obs. - Calc.). Table 2.4 shows the zero points and the values obtained on each night for the magnitude of HD 168476, comparison and check stars, together with colours and errors in the form of the standard deviation from the mean. Table 2.5 shows the differential 'b' magnitudes found for HD 168476 relative to HD 167918 in the 1978 run. Data for the period between 244 3378 and 244 3387 was kindly supplied by Dr. D. Kilkenny (1979). In the overall programme, four stars (HD 5737,

HD 6178, HD 120640, HD 143699) were found with photometry in the catalogue by Lindemann & Hauck (1973). These showed no significant residuals in (b-y), m_1 and c_1 (Walker & Kilkenny, 1979).

Table 2.3 Values used for scale factor, extinction and colour term

Year		(u-b)	(v-b)	(b-y)	V	no of nights
1976	Scale factor (SF)	1.005	1.029	1.049	1.000	4
	Extinction x SF	0.380	0.120	0.073	0.141	
	Colour term				0.020	
1977	SF	0.990	0.970	1.040	1.000	1
	Extinction x SF	0.424	0.113	0.061	0.132	
1978	SF	0.997	0.999	1.022	1.000	5
	Extinction x SF	0.385	0.104	0.063	0.127	
	Colour term				0.034	

Table 2.4 Zero points determined from standard stars, observations and means of programme stars

Date JD 244	Star	(u-b)	sd rmse	(v-b)	sd rmse	(b-y)	sd rmse	V	sd rmse	n
1976										
2972	Zero pt.	0.566±.004		0.258±.007		0.375±.007		8.109±.012		18s
	HD 168476	0.398	13	0.116	8	0.048	7	9.298	5	10o
	HD 168910	1.661	57	0.356	17	0.150	9	9.865	12	10o
	HD 167918	0.658	1	0.084	1	-0.008	6	7.808	8	2o
2974	Zero pt.	0.582	7	0.265	7	0.376	6	8.147	8	16s
	HD 168476	0.392	6	0.102	7	0.050	8	9.301	6	12o
	HD 168910	1.679	20	0.356	11	0.145	6	9.868	5	12o
	HD 167918	0.657	6	0.076	6	0.003	2	7.805	8	3o
2978	Zero pt.	0.518	24	0.241	14	0.345	4	8.041	15	3s
(poor)	HD 168476	0.418		0.130		0.040		9.315		1o
	HD 168910	1.675		0.367		0.155		9.880		1o
2979	Zero pt.	0.569	9	0.260	10	0.366	11	8.109	11	14s
	HD 168476	0.398	11	0.114	5	0.033	12	9.324	10	7o
	HD 168910	1.668	14	0.359	11	0.137	10	9.886	21	10o
	HD 167918	0.670		0.084		0.007		7.798		1o
2980	Zero pt.	0.573	10	0.268	13	0.356	7	8.106	14	14s
	HD 168476	0.384	6	0.118	6	0.034	9	9.324	4	5o
	HD 168910	1.675	12	0.357	15	0.142	18	9.900	12	10o

Table 2.4 (cont.)

Date	Star	(u-b)	sd	(v-b)	sd	(b-y)	sd	V	sd	n
1977										
3299	Zero pt.	0.513±.008		-0.050±.005		0.766±.005		3.940±.010		18s
	HD 168476	0.399	4	0.092	6	0.040	7	9.275	7	12o
	HD 167918	0.657	5	0.073	6	-0.005	6	7.796	6	5o
	CPD-56°8745	1.627	15	0.344	9	0.174	9	10.251	6	4o
DK 3378	HD 168476	0.402		0.099		0.028		9.303		1o
	HD 167918	0.648		0.072		-0.007		7.809		1o
DK 3379	HD 168476	0.403	9	0.101	5	0.043	7	9.284	7	5o
	HD 167918	0.652	4	0.076	2	-0.004	5	7.800	2	4o
DK 3380	HD 168476	0.389	16	0.094	3	0.027	4	9.302	7	2o
	HD 167918	0.656	4	0.075	3	-0.010	9	7.807	7	2o
DK 3381	HD 168476	0.407		0.094		0.051		9.274		1o
	HD 167918	0.652		0.071		-0.004		7.803		1o
DK 3382	HD 168476	0.404		0.102		0.039		9.301		1o
DK 3384	HD 168476	0.410		0.102		0.047		9.292		1o
	HD 167918	0.648		0.072		0.003		7.802		1o
DK 3386	HD 168476	0.405		0.091		0.049		9.267		1o
	HD 167918	0.653		0.072		-0.009		7.812		1o
DK 3387	HD 168476	0.390	1	0.088	2	0.046	17	9.283	25	2o
	HD 167918	0.659	4	0.077	1	0.000	2	7.807	3	2o
1978										
3659	Zero pt.	0.180±.005		-0.235±.004		0.883±.003		17.655±.008		13s
3660	Zero pt.	0.190	9	-0.234	4	0.889	4	17.696	5	11s
	HD 168476	0.392		0.102		0.047		9.311		1o
	HD 167918	0.650		0.075		-0.001		7.809		1o
	CPD-56°8745	1.653		0.348		0.174		10.248		1o
3662	Zero pt.	0.185	10	-0.230	4	0.891	5	17.701	8	11s
	HD 168476	0.389		0.115		0.046		9.298		1o
3663	Zero pt.	0.176	9	-0.236	3	0.887	7	17.700	6	14s
3665	Zero pt.	0.182	13	-0.233	5	0.888	6	17.704	8	14s
	HD 168476	0.398		0.108		0.048		9.303		1o
Mean of obs	HD 168476	0.396±.010		0.104±.011		0.043±.010		9.297±.019		64o
	HD 167918	0.656	6	0.076	5	-0.003	6	7.803	7	24o
	HD 168910	1.671	32	0.355	12	0.142	11	9.879	20	39o
	CPD-56°8745	1.634	18	0.345	8	0.174	8	10.251	6	5o

Note 's' indicates the number of standard stars observed
'o' indicates the number of programme star observations made

Table 2.5 Differential 'b' magnitudes

HJD 244	HD168476-HD167918 Δb	sd	n	CPD-56°8745-HD167918 Δb	sd	n	HD167918 b	sd	n
3659	1.551 ±	0.003	12	2.621 ±	0.005	5	7.774 ±	0.005	12
3660	1.555	0.003	15	2.622	0.005	8	7.789	0.002	15
3662	1.561	0.001	15	2.623	0.003	7	7.783	0.002	13
3663	1.554	0.002	11	2.620	0.006	6	7.790	0.004	12
3665	1.559	0.003	15	2.625	0.003	7	7.788	0.004	14

From the mean values displayed in table 2.4 it can be seen that the standard deviation in V of HD 168476 is almost three times that of HD 167918. Bartlett's statistic (Stibbs, 1979) is used to test if the data is a random sample from a normal distribution of values. The data for 244 2972, 2974, 2979, 2980, 3299, 3379 shown in table 2.4 were used.

Bartlett's statistic $X = \dfrac{\upsilon \ln \hat{\sigma}^2 - \Sigma_i^k \upsilon_i \ln \hat{\sigma}_i^2}{1 + \frac{1}{3(k-1)}\left\{\Sigma \frac{1}{\upsilon_i} - \frac{1}{\upsilon}\right\}}$

where $\upsilon_i = n_i - 1$, n_i being the number of observations in a night

$\upsilon = \Sigma_i \upsilon_i$

$\hat{\sigma}_i^2$ is the unbiased estimate of the standard deviation from Bessel's law

and $\hat{\sigma}^2 = \dfrac{(n_1-1)\hat{\sigma}_1^2 + (n_2-1)\hat{\sigma}_2^2 + \ldots + (n_k-1)\hat{\sigma}_k^2}{n_1 + n_2 + \ldots + n_k - k}$

where k is the number of nights

'X' has a χ^2_μ distribution where $\mu = k - 1$.

From the data $X = 5.37$

From Conover (1971) p. 367 $\chi^2_{5,.95} = 11.07$

Thus the data is from a normal distribution, with comparable variances, an indication of no variability in a few hours, so that a 'one-way analysis of variance' may be applied to the data.

From Stibbs (1979) the ratio A/B is tested against tables in Fisher & Yates (1945).

$$A = \frac{(\Sigma T_i^2/n_i - T^2/N)}{k - 1}$$

$$B = \frac{(S - \Sigma T_i^2/n_i)}{N - k}$$

where $T_i = \sum_{j=1}^{n_i} X_{ij}$ $\qquad T = \sum_{i=1}^{k} T_i$

$S_i = \sum_{j=1}^{n_i} X_{ij}^2$ $\qquad S = \sum_{i=1}^{k} S_i$

X_{ij} is the ith observation on the jth night, for n_i observations in one night and k nights, with a total of N values.

For HD 168476 $A = 0.0031$, $B = 4.37 \times 10^{-5}$ $\Big\}$ $F_{5,45} = 71.91$

From the tables at 1.0% level $F_{5,44} = 3.46$

at 0.1% level $F_{5,40} = 5.13$

Therefore, this test shows that the V magnitude of HD 168476 is varying with a probability of more than 99.9%.

In a similar manner the colours (b-y), (v-b) and (u-b), also the indices m_1 and c_1 were tested. Also, the V magnitude and colours of the comparison star HD 167918 were tested in the same way.

From the tables at 5% level $F_{5,44} = 2.43$ $\qquad F_{5,12} = 3.11$

	observed $F_{5,45}$ HD 168476	$F_{5,12}$ HD 167918
V	71.91	1.92
(b - y)	5.97	1.41
(v - b)	21.61	1.66
(u - b)	3.71	0.78
m_1	10.04	
c_1	36.99	

Thus it can be seen that the V magnitude and most probably the colours of HD 168476 are variable.

In order to remove the restraint of normality on the data for HD 168476 the median test (Conover, 1971, p. 168) was used, as suggested by Stibbs (1979). A contingency table (see table 2.6) was set up with the number of observations displayed with values greater than or less than and equal to the median value. This was then tested on the hypothesis that all the values came from the same population i.e. no variability. The data from 1976 to 1978 were tested.

Table 2.6 Contingency table for photometric groups 244 2972 - 2980 and 244 3299 - 3665

	244 2972 - 2980	244 3299 - 3665	
$>$	23	6	29
$\leqslant$	11	23	34
	34	29	63

median = 9.298

For 1 degree of freedom at 0.95 T = 3.84

at 0.995 T = 7.88

(Values obtained from Selby (1971), p. 612)

$$T_{ob} = \frac{N^2}{ab}\sum_{i=1}^{a}\frac{O_{1i}^2}{n_i} - \frac{Na}{b}$$

where N is the total number of observations

a is the number greater than the median

b is the number less than or equal to the median

n_i is the total number in the ith time interval

and O_{1i} is the number of values greater than the median in the ith time interval

$$T_{ob} = 13.89$$

The hypothesis that the V magnitude of HD 168476 is not variable must therefore be rejected, for the time-scale of years.

The data for 1976 was further investigated to examine the possibility of variability during several nights (see table 2.7).

Table 2.7 Contingency table for photometric groups 244 2972 - 74, 244 2979 - 80

244	2972 - 74	2979 - 80	
>	5	12	17
≤	17	0	17
	22	12	34

median = 9.303

$$T_{ob} = 18.55$$

In this case, the hypothesis that the V magnitude does not vary over several nights must be rejected.

Table 2.5 and Bartlett's statistic show that the variability will be on a time-scale longer than a few hours, approximately 0.4 days (twice the maximum length of time that the star was observed in one night). Table 2.5 shows from the standard

deviations in the 'b' magnitudes and the differential 'b' magnitudes the accuracy that can be obtained. Any variations on a time-scale of a few hours must be very small indeed, i.e. a few ten-thousandths of a magnitude. It was not possible to find a period for the star due to paucity of observations over a period of longer than one week. Landolt (1973) suspected a slight secular brightening in HD 168476 over a decade, after comparison with the observations of Hill (1969a). The observations given here show that this trend has reversed (see figure 2.6) suggesting that the star is variable on a long time-scale. The data for figure 2.6 came from observations in table 2.4 together with those of Hill (1969a) and Landolt (1973). Plotted in figure 2.7 are the data for periods of several nights showing the slight variations in HD 168476.

2.6 Discussion

HD 168476 was plotted on the (b-y) - m_1 and (b-y) - c_1 diagrams (figures 2.8 and 2.9) with several other extreme helium-rich, intermediate helium-rich stars and helium-rich subdwarfs. Where possible the reddening of the extreme helium-rich stars was removed, but this should only be important for HD 160641 and BD-1°3438, which are very near the Galactic Plane. In all cases the reddening E(B-V) was found (except for HD 168476 where the model gave intrinsic (b-y)) and converted to E(b-y) via :-

$$E(b-y) = 0.72\ E(B-V)$$

from Crawford (1973). The reddening in m_1 and c_1 was then calculated using

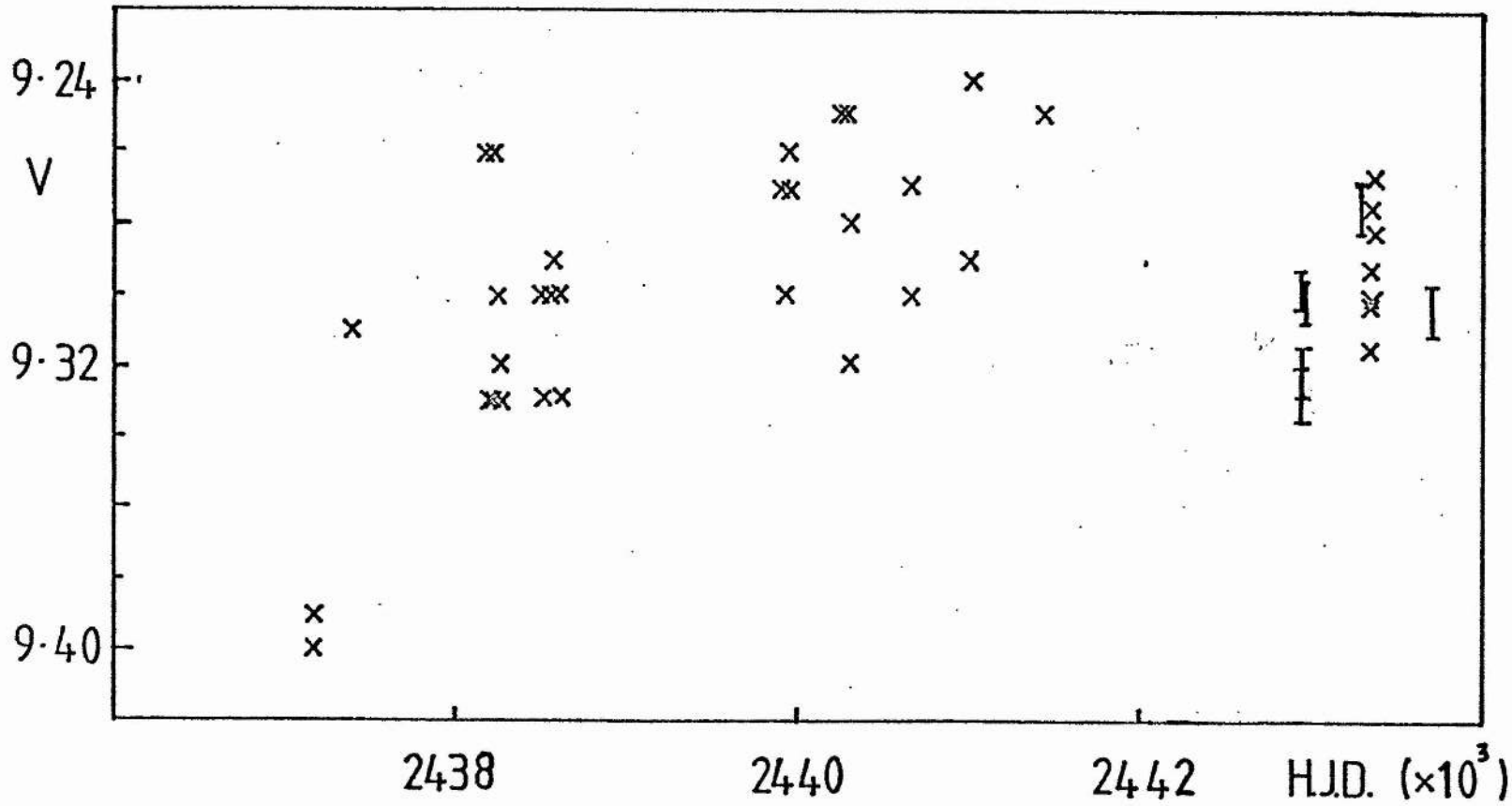

Figure 2·6 V magnitudes of HD 168476 1960–1978

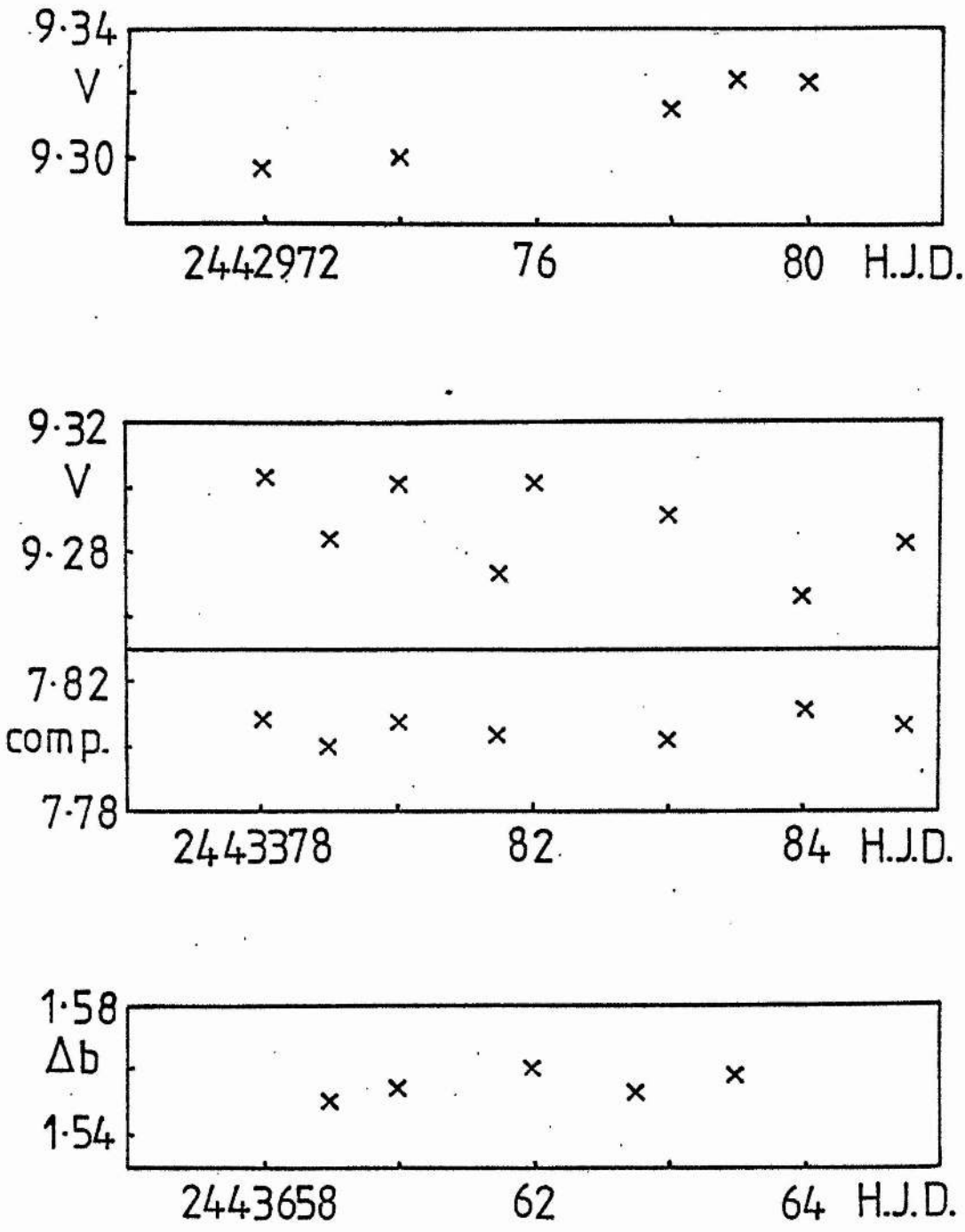

Figure 2·7 V magnitudes or differential b magnitudes for observing runs of several nights

$$E(m_1) = -0.3 \times E(b-y)$$

$$E(c_1) = 0.2 \times E(b-y)$$

The intermediate helium-rich stars used will all probably be reddened to some extent, since they are generally found in the plane of the galaxy (see table 1.1), HD 264111 ($b = 1^{\circ}$) and several of the Osmer & Peterson (1974) stars appear significantly affected. For BD-9°4395 computed intrinsic colours were available from Kaufmann & Schönberner (1977) on the Johnson (UBV) system, so that E(b-y) was easily computed. The difference in the computed theoretical colours for BD-9°4395 compared with the expected intrinsic colours from its spectral type was assumed to arise from it being an extreme helium-rich star. Thus the difference between the two was applied as a correction to the expected intrinsic colours of HD 160641, so that an estimate of the reddening could be obtained. For BD-1°3438 an estimate of $E(B-V) \sim 0.5$ mag. given by MacConnell et al. (1972) was used. Table 2.8 shows values obtained for V, (b-y), m_1 and c_1 from Walker & Kilkenny (1979) for several helium-rich stars and the number of observations used, with additional data for the intermediate helium-rich stars and helium-rich subdwarfs from Kilkenny (1977), Kilkenny (1978) and Osmer & Peterson (1974).

Table 2.8 Magnitudes and colours of helium-rich stars

Star	V	(b-y)	m_1	c_1	n	E(b-y)	He type	Source
HD 124448	9.99	-0.005	0.055	0.123	12		ext	WK
BD -9°4395	10.5	0.14	0.00	-0.15	1	0.22	ext	WK
BD +13°3224	10.6	-0.07	0.07	-0.06	1		ext	WK
HD 160641	9.84	0.200	-0.053	-0.125	10	0.3	ext	WK
BD -1°3438	10.3	0.38	0.04	0.28	1	0.4	ext	WK
HD 168476	9.30	0.043	0.061	0.188	64	0.09	ext	WK
HD 49798	8.30	-0.122	0.064	-0.218	3		SdO	K2
HZ 44	11.71	-0.151	0.118	-0.280	2		SdO	K1
HD 127493	10.05	-0.111	0.046	-0.206	7		SdO	WK
HD 37776	7.01	-0.056	0.099	0.061	3		int	K2
HD 37479	6.71	-0.072	0.097	0.049			int	OP
HD 264111	9.63	0.102	0.034	0.058	3		int	K1
HD 60344	7.75	-0.06	0.07	0.09			int	OP
CPD-46°3093	10.0	0.14	0.04	0.02			int	OP
HD 133518	6.40	-0.024	0.090	0.173	14		int	WK
HD 144941	10.11	0.07	0.07	0.06			int	OP
CPD-69°2698	9.36	-0.141	0.069	0.050	9		int	WK
HD 168785	8.49	0.08	0.04	0.05			int	OP

notes :-
ext - extreme helium-rich star
SdO - helium-rich subdwarf
int - intermediate helium-rich star
WK Walker & Kilkenny (1979)
K2 Kilkenny (1978)
K1 Kilkenny (1977)
OP Osmer & Peterson (1974)

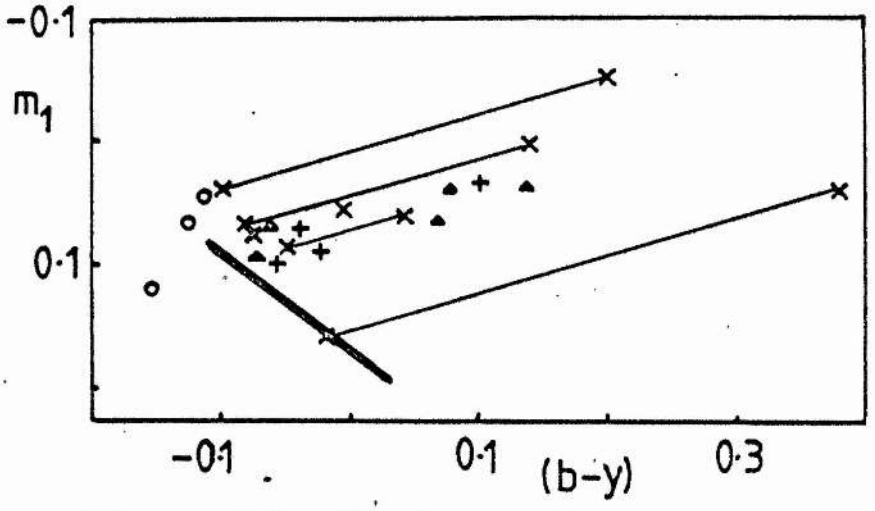

Figure 2·8 (b-y) – m_1 diagram

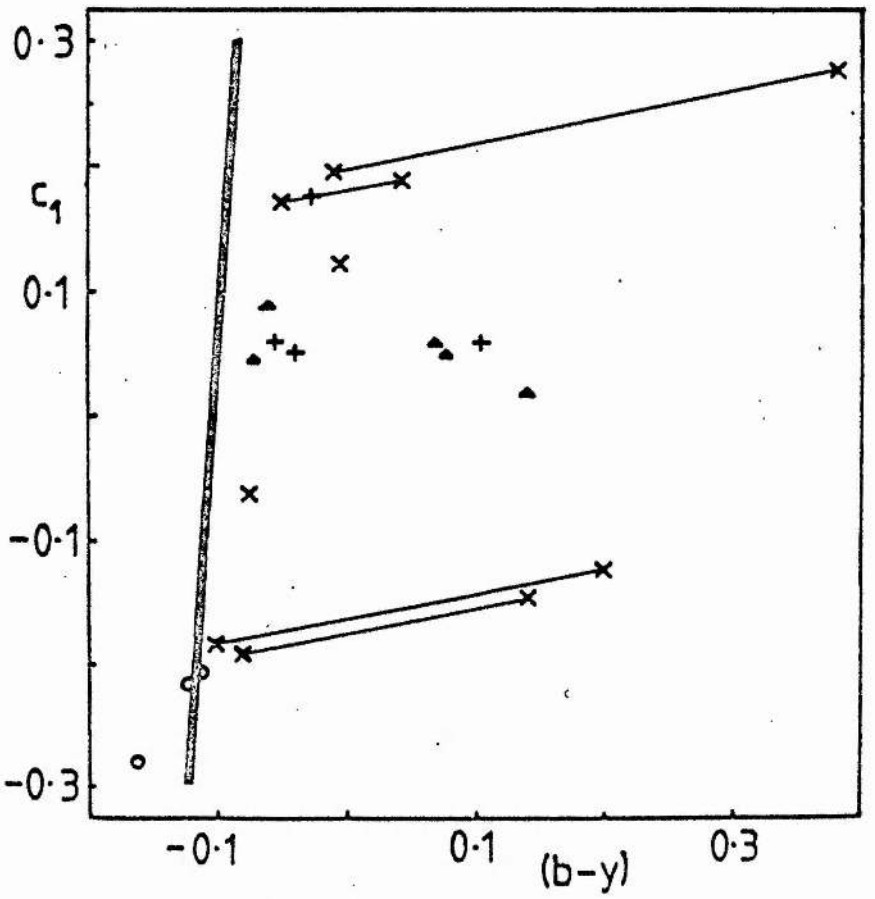

Figure 2·9 (b-y) – c_1 diagram

x extreme helium-rich star
\+ intermediate helium-rich star
△ OP intermediate helium-rich star
o helium-rich subdwarf

The (b-y) - m_1 and (b-y) - c_1 diagrams (figures 2.8 and 2.9) show that it is not possible to recognise the peculiarity of helium overabundance by 'uvby' photometry. The solid lines in the diagrams are the intrinsic colour lines taken from Slettebak et al. (1968) for (b-y) - m_1 and Crawford (1973) for (b-y) - c_1. The intrinsic colours of the helium-rich stars do not appear significantly different from those of normal stars, a fact that Hunger & Van Blerkom (1967) noted from flux calculations. In the (b-y) - c_1 diagram it is possible to suggest that the extreme helium-rich stars form a sequence in c_1. On spectral evidence (Kaufmann & Schönberner, 1977) HD 160641 is believed to be hotter than BD-9°4395, which is reflected in the dereddened colour (b-y). Figure 3 of Walker & Kilkenny (1979) showed a graph of the reddening free parameter [u-b] against θ_e for the extreme helium-rich stars, with the calibration from Philip & Newell (1975). It showed that the extreme helium-rich stars were cooler at the same [u-b] than normal B stars. Their c_1 indices are naturally very different. The lack of hydrogen partly explains the proximity of the hot extreme helium-rich stars, such as HD 160641 and BD-9°4395 to the SdO stars in the (b-y) - c_1 diagram.

Several different types of variability have been discovered in the extreme helium-rich stars. MV Sgr. is known to be a hot extreme helium-rich R CrB star (Hoffleit, 1959). BD+13°3224 has a photometric variation (Landolt, 1975) with amplitude in V of 0.1 mag. and period 0.1 days, with variability in (B-V) and (U-B). There is evidence to suggest that HD 160641 may have a period of about 0.7 days for its variation in V, but no variations have been detected in its colours (Landolt, 1975; Walker & Kilkenny, 1979).

As noted before HD 168476 is found to be variable in its V magnitude on a time-scale of days, but with a period longer than 0.4 days. HD 124448, however, has only a little evidence to suggest that it is variable (Landolt, 1973; Walker & Kilkenny, 1979). This leads to the conclusion that variability of a specific nature is not a characteristic of the group of extreme helium-rich stars, but rather a property of individual members of the group. The extreme helium-rich stars are closely related to the R CrB stars, HD 168476 being one of the nearest in the log T_e - log g diagram, and so its variability is of great interest in the light of the variability of the R CrB stars (Schönberner & Wolf, 1974). The variability of the R CrB stars is mostly irregular, although a period of 39 days was found for RY Sgr. (Alexander et al., 1972).

3 RADIAL VELOCITY STUDY

3.1 Introduction

The Cassegrain two-prism spectrograph was used with the 1.9m Radcliffe telescope at the South African Astronomical Observatory (SAAO), to obtain spectra for radial velocity measurements. The spectrograph, consisting of two 64° light/flint glass prisms set permanently for minimum deviation at 4200A, was carefully designed to minimise flexure (Jackson, 1951) and tests (Feast et al., 1954) with the telescope observing far into the east and west, discovered no flexure effects. The 'c' camera was used, which had a dispersion of 49A/mm at Hγ, and the length of the slit was determined by either dekker 2 (length 1mm projected at plate to 0.024mm) or dekker 3 (length 2mm), since only two adjacent dekkers could be collimated satisfactorily at any one time. (SAAO Facilities Manual) The slit width was set to around 0.075mm (projected width at plate 0.018mm). The slit jaws of the spectrograph were curved so that they produced straight lines on the photographic plate, avoiding any necessity for correction. An iron arc was used to give the wavelength calibration.

3.2 Observations

IIaO plates were used for the observations, after being baked in air for 48 hours at 50°C. The wavelength region covered was around 3850A to 4950A for the star, with arc lines to the blue and red respectively of these values. A quartz-halogen lamp emitting a continuous spectrum was available to give a wedge calibration, with arc lines from a mercury lamp for the

wavelength scale.

Seven exposures of stellar spectra could be made on one plate, which was developed fairly soon after the exposure to check exposure time and the focus of the telescope. The 1976 plates were developed in D-19 for 5 minutes at 20°C, and then fixed in a conventional fixer for 10 minutes before washing for about 30 minutes. In 1977 a different fixer 'Amfix' was used with its hardener, which required only 4 minutes to fix the plate before washing, and the addition of a wetting agent to ensure even drying. In 1977 a bubble development system was used, passing a 0.6 second burst of nitrogen through the developer every 8 seconds.

A focus plate was taken using the arc spectrum. Several standard stars were observed to check the radial velocities obtained, both late and early spectral types. Although the late spectral types had more lines so that a better radial velocity could be determined, it was feared that a shift in radial velocity might be introduced through guiding on a 'red' image as opposed to the 'blue' one of the early type standards and programme stars, so that several early type standard stars were used. However, no systematic difference was found for the two types of standard. Table 3.1 shows the radial velocity standards used.

The allocations of observing time for the project which involved simultaneous photometry and spectroscopy are shown in Table 3.2.

Table 3.1 Radial velocity standards used

Star	Sp tp	Vel	Ref	Star	Sp tp	Vel	Ref
HD 6085	gK1	+11.5±0.5	1	HD 162021	KOIII	-22.9±0.3	4
HD 113537	F5III	-1.4±1.0	4	HD 168454	gK2	-20.0±0.2	1
HD 120908	B5V	+8.0±1.2	1	HD 180540	gG5	+15.2±0.6	1
HD 150041	BOIIk	-18 ± 2	2	HD 210934	B8III	-5.8±1.2	1
HD 157457	K1III	+17.4±0.2	3	HD 219784	sgG8	+15.6±0.5	1

Source :- 1 Wilson (1953)
2 Feast et al. (1954)
3 Pearce (1955)
4 Evans et al. (1959)

Table 3.2 Observing time used for radial velocity work

Date	1976 May	1976 July	1977 June
Allocation (nights)	4	7	7
Usable	1 whole 2 ½-nights	3 whole 2 < 2hrs	4 whole 1 ⅔-night
Assistance	PWH	WM + SAAO technician	PWH + AELG (1 night)
Comments			Thin cloud on 4 nights

Notes :- PWH P. W. Hill
WM W. Martin (SAAO)
AELG A. E. Lynas-Gray

3.3 Reductions

The spectral lines were measured in three visits to the Royal Greenwich Observatory, using their radial oscilloscope measuring machine (see figure 3.1, Murdin, 1978). The spectrum plate was set up on a Hilger and Watts long screw measuring instrument in the usual way, but instead of measuring the spectrum by inspection through the eyepiece, the light was passed through a rotating quartz octagon onto a 1P28 photomultiplier. This sent the signal to an oscilloscope on which the line and its reverse were shown, so that when these coincided the reading was noted via an Addo-X machine. The 1P28 received only the blue light from a dichroic filter in the light path, the yellow light was reflected onto a screen, so that the spectral image could be seen and easily adjusted. The spectrum was measured in the usual manner, in both the forward and reverse directions, setting on the line from one side only, to reduce the errors from backlash to a minimum.

In May and July 1976, 119 spectra were obtained, of which 16 were of HD 168476 and 18 were of standard stars. Unfortunately, of those taken in May, from the seven standard star spectra, four spectra of one star HD 113537 were very discrepant (see table 3.3) suggesting the star might be variable. In June 1977, 117 spectra were obtained of which 24 were of HD 168476 and 14 were of standard stars. In this run 11 wedge calibration spectra were taken to enable the conversion of density of the emulsion into intensity. In addition 10 spectra of HD 168476 had been taken by Dr. D. Kilkenny in 1971 and these were scanned at the RGO, as well as 13 spectra of HD 168476 taken by M. W. Feast, P. W. Hill, A. D. Thackeray and A.J. Wesselink between 1953 and 1964. Three of these spectra were taken at the higher dispersion of 29A/mm.

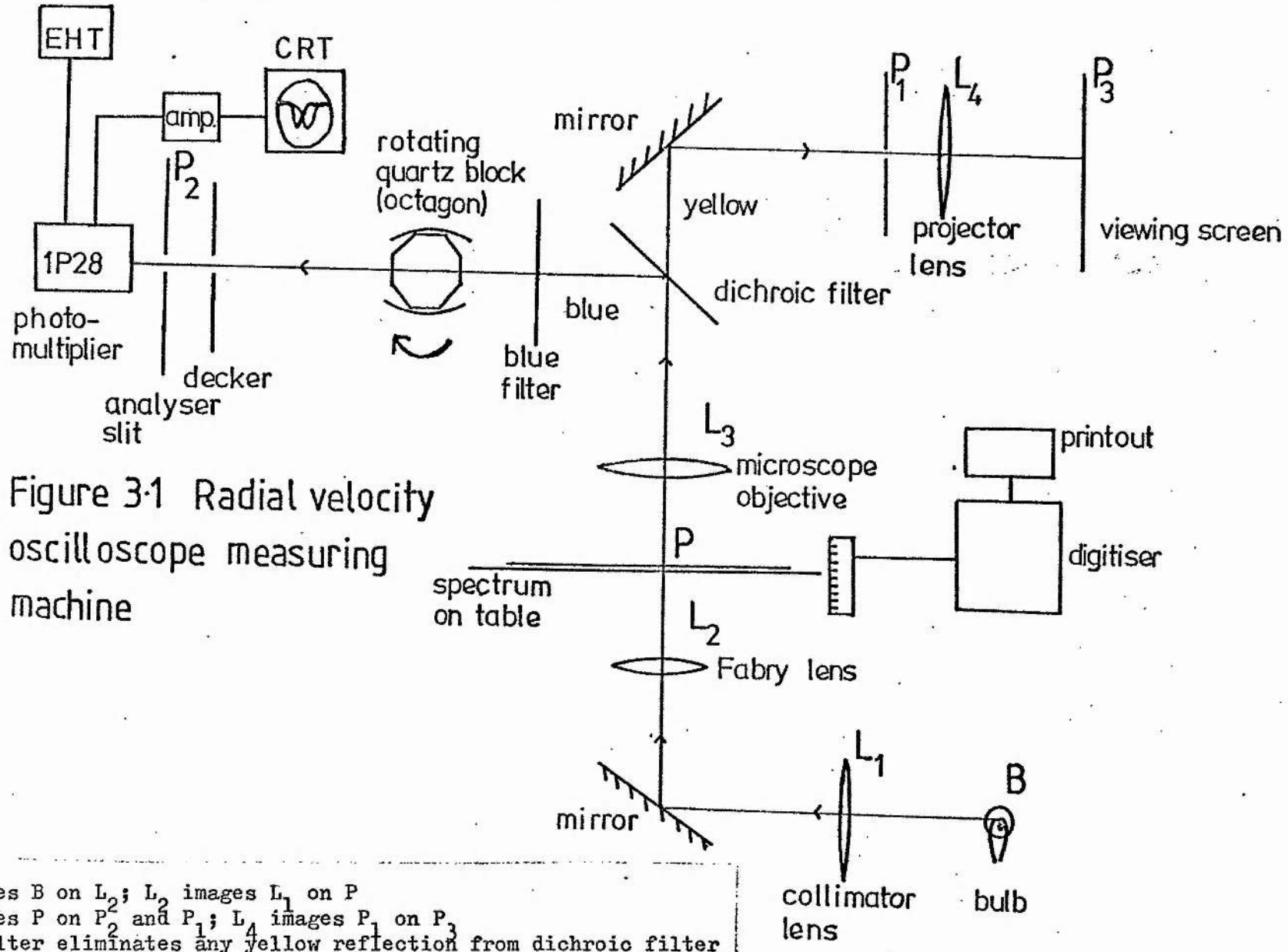

Figure 3·1 Radial velocity oscilloscope measuring machine

L_1 images B on L_2; L_2 images L_1 on P
L_3 images P on P_2 and P_1; L_4 images P_1 on P_3
Blue filter eliminates any yellow reflection from dichroic filter

These earlier plates had been scanned with the same machine by Dr. P. W. Hill, with other spectra (see table 3.8), and were rescanned to check for significant errors between measurements.

The measurements made at the RGO were reduced using programs written by Dr. P.W. Hill. The Hartmann formula was used :-

$$\lambda = \lambda_0 + \frac{c}{d_0 - d}$$

where λ_0, c and d_0 are calculated constants and d is the measured position of the stellar line. The constants were calculated from the positions of three arc lines and the results from many spectra averaged. This formula is not exact and a polynomial up to degree five was fitted by the computer program to the residuals from the Hartmann curve to give the correction curve. Between 80 and 100 spectral measurements were used to determine the Hartmann constants for the 1976 July and 1977 June observing runs. The arc line at 4071A had conspicuously large residuals and so was not used. It may have two components to it. A few other arc lines, one or several of 4891A, 4871A, 4859A, 4315A, 4132A, 3930A, were occasionally given half weight in the program due to their large residuals from the correction curve. The radial velocity calculated was then corrected for the diurnal motion of the earth and the annual motion of the sun. Schlesinger (1899) gives these corrections. The diurnal correction is :-

$$V_d = \frac{2\pi A}{\tau} r \cos\phi \sin H \cos\delta$$

where A is the equatorial semi-diameter of the earth

r is the radius vector from the centre of the earth to the

observer

τ is the length of a sidereal day in seconds of mean time

H = Sidereal time - α

The annual correction was computed in the form

$$V_a = lX' + mY' + nZ'$$

$$l = \cos\alpha \cos\delta$$

$$m = \sin\alpha \cos\delta \cos\varepsilon - \sin\delta \sin\varepsilon$$

$$n = \sin\alpha \cos\delta \sin\varepsilon + \sin\delta \cos\varepsilon$$

X', Y', Z' are the diurnal corrections from the equatorial rectangular coordinates of the sun obtained from the Astronomical Ephemeris, instead of the ecliptic coordinates used by Schlesinger.

3.4 Results

3.4a Standard stars

The stellar line wavelengths were taken from Plaskett et al. (1932) and where appropriate (i.e. 4861A, 4471A, 4026A) the wavelengths or velocities were corrected according to Petrie (1953) and Feast et al. (1957). Table 3.3 shows the results obtained corrected for the earth's motion. Most spectra were measured only once, but some, indicated in the table, were measured twice to check that my measurement technique and the machine remained constant.

Table 3.3 Radial velocities of standard stars

Year	Star	Rad vel km/s	s.e.	no of lines	no of meas.	O-S
1976 May	HD 113537	-24	3	9	1	-23
		-21	2	7	2	-20
		-20	4	7	1	-19
		+4	2	8	1	+3
	HD 168454	-17	3	4	1	+3
		-22	3	6	1	-2
		-29	4	8	1	-9
1976 July	HD 6085	+16	5	7	1	+4
	HD 120908	+4	4	10	1	-4
		0	3	6	1	-8
	HD 150041	-13	3	8	1	+5
		-20	3	10	2	-2
	HD 162021	-25	2	15	2	-2
	HD 180540	+11	2	14	1	-4
		+13	2	18	2	-2
	HD 207971	-4	3	5	1	-2
	HD 210934	-10	3	5	2	-4
	HD 219784	+11	2	13	1	-5
1977 June	HD 113537	-2	4	10	1	-1
	HD 120908	+6	3	8	1	-2
		+12	4	7	1	+4
		-2	3	11	1	-10
		+8	6	9	1	0
		+7	2	7	1	-1
	HD 139129	-7	3	8	1	+5
		-9	3	7	1	+3
	HD 150041	-30	4	10	1	-12
	HD 157457	+27	2	11	1	+10
	HD 162021	-31	4	11	1	-8
	HD 207971	-3	5	7	1	-1
		-6	3	8	1	-4
		+1	9	6	1	+3

O-S observed velocity from measures - standard (table 3.1)

1976 July mean residual = -2.2 ± 3.8 (s.d.)

1977 June mean residual = -1.0 ± 6.1 (s.d.)

From Wayman (1961) a weight can be attached to each spectrum :-

$$W_i = \frac{100}{(a + 2.2e_i^2)}$$

where 'a' is a constant for the c camera, equal to 3.87 and e_i is the internal probable error of a single measurement of the spectrum, expressed as :-

$$e_i = 0.6745\sigma_i$$

where σ_i is the standard deviation of the mean. By using these weights with the differences between the radial velocities calculated here and the published value, a root-mean-square error was found of $\pm$ 2.8 km/s, the error in the radial velocity of a spectrum due to internal and external errors.

3.4b HD 168476

In table 3.4, shown below, the line wavelengths used in the analysis are given. These lines are the same as are used in section 3.4a, with some additions from Moore (1945). It is felt that for HD 168476 they are possibly not the most suitable set of wavelengths to be used due to the fact that the wavelengths make allowance for blending in normal stars, which may not be valid in the case of HD 168476. However, until definite values can be put upon any wavelength changes necessary, this set is used, and the radial velocities will be consistent with values of HD 168476 previously determined. Table 3.5 shows the mean radial velocity with standard error from the mean, for the measurements made here,

Table 3.4 Spectral line wavelengths for HD 168476 used in the radial velocity determination

λ	Ion	λ	Ion
4481.228	Mg II	3968.465	Ca II
4471.477	He I	3964.727	He I
4437.549	He I	3935.914	He I
4387.928	He I	3933.664	Ca II
4267.160	C II	3926.530	He I
4168.970	He I	3920.677	C II
4143.759	He I	3918.977	C II
4130.876	Si II	3888.646	He I
4128.051	Si II	3867.528	He I
4120.812	He I	3862.590	Si II
4026.189	He I	3856.028	Si II
4009.270	He I	3819.640	He I
3994.996	N II		

together with the number of lines used. The radial velocities determined by Dr. D. Kilkenny and Dr. P. W. Hill for spectra also measured by the writer are shown in table 3.6, with the residual of "this thesis - Hill/Kilkenny". Table 3.7 shows the radial velocities measured by Hill (1978) for spectra which the writer did not re-measure. The mean radial velocity for the 10 lines common to the measurements in 1976 July and from 13 lines common to the measurements in 1977 June is shown in table 3.8. Table 3.9 shows the mean radial velocity for the thirteen lines, found from 1976 July and 1977 June.

Table 3.5 Mean radial velocities for HD168476 (all available lines)

H.J.D.	rad vel	se.	no of lines		H.J.D.	rad vel	se.	no of lines
2434510.505	-159	± 4	13		2442971.471	-170	± 4	14
520.556	-165	1	18	+	971.505	-168	3	15
585.385	-168	1	20	+	971.545	-164	3	14
586.281	-170	4	15		975.383	-168	4	13
587.271	-167	4	9		975.419	-172	3	17
588.299	-170	2	19	+	975.454	-177	2	11
648.244	-168	3	15		975.508	-181	3	14
2438155.532	-167	2	22		2443299.522	-172	2	20
264.271	-177	2	22		299.559	-171	2	22
508.582	-161	2	19		299.594	-172	2	24
537.657	-176	3	18		300.475	-173	2	25
567.477	-172	2	14		300.509	-178	1	24
619.327	-172	2	19		300.536	-175	2	20
2441117.479	-170	2	17		300.565	-172	2	23
136.398	-172	1	18		300.598	-173	2	25
167.313	-168	4	13		300.630	-174	1	20
168.252	-167	2	19		302.450	-174	2	25
168.289	-171	3	19		302.611	-176	2	23
168.327	-165	2	21		302.646	-174	2	24
168.391	-173	2	13		303.512	-179	1	25
168.436	-172	2	17		303.538	-182	1	21
168.474	-174	4	16		303.564	-181	2	24
169.337	-173	2	22		303.594	-178	1	23
2442913.599	-182	2	15		303.631	-179	2	21
913.630	-188	3	15		304.437	-177	2	20
913.670	-184	2	13		304.467	-178	2	21
970.407	-170	2	18		304.500	-179	1	20
970.446	-170	2	17		304.532	-179	2	18
970.507	-172	2	15		304.564	-178	2	19
970.539	-170	2	19		304.605	-177	2	20
971.404	-168	3	14		304.694	-176	2	20
971.434	-163	4	13					

+ signifies 'b' dispersion (29A/mm)

mean radial velocity = -172.9 ± 0.7 (s.e.) km/s

Table 3.6 Common radial velocities measured by Kilkenny and Hill

D. Kilkenny		P. W. Hill	
H.J.D.	rad vel	H.J.D.	rad vel
2441117.479	-172	2434510.505	-161
136.398	-176	520.556	-166
167.313	-169	585.385	-165
168.252	-166	586.281	-170
168.289	-171	587.271	-169
168.327	-163	588.299	-168
168.391	-171	648.244	-166
168.436	-174	8155.532	-163
168.474	-170	264.271	-173
169.337	-172	508.582	-160
		567.477	-169
		619.327	-171

Residual
'thesis - Kilkenny'
= -0.1 ± 2.4 (10)

'thesis - Hill'
= -1.3 ± 2.1 (12)

Table 3.7 Radial velocities up to 1964 measured by Hill

H.J.D.	rad vel	no of lines	H.J.D.	rad vel	no of lines
2434195.454	-170	15	2437505.538	-179	33 *
222.433	-159	13	506.533	-181	46 *
241.347	-156	14	537.374	-171	36 *
251.313	-166	14	561.334	-176	13 *
279.280	-165	11	566.314	-172	34 *
286.213	-167	11	8167.512	-172	17
295.211	-157	16	169.465	-168	17
459.611	-164	17	226.322	-166	16
497.580	-162	11	227.388	-151	14
497.618	-169	12	241.281	-167	12
530.557	-160	12	248.343	-163	15
534.436	-177	10	250.247	-159	13
578.539	-165	16	269.254	-171	16
579.287	-171	17	271.223	-168	16
580.289	-170	15	275.288	-169	12
640.236	-169	21 +	277.263	-163	13
7094.514	-173	97 *	625.287	-172	27 *
183.275	-166	15 *	625.469	-168	29 *
185.307	-174	31 *			

+ signifies "b" dispersion (29A/mm)

* signifies Coudé plate (15.6A/mm)

mean radial velocity = -170.9 ± 0.7 (s.e.) km/s

(100 obs.)

Table 3.8 Mean radial velocities from 10 or 13 lines, by night

H.J.D.	rad vel	s.e.	note	H.J.D.	rad vel	s.e.
2442970.407	-166	2		2443300.565	-172	2
970.446	-168	2	*	300.598	-172	2
970.507	-169	2		300.630	-173	2
970.539	-167	3		302.450	-172	2
971.404	-172	3		302.611	-174	2
971.434	-162	3		302.646	-171	3
971.471	-167	2		303.512	-178	2
971.505	-167	4		303.538	-180	2
971.545	-161	3	*	303.564	-178	2
975.383	-166	3		303.594	-177	1
975.419	-172	3		303.631	-180	2
975.454	-177	3	*	304.437	-175	2
975.508	-178	3		304.467	-179	2
3299.522	-171	2		304.500	-179	1
299.559	-171	3		304.532	-178	2
299.594	-169	2		304.564	-175	3
300.475	-169	3		304.605	-177	2
300.509	-174	2		304.694	-174	3
300.536	-174	2				

Notes :- 2442970.446 9 lines, 4120A not measured

971.545 9 lines, 4120A not measured

975.383 9 lines, 4026A not measured

Table 3.9 Mean radial velocities from 10 or 13 lines, by line

	Ion	1976 rad vel	s.e.	no of spectra	1977 rad vel	s.e.
4481	Mg II	-169	± 2	13	-177	± 3
4471	He I	-168	2	13	-170	2
4387	He I	-172	3	13	-180	2
4267	C II	-169	2	13	-171	2
4143	He I	-171	3	13	-178	2
4130	Si II	-168	3	13	-168	3
4128	Si II	-168	2	13	-175	2
4120	He I	-166	3	11	-174	2
4026	He I	-168	4	12	-170	2
4009	He I	-170	6	13	-177	2
3968	Ca II	-166	2	13	-175	1
3964	He I	-171	4	10	-177	1
3933	Ca II	-171	3	11	-180	1

Note :- In 1977 there were 24 spectra used for each line average.

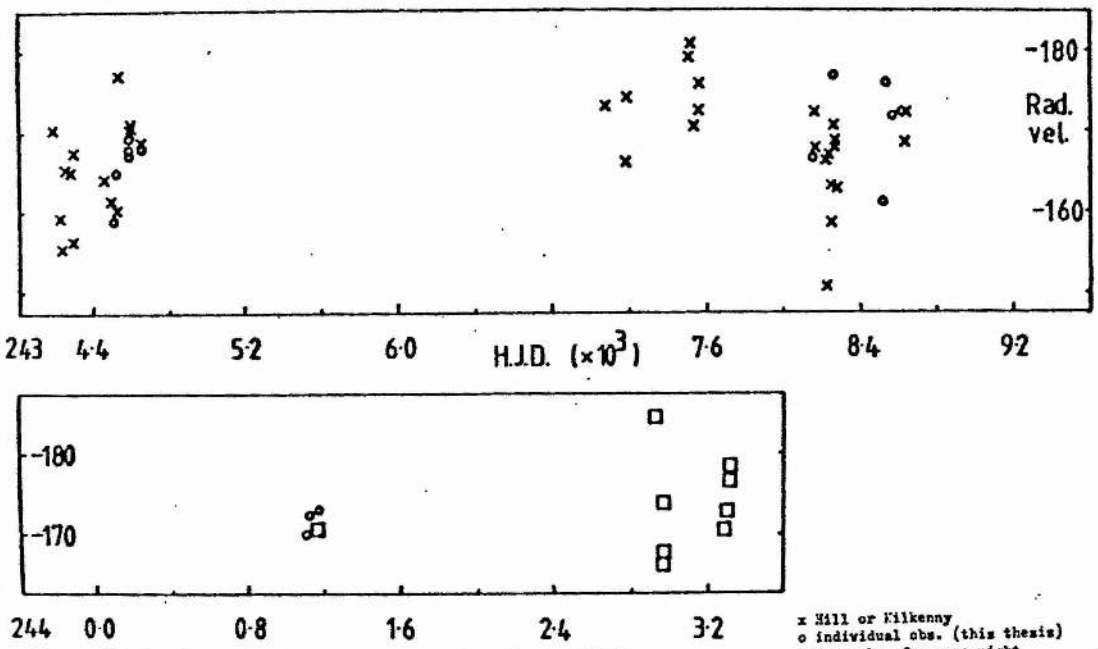

Figure 3·2 Radial velocity measurements of HD168476

3.5 Discussion

There are no significant differences between the radial velocities obtained by Dr. D. Kilkenny and Dr. P. W. Hill and the writer. Table 3.9 shows that the measurement errors were larger than any wavelength shift introduced by using an unsuitable wavelength. One problem with the 1976 July run was the apparent absence of the 4120A He I line in two spectra (noted in table 3.8), although each spectrum was measured twice. Upon scanning with the Joyce-Loebl machine at St. Andrews Observatory the line was clearly identifiable. Thus a line profile variation was suspected, with the result that the line would not be easily measured. The data from tables 3.5 and 3.7 are plotted in figure 3.2. Possible maxima are seen at 243 4534, 243 7505 and 244 2913, and minima at 243 4241, 243 3827 and 244 2971, but these must naturally be very tentative, and a considerable amount of scatter in the data is clearly visible.

To test whether the star's radial velocity is variable first the χ^2 - test (Trumpler & Weaver, 1953, page 205 et seq.) was used. The hypothesis of constant radial velocity was tested in the form that the semi-amplitude of the variation in radial velocity is zero and this is rejected whenever

$$\frac{1}{\epsilon^2} \sum_{j=1}^{n} (x_j - \bar{x})^2 \geq \chi^2_{a,n-1}$$

where $\chi^2_{a,n-1}$ is tabulated in Trumpler & Weaver, for $(n - 1)$ degrees of freedom and probability 'a'. $\bar{x}$ is the mean radial velocity and ϵ^2 is the expected standard deviation from the mean, found from the standard stars (using the probable error quoted on page 52).

For the data obtained in 1977 :-

$n = 24$ $\quad \bar{x} = -174.6$ km/s

$\sigma = 4.2$ km/s

$\sigma^2 = 17.64$

$$\frac{1}{\sigma^2}\sum_{j=1}^{24}(x_j - \bar{x})^2 = 15.47$$

At $a = 0.10$ $\chi^2_{0.10,23} = 32.01$

Thus the hypothesis that the semi-amplitude of the variation in radial velocity is zero may not be rejected. However, table 3.5 suggests a systematic trend in the 1977 run. Thus it is important to make use of tests that are more sensitive.

In section 2.5 Bartlett's statistic was used to check that the photometric observations were randomly selected from a normal population. This statistic is now applied to the radial velocities using table 3.10.

Table 3.10 Standard deviations and degrees of freedom for radial velocities by year

Year	1952	1953	1960	1961	1963	1964	1971	1976	1977
$\hat{\sigma}_i$	5.7	4.5	4.3	4.1	6.5	5.1	3.0	7.2	3.0
ν_i	6	15	2	4	12	6	9	15	23

$\nu = 91$, $k = 9$

$\chi^2_{obs} = 19.08$

From Conover (1971, page 367) $\chi^2_{8,.99} = 20.09$

$\chi^2_{8,.975} = 17.53$

Thus at any probability level less than 0.99 the hypothesis that the radial velocities were randomly selected from an assumed normal population with comparable variances must be rejected.

At the suggestion of Prof. D. W. N. Stibbs (1979) the median test (Conover, 1971 and section 2.5) was used since this does not require a normal population of data. First the possibility of variability in all 100 radial velocities was examined. They were divided into three groups by H.J.D. 243 4195 - 243 7185 (1952 - 1960), 243 7505 - 243 8625 (1961 - 1970) and 244 1117 - 244 3304 (1971 -1977). The contingency table is shown in table 3.11.

Median = -171.0 km/s

From Conover (1971, page 367)

for 2 degrees of freedom at 0.95 $T = 5.99$

at 0.995 $T = 10.6$

from table 3.11 $T_{ob} = 25.23$

Thus the hypothesis of non-variability of the radial velocity over the time 1952 - 1977 must be rejected.

To investigate the data further (Stibbs, 1979) the radial velocities for 1971 to 1977 were examined, dividing the data into two groups 244 1117 - 244 2975 (1971 - 1976) and 244 3299 - 244 3304 (1977), see table 3.12.

Median = -173.4 km/s

for 1 degree of freedom at 0.95 $T = 3.84$

at 0.995 $T = 7.88$

from table 3.12 $T_{ob} = 11.54$

This most strongly suggests that there is a variation on a time-scale of days, since the combined data for 1971 and 1976 should tend to smooth out any short periods observable in the 1977 data.

Table 3.11 Contingency table for groups 243 4195 - 243 7185, 243 7505 - 243 8625, 244 1117 - 244 3304

	243 4195 - 243 7185	243 7505 - 243 8625	244 1117 - 244 3304	
>	23	13	14	50
≤	3	11	36	50
	26	24	50	100

Table 3.12 Contingency table for groups 244 1117 - 244 2975, 244 3299 - 244 3304

	244 1117 - 244 2975	244 3299 - 244 3304	
>	19	6	25
≤	7	18	25
	26	24	50

Table 3.13 Contingency table for groups 244 3299 - 302, 303 - 304

	299 - 302	303 - 304	
>	11	2	13
≤	1	10	11
	12	12	24

Table 3.14 Contingency table for groups 244 3299 - 302, 303 - 304; using set of common 13 lines

	299 - 302	303 - 304	
>	12	2	14
≤	0	10	10
	12	12	24

Table 3.15 Contingency table for groups of radial velocities from 13 lines, radial velocities from all lines

	13 lines	All lines	
>	14	9	23
≤	10	15	25
	24	24	48

In order to examine the possibility of variability on the time-scale of days, the data for 1977 was tested, although this was regarded as more doubtful due to the expected value in the contingency table falling as low as five. (see table 3.13)

Median = -176.0 km/s

for 1 degree of freedom at 0.95 T = 3.84

at 0.995 T = 7.88

from table 3.13 T_{ob} = 13.59

To confirm this variability on a time-scale of days the Cox & Stuart test for trend (Conover, 1971, p. 130) was used (Stibbs, 1979). The twelve velocities from the nights 244 3303 and 3304 were arranged into pairs and these compared. If the first was less than the second a plus sign was given and if greater a minus sign.

Using the two-tailed test

(-178.5, -178.4)	+
(-181.6, -179.1)	+
(-180.9, -178.6)	+
(-178.1, -178.0)	+
(-178.8, -176.5)	+
(-176.9, -175.5)	+

n = 6 T = 6

If $2\alpha_1$ = 0.04 sets the critical level of acceptance or rejection, from Conover table 3 (page 369)

t = 0

Thus if $T \leq t$ or if $T \geq n - t$ a trend exists.

Since T = n - t a trend in the radial velocities over the two nights does exist with a possibility of 0.96.

To check if the variation is due to wavelength shifts in the

lines caused by an unsuitable value being used, the radial velocities determined from the common set of 13 lines were examined for short term variations, see table 3.14.

Median = -175.1 km/s

for 1 degree of freedom at 0.95 T = 3.84

at 0.995 T = 7.88

from table 3.14 T_{ob} = 17.14

In order to check that the wavelengths did not affect the radial velocity tests for variability, the set containing the velocities from the 13 lines were tested against the set determined from all available lines, see table 3.15.

Median = -175.4 km/s

for 1 degree of freedom at 0.95 T = 3.84

at 0.995 T = 7.88

from table 3.15 T_{ob} = 2.09

Thus at the 0.95 level of confidence it is not possible to reject the hypothesis that the radial velocities determined from a set of 13 lines came from the same population as radial velocities determined from all available lines.

As a final check that the variations were not an instrumental effect caused by taking observations in different years, the radial velocities of HD 120640 (B2III, Houk, 1978) were tested in the same way as the radial velocities of HD 168476 taken on the same observing runs. Table 3.16 shows the radial velocities of HD 120640 taken in May and July 1976 and June 1977. Table 3.17 shows the resulting contingency tables for HD 168476 and HD 120640.

Table 3.16 Radial velocities determined for HD 120640

HJD 244	rad vel	HJD 244	rad vel	HJD 244	rad vel
2913	-9	2974	+2	3300	-7
2913	-2	2975	-7	3302	-8
2970	-4	2975	-4	3302	-5
2970	-2	2975	-7	3302	-1
2972	0	3299	-1	3302	-2
2972	-5	3299	-2	3302	-3
2972	+1	3299	+1	3303	-7
2973	-7	3299	-6	3303	-7
2973	-7	3299	-9	3303	-13
2973	-6	3299	-7	3304	-3
2974	-2	3300	-4	3304	-7
2974	-6			3304	-6

Table 3.17 Contingency tables for data from HD 120640 and HD 168476

244	2913 - 2975	3299 - 3304	
HD 168476			
>	11	9	20
≤	5	15	20
	16	24	40
HD 120640			
>	9	8	17
≤	7	11	18
	16	19	35

	HD 168476	HD 120640
median	-174.8	-5.1
T_{ob}	3.75	0.70
z	1.65	0.23
P	~ 0.95	0.59

P was determined by calculating a parameter 'z' (Stibbs, 1979) and examining tables (Conover p. 366) where $z = w_p$.

$$z = \frac{(\nu^{-1}\chi^2)^{1/3} - (1 - 2/9\nu)}{\sqrt{2/9\nu}}$$

where $T_{ob} = \chi^2$, ν is the number of degrees of freedom (= 1 here).

The variation in radial velocity is therefore not an instrumental effect or an effect of selecting unsuitable wavelengths for the lines. Use of a period-finding program written by Morbey (1973) of Dominion Astrophysical Observatory and lent by Dr. R. W. Hilditch, failed to show any periods either on a short time-scale or on a long time-scale, so that it suggests that the period may not be a simple one. The technique of Lucy (1976) found sixteen peiods for α Cygni, ranging from 6.9 to 100.8 days. This may be a useful technique for HD 168476 but α Cygni was a much brighter star. 447 radial velocities were accurately determined for it, including a set of 144 radial velocities determined in one year (1931). This is a considerably larger sample for their harmonic analysis than is available for HD 168476 with a total of 100 radial velocities, with a maximum of 24 taken in one year (1977). Obviously many more radial velocities of HD 168476 must be obtained over a period of years for this technique of harmonic analysis to be successfully applied.

4 THE ULTRA-VIOLET SPECTRUM

4.1 Observations

The International Ultraviolet Explorer (IUE) satellite and its in-flight performance have been described in Boggess et al. (1978a) and Boggess et al. (1978b) respectively. Low resolution spectra of HD 168476 were taken by Dr. P. M. Gondhalekar as part of the high-priority programme, with both short wavelength and long wavelength cameras. The wavelength regions covered were between 1150A and 3000A, the long wavelength end being cut off by a telemetry fault. Dr. A. E. Lynas-Gray and the writer identified ions similar to those found in the spectra obtained from ground based observations and features were noted which might be due to C I, N I, Si I and S I (Lynas-Gray, Walker & Hill, 1979). These features may have been formed in a cool outer shell. At Lyman-α there was only a weak emission feature, most probably geocoronal in origin.

One high-resolution spectrum was obtained of HD 168476, exposure 120 minutes, by Lynas-Gray and the writer on 1978 June 14 commencing at 03:36:29 from the Villafranca satellite tracking station of the European Space Agency. The third file of the provided magnetic tape was used for the analysis and this contained an image which had been corrected geometrically and photometrically, with the background removed and calibrated as IUE flux units. A program was written to plot the spectral orders using the IBM 360/44 computer of the University of St. Andrews. Preliminary identifications of possible lines were made on these plots. The spectra were then displayed on a video terminal using the University of St. Andrews Observatory Nova and Honeywell 316

computers under FORTH control (with the aid of R. Stapleton, P. Bunclark, G. Stewart). These spectra had been smoothed using the running mean of five points, to reduce noise. For the lines indicated on the screen the wavelengths were printed out for later identification and the lines noted on the plots. For one order (94) the numbers obtained were incorrect due to a computer error and one order (92) was not measured (by mistake), so that for these two orders (2440A to 2475A and 2496A to 2529A) the wavelengths of the lines were measured directly from the unsmoothed plots.

The spectrum was underexposed so that only orders 104 and 101 to 72 were examined; those orders covered 2207A to 2235A and 2270A to 3233A. At the longer wavelengths, comparison with ground based observations analysed in chapter 5 was possible. Using a radial velocity of -171 km/s for HD 168476 (see chapter 3) a correction was made to each order to determine the stellar wavelengths. This correction varied from 1.3A to 1.8A on the orders used. Data from Morton (1979) were used to identify lines connected with the ground state, both for the interstellar and the stellar lines. Additional data were taken from Moore (1950), Moore (1965, 1967, 1970, 1975) for stellar wavelengths. Line wavelengths due to interstellar molecules were found from Jenkins et al. (1973) and Snow (1976).

4.2 Results

Table 4.2 shows the identifications made from the spectrum. The multiplet number of the line is shown in brackets. These lines represent only a small number of the lines found in the spectrum. It is suspected that some of the lines will be identified

as high multiplet numbers of the transition elements (e.g. Cr II (325)) but since this was uncertain the identifications were not always inserted. The multiplet tables are obviously incomplete in the ultraviolet for most elements. Hill (1962) uses a formula from Fowler (1922) to obtain He I line wavelengths. This formula was used to find ultraviolet wavelengths for He I, with several iterations from the expected series limit at 2601A. The results are shown in table 4.1. The formula used was :-

$$\tilde{\nu} = A - \frac{R}{(n + \mu + \frac{a}{n-1})^2}$$

where $\tilde{\nu}$ is the wavenumber of the line

A is the wavenumber of the series limit

R is the Rydberg constant for helium

n is the principal quantum number

a, μ are constants, calculated from the wavenumbers of two known members of the series.

Table 4.1 Ultraviolet wavelengths of He I

n	λ_{ob}	λ_{calc}	n	λ_{ob}	λ_{calc}
4	3187.74	3188.23	15		2633.4
5	2945.10	2945.27	16		2629.3
6	2829.07	2829.16	17		2625.8
7	2763.8	2763.8	18		2623.0
8	2723.2	2723.2	19		2620.6
9	2696.1	2696.1	20		2618.5
10	2677.1	2677.1	21		2616.7
11	2663.3	2663.3	22		2615.2
12	2652.8	2652.9	23		2613.9
13	2644.8	2644.8	24		2612.7
14		2638.5	∞		2599.7

Using $n = 3$ 3888.65A

$n = 4$ 3187.74A

$a = 3.85 \times 10^{-3}$

$b = -7.03 \times 10^{-2}$

In table 4.1 the observed wavelengths were taken from Moore (1950), and from n = 11 the wavelengths were taken from Harrison (1969).

In table 4.2 the first column gives the wavelength identified on the spectrum, the second column the wavelength corrected for the radial velocity. An estimate of the intensity of the line is given in column 3. Then follows any identification made for the rest wavelength in the interstellar medium (I.S. ID) and any stellar identification made. The order of the spectrum is also given (ORDR). In all 391 lines were identified either with stellar or interstellar wavelengths.

Table 4.2

ULTRAVIOLET ABSORPTION LINE WAVELENGTHS

REST	STAR	I	I.S. ID	STELLAR ID		ORDR
2207.3	2208.6	s		2208.61 Ca II (8)		104
2208.2	2209.5	s	2207.98 Si I (3)			
2209.3	2210.6	s		2210.89 Si I (3)		
2210.1	2211.4	s		2211.74 Si I (3)		
2211.2	2212.5	s	2211.32 Si I (3)			
2215.7	2217.0	m		2216.67 Si I (3)		
2216.8	2218.1	s	2216.67 Si I (3)	2218.06 Si I (3)		
2218.1	2219.4	s		2218.92 Si I (3)		
2218.8	2220.1	s	2218.31 Si I (3)			
2233.7	2235.0	s		2235.21 N II (18.02)		
2275.4	2276.7	s	2275.47 Ca I (6)			101
2279.4	2280.7	m		2281.00 P II (6)		
2283.7	2285.0	m		2285.11 P II (7)		
2285.9	2287.2	s		2286.69 N II (16.02,20.02)		
2287.6	2288.9	s		2288.44 N II (16.02,20.02)		
2288.9	2290.2	s		2290.26 N II (20.02)		
2290.2	2291.5	s		2291.65 N II (16.02)		
2292.0	2293.3	m		2293.32 N II (20.02)		
2295.8	2297.1	s		2297.28 Ni II (11)		
2298.4	2299.7	s		2298.95 Mn II (2)	*	
2298.9	2300.2	s	2298.95 Mn II (2)			
2299.6	2300.9	s	2299.84 SiO			
2301.6	2302.8	m		2302.98 Ni II (11)	*	
2303.6	2304.9	m		2305.00 Mn II (2)	*	
2305.0	2306.3	w	2305.00 Mn II (2)			100
2306.8	2308.2	m		2307.86 Si II (18.02)		
2311.2	2312.5	m	2310.95 Ni I (10)			
2312.5	2313.8	m	2312.34 Ni I (10)			
2314.4	2315.7	m	2313.98 Ni I (10)	2316.03 Ni II (11)		
				2316.76 N II (16)		
2318.2	2319.5	m		2319.94 N II (16)		
2320.4	2321.7	m	2320.03 Ni I (9)	2321.65 N II (16)	*	
2321.9	2323.2	w	2321.38 Ni I (9)	2323.50 C II (0.01)		99
2323.5	2324.8	m	2323.50 C II (0.01)	2324.69 C II (0.01)	*	
				2325.16 N II (16)		
2323.9	2325.2	m		2325.40 C II (0.01)		
2324.7	2326.0	s		2324.69 C II (0.01)		
2325.4	2326.7	w		2326.93 C II (0.01)		
2325.8	2327.1	w	2325.40 C II (0.01)	2327.39 Fe II (3)		
			2325.79 Ni I (9)			
2326.5	2327.8	m	2326.93 C II (0.01)	2328.12 C II (0.01)		
				2328.51 Si II (0.01)		
2328.0	2329.3	w	2328.12 C II (0.01)			
2328.7	2330.0	m	2328.51 Si II (0.01)		*	
2331.0	2332.3	m		2332.80 Fe II (3)		

REST	STAR	I	I.S. ID	STELLAR ID		ORDR
2332.7	2334.0	m	2332.80 Fe II (3)			
2333.4	2334.7	m		2334.51 Si II (0.01)		
				2334.59 Ni II (20)		
2334.4	2335.7	w	2334.51 Si II (0.01)			
2337.2	2338.5	m		2338.01 Fe II (3)		
2337.8	2339.1	m	2338.01 Fe II (3)			
2341.8	2343.1	m		2343.50 Fe II (3)		
2342.8	2344.1	m		2344.20 Si II (0.01)	*	
				2344.28 Fe II (3)		
2343.6	2344.9	s	2343.50 Fe II (3)			
2344.8	2346.1	m	2344.20 Si II (0.01)		*	
			2344.28 Fe II (3)			
2347.3	2348.6	m		2348.30 Fe II (3)	*	
2348.4	2349.7	m	2348.30 Fe II (3)			98
			2348.61 Be I (1)			
2348.9	2350.2	m		2350.17 Si II (0.01)		
2350.4	2351.7	m	2350.17 Si II (0.01)			
2358.0	2359.3	m		2359.11 Fe II (3)		
2358.5	2359.8	m	2359.11 Fe II (3)			
2363.3	2364.6	m		2364.73 Cr I (1)		
				2364.83 Fe II (3)		
2364.7	2366.0	m	2364.73 Cr I (1)	2365.91 Cr I (1)		
			2364.83 Fe II (3)	2366.05 Si II (18.01)		
2365.7	2367.1	m	2365.91 Cr I (1)	2366.81 Cr I (1)	*	
				2366.86 Fe II (2)		
				2366.97 Si II (18.01)		
2367.0	2368.3	m	2366.81 Cr I (1)		*	
			2366.86 Fe II (2)			
			2367.05 Al I (4)			
2370.5	2371.9	w		2372.12 Mn I (2)		97
2372.0	2373.4	m	2372.07 Al I (3)	2373.73 Fe II (1)	*	
			2372.12 Mn II (2)			
2373.0	2374.3	m		2374.26 Si II (18.01)		
2373.5	2374.8	m	2373.18 Al I (4)	2374.82 Ca I (1)	*	
			2373.73 Fe II (1)			
2374.7	2376.1	m	2374.82 Ca I (1)		*	
2376.1	2377.5	m		2377.18 Mn I (2)		
2377.7	2379.0	m	2377.18 Mn I (2)		*	
			2378.40 Al I (3)			
2380.5	2381.9	m	2380.48 Ca I (6)			
			2380.76 Fe II (3)			
2380.9	2382.3	m		2382.03 Fe II (2)		
2381.7	2383.1	s		2383.06 Fe II (2)		
2382.6	2384.0	m	2382.35 Fe II (2)	2384.05 Mn I (2)		
2384.3	2386.2	m	2384.05 Mn I (2)			
			2384.39 Ni I (10)			
2385.7	2387.1	m		2386.78 N II (18.06)		
2386.8	2388.2	s		2388.23 N II (18.06)		
				2388.63 Fe II (2)		
2388.2	2389.6	m	2388.63 Fe II (2)			

REST	STAR	I	I.S. ID	STELLAR ID		ORDR
2389.8	2391.2	m		2390.87 N II (18.06)	*	
2392.8	2394.2	m		2394.52 Ni II (20)		
2394.1	2395.5	s		2395.54 Fe II (2)	*	
2395.4	2396.8	m	2395.54 Fe II (2)			96
2396.9	2398.2	m		2398.56 Ca I (5)	*	
2397.9	2399.3	s		2399.24 Fe II (2)	*	
2398.5	2399.9	s	2398.56 Ca I (5)			
2399.6	2401.0	s	2399.24 Fe II (2)			
2402.9	2404.3	s		2404.68 Fe II (2)	*	
2404.9	2406.3	s	2404.68 Fe II (2)	2406.66 Fe II (2)		
2406.8	2408.2	s	2406.66 Fe II (2)			
2407.7	2409.1	m	2407.25 Ca I (6)			
2409.2	2410.6	m		2410.52 Fe II (2)		
2409.9	2411.3	m		2411.06 Fe II (2)		
2411.4	2412.8	m	2411.06 Fe II (2)			
			2411.62 Co I (6)			
2412.3	2413.7	m		2413.31 Fe II (2)		
2413.1	2414.5	m	2413.31 Fe II (2)			
2415.1	2416.5	m		2416.13 Ni II (20)	*	
2433.0	2434.4	s		2435.16 Si I (45)		95
2437.6	2439.0	m		2438.77 Si I (2)		
2438.5	2439.9	m	2438.77 Si I (2)			
2442.0	2443.4	w		2443.36 Si I (2)		
2443.7	2445.1	s	2443.36 Si I (2)			94
2446.4	2447.8	m		2447.71 Fe I (9)	*	
2447.4	2448.8	m	2447.71 Fe I (9)		*	
2450.8	2452.2	m		2452.12 Si I (2)	*	
2452.3	2453.7	m	2452.12 Si I (2)		*	
2460.3	2461.8	m		2461.27 N II (23)		
2462.7	2464.1	m	2462.65 Fe I (9)			
2473.2	2474.6	s		2474.22 Ti II (2)	*	
2474.8	2475.2	m	2474.22 Ti II (2)		*	
2476.5	2477.9	m		2478.23 Ti II (2)		93
2478.1	2479.5	m	2478.23 Ti II (2)			
2483.4	2484.8	w	2483.27 Fe I (9)			
2489.4	2490.8	m		2490.28 N II (18.01,20)		
2497.2	2498.6	m	2497.40 B I (1)		*	
2499.3	2500.7	m		2500.93 Si II (18)	*	
2500.3	2501.6	m		2501.97 Si II (18)	*	
2501.0	2502.4	m	2501.13 Fe I (7)		*	
2503.7	2505.0	m		2504.71 Si II (17.03)	*	
2506.5	2507.9	m	2506.90 Si I (1)		*	
2507.5	2508.9	m		2509.11 C II (14)	*	
2510.5	2511.9	s		2511.71,12.03 C II (14)		92
2511.7	2513.1	m	2512.18 Na I (5)			
2513.0	2514.4	m		2514.32 Si I (1)		
2513.4	2514.8	m		2514.63 V II (21)		
2514.8	2516.2	m	2514.32 Si I (1)			
2516.6	2518.0	w	2516.11 Si I (1)	2518.29 Cr II (308)		
2517.6	2519.0	m		2519.20 Si I (1)		

REST	STAR	I	I.S. ID	STELLAR ID		ORDR
2518.7	2520.1	s		2520.22 N II (19)		
2519.3	2520.7	m	2519.20 Si I (1)	2520.79 N II (19)		
2521.4	2522.8	m		2522.31 N II (19)	*	
2521.8	2523.2	w		2523.24 Cr II (308)		91
2523.4	2524.8	m	2522.85 Fe I (7)	2524.49 N II (19)	*	
2524.4	2525.8	m	2524.11 Si I (1)	2525.62 Ti II (4)	*	
2525.2	2526.6	m		2526.17 N II (19)	*	
2526.5	2527.9	m		2527.90 V II (50)	*	
2527.7	2529.1	m		2528.66 V II (50)	*	
2528.1	2529.5	m	2528.51 Si I (1)			
2530.1	2531.5	m		2531.27 Ti II (4)		
2533.7	2535.1	m		2534.64 Ti II (4)		
2537.0	2538.4	s		258.31 Cr II (308)		
2539.0	2540.4	m		2540.86 Sc II (1)		
2539.9	2541.3	w		2541.40 Ca I (4)		
2541.2	2542.6	m	2540.86 Sc II (1)			
			2541.40 Ca I (4)			
2543.5	2544.9	m	2543.85 Na I (4)	2545.28 Sc II (1)		
2545.3	2546.7	w	2545.28 Sc II (1)			
2551.3	2552.8	m		2552.38 Sc II (1)		90
2555.8	2557.2	m	2555.84 Sc II (1)		*	
2558.4	2559.8	m		2560.26 Sc II (1)	*	
2560.3	2561.7	s	2560.26 Sc II (1)		*	
2561.8	2563.2	s		2563.23 Sc II (1)	*	
2563.6	2565.1	w	2563.23 Sc II (1)			
2567.7	2569.2	m	2567.98 Al I (3)			
2574.9	2576.4	s	2575.18 Al I (2)	2576.11 Mn II (1)		
2576.0	2577.5	s	2576.11 Mn II (1)			
2577.1	2578.6	m		2578.81 Mn II (89)	*	
2577.7	2579.2	s		2579.12 Cr II (262)		89
2584.0	2585.5	s		2585.88 Fe II (1)	*	
2585.9	2587.4	s	2585.88 Fe II (1)		*	
2589.3	2590.8	m		2590.94 N II (18)		
2589.9	2591.4	m		2591.43 Mn II (36)		
2591.6	2593.1	m		2593.73 Mn II (1)		
2593.2	2594.7	m	2593.73 Mn II (1)			
			2593.88 Na I (3)			
2596.9	2598.4	w		2598.37 Fe II (1)		
2597.4	2598.9	m		2599.40 Fe II (1)		
2599.0	2600.5	s	2599.40 Fe II (1)			
2603.1	2604.6	w		2604.42 Si II (15)		
2603.6	2605.1	m		2605.70 Mn II (1)		
2605.1	2606.6	s	2605.70 Mn II (1)	2606.08 Si II (15)		
				2607.01 Fe II (1)		
2607.2	2608.7	w	2607.01 Fe II (1)		*	
2610.1	2611.6	m		2611.23 Sc II (3)	*	
				2611.87 Fe II (1)		
2612.0	2613.5	s	2611.87 Fe II (1)	2613.82 Fe II (1)	*	
2616.1	2617.6	s		2617.66 Ca I (3)	*	
2617.2	2618.7	w	2617.62 Fe II (1)	2618.5 He I		88

REST	STAR	I	I.S. ID	STELLAR ID		ORDR
			2617.66 Ca I (3)			
2618.4	2619.9	m		2619.80 Ti I (5)	*	
2618.9	2620.4	m		2620.41 Fe II (1)		
				2620.53 He I		
2620.0	2621.5	m	2619.80 Ti I (5)	2621.67 Fe II (1)		
			2620.41 Fe II (1)			
2621.8	2623.3	w	2621.67 Fe II (1)	2622.95 He I		
2623.7	2625.2	s		2625.66 Fe II (1)		
2624.5	2626.0	m	2625.66 Fe II (1)	2625.81 He I		
2626.5	2628.0	m		2628.29 Fe II (1)		
2627.8	2629.3	m		2629.1 S II (11)		
				2629.23 He I		
2628.2	2629.7	m	2628.29 Fe II (1)			
2629.4	2630.9	m		2631.14 Fe II (1)		
2631.4	2632.9	w	2631.14 Fe II (1)	2632.37 Ti I (5)		
			2632.37 Ti I (5)	2633.38 He I		
2636.5	2638.0	m		2638.46 He I		
2639.6	2641.1	w		2641.09 Ti I (5)		87
2641.0	2642.5	w	2641.09 Ti I (5)			
2643.4	2644.9	m		2644.80 He I	*	
2644.3	2645.8	m	2644.25 Ti I (5)	2645.70 Ne I	*	
				2646.08 Ti II (29)		
2646.6	2648.1	m	2646.63 Ti I (5)		*	
2651.6	2653.1	m		2652.85 He I		
2652.7	2654.2	m	2652.48 Al I (1)			
2659.7	2661.2	w		2660.79 Mg II (4)		
2660.6	2662.1	w	2660.39 Al I (1)	2661.73 Cr II (8)		
2661.5	2663.0	m		2663.27 He I		
2662.6	2664.1	m		2663.67 Cr II (8)		
2666.9	2668.4	m		2668.71 Cr II (8)		
2667.7	2669.2	m		2669.17 Al II (1)		
2668.4	2669.9	m		2670.0 S II (11)	*	
2670.7	2672.2	m		2672.01 V II (3)	*	
2673.4	2674.9	m		2675.44 Ne I (13)		86
2675.3	2676.7	m		2677.14 He I	*	
2676.9	2678.4	m		2678.11 V II (3)		
				2678.79 Cr II (7)		
2680.3	2681.7	m	2680.37 Na I (2)	2682.21 Si II (20)		
2681.7	2683.2	m		2682.99 V II (3)		
2682.7	2684.2	s	2682.99 V II (3)			
2686.2	2687.7	m		2687.96 V II (3)		
2687.0	2688.5	m		2688.72 V II (3)		
2688.8	2690.3	w		2690.56 V II (3)		
2694.1	2695.6	w		2696.10 He I		
2697.0	2698.5	s		2698.40 Cr II (7)		
2699.1	2700.6	m		2700.94 V II (1)		
2704.8	2706.3	m		2706.17 V II (1)	*	
2708.2	2709.7	m		2709.84 N II (22)	*	
2714.3	2715.9	s		2715.67 V II (1)		85
2717.0	2718.6	w	2716.92 CaII			

REST	STAR	I	I.S. ID	STELLAR ID		ORDR
2717.7	2719.3	m		2719.03 Fe I (5)		
				2719.39 Ti II (13)		
2719.0	2720.6	w	2719.03 Fe I (5)	2720.90 Fe I (5)		
2720.0	2721.6	m		2721.64 Ca I (2)		
2721.1	2722.7	m	2720.90 Fe I (5)	2722.25 Si II (19)		
2721.5	2723.1	m	2721.64 Ca I (2)	2723.19 He I		
				2723.22 V II (1)		
2722.7	2724.3	m	2723.58 Fe I (5)			
2725.6	2727.2	s		2726.70 Si II (19)		
2726.8	2728.4	m		2728.64 V II (1)		
2730.0	2731.6	w		2731.90 Cr I (7)		
2732.1	2733.7	m		2733.91 V II (1)		
2734.8	2736.4	m		2736.46 Cr I (7)		
2735.3	2736.9	m		2737.31 Fe I (5)	*	
2737.7	2739.3	s	2737.31 Fe I (5)		*	
2738.0	2739.6	s		2739.72 V II (1)		
2741.4	2743.0	s	2741.19 Li I (1)	2742.41 Fe I (5)	*	
2743.0	2744.6	m	2742.41 Fe I (5)			84
2744.8	2746.4	s		2746.91 C II (15)		
2747.3	2748.9	s		2748.98 Cr II (6)		
2748.9	2750.5	m		2750.14 Fe I (5)		
				2750.72 Cr II (6)		
2749.8	2751.4	m	2750.14 Fe I (5)	2751.70 Ti II (31)		
2754.9	2756.5	w		2756.33 Fe I (5)		
2756.8	2758.4	w	2756.33 Fe I (5)			
2760.5	2762.1	m		2762.58 Cr II (6)		
2761.7	2763.3	m		2763.80 He I		
2764.3	2765.9	m		2766.56 Cr II (6)		
2765.7	2767.3	m		2767.28 Ne I	*	
2772.9	2774.5	m	2772.11 Fe I (5)			83
2773.5	2775.1	m		2775.05 Ne I		
2788.9	2790.5	s		2790.77 Mg II (3)		
2793.2	2794.8	s		2794.82 Mn I (1)		
2793.9	2795.5	s		2795.52 Mg II (1)		
2796.0	2797.6	s	2794.82 Mn I (1)	2797.99 Mg II (3)		
			2795.53 Mg II (1)	2798.27 Mn I (1)		
2798.9	2800.5	m	2798.27 Mn I (1)	2799.22 N II (21)	*	
2799.4	2801.0	w		2801.08 Mn I (1)		
2801.2	2802.8	s	2801.08 Mn I (1)	2802.70 Mg II (1)	*	
2802.6	2804.2	s	2802.70 Mg II (1)	2804.07 C II (48)	*	
2803.7	2805.3	m		2805.00 Ti II (25)		82
				2805.20 C II (48)		
2808.1	2809.7	w		2810.28 Ti II (25)		
2814.2	2815.8	m		2816.19 Al II (7)		
2816.1	2817.7	m		2817.84 Ti II (25)		
2820.4	2822.0	m		2822.17 Sc II (5)		
2823.9	2825.5	m		2825.44 Ne I		
2825.6	2827.2	m		2826.69 Sc II (5)		
2826.9	2828.5	m		2828.15 Ti II (25)		
				2828.80 Ti II (24,25)		

REST	STAR	I	I.S. ID	STELLAR ID		ORDR
				2829.07	He I (12)	
2834.0	2835.6	m		2835.23	Ne I	*
				2835.63	Cr II (5)	
2834.8	2836.4	m		2836.71	C II (13)	*
2835.8	2837.4	s		2837.60	C II (13)	*
2841.5	2843.1	m		2843.24	Cr II (5)	*
2846.0	2847.6	m		2847.73	S II (10)	81
2847.7	2849.3	m		2849.83	Cr II (5)	
2849.6	2851.2	m		2851.09	Ti II (16)	
				2851.35	Cr II (82)	
2851.7	2853.3	m	2852.12 Mg I (1)			
2854.2	2855.8	m		2855.67	Cr II (5)	
2858.9	2860.5	m		2860.92	Cr II (5)	
2860.6	2862.2	m		2862.07	Ne I	
				2862.57	Cr II (5)	
2863.2	2864.8	m		2865.10	Cr II (5)	
2864.8	2866.4	m		2866.72	Cr II (5)	
2867.2	2868.8	m		2868.73	Ti II (5)	
2871.3	2872.9	m		2872.66	Ne I	*
2874.7	2876.3	m		2876.24	Cr II (5)	*
2876.5	2878.1	m		2878.45	Cr II (5)	
2879.9	2881.5	w		2881.01	S II (10)	80
				2881.58	Si I (43)	
2885.6	2887.2	m		2887.46	Si II (17.01)	
2887.5	2889.1	m		2888.92	Ti II (5)	
2889.1	2890.6	m		2891.05	Ti II (5)	
2890.6	2892.2	m		2892.28	V II (12)	
2892.2	2893.8	m		2893.31	V II (12)	
2902.3	2903.9	m		2904.28	Si II (17)	
2904.2	2905.8	m		2905.69	Si II (17)	
2907.2	2908.9	m		2908.81	V II (12)	*
2908.3	2909.9	m		2909.91	Ti II (1)	
2909.6	2911.2	m	2909.91 Ti II (1)	2911.46	Ne I	*
2911.6	2913.3	m	2912.16 Fe II (1)	2913.08	Ti II (1)	*
				2913.17	Ne I (12)	
2913.3	2914.9	m	2913.08 Ti II (1)			*
2922.4	2924.1	w		2924.30	V II (10)	79
2926.6	2928.3	s		2928.63	Mg II (2)	
2928.7	2930.4	m		2930.80	V II (12)	
2929.3	2931.0	w	2929.01 Fe I (1)			
2931.0	2932.7	m		2932.72	Ne I (14)	
				2933.05	Mn II (5)	
2932.3	2934.0	m		2933.53	Ti I (1)	
2933.0	2934.7	m	2933.53 Ti I (1)	2934.72	Mn II (50)	
2934.7	2936.4	s		2936.50	Mg II (2)	
2936.4	2938.1	w	2936.90 Fe I (1)			
2937.4	2939.1	s	2937.29 Ti I (1)	2939.30	Mn II (5)	
2939.7	2941.4	m		2941.34	Fe I (1)	
				2941.37	V II (10)	
				2941.96	Ti I (1)	

REST	STAR	I	I.S. ID	STELLAR ID	ORDR
				2941.99 Ti II (26)	
2941.0	2942.7	m	2941.34 Fe I (1)		
2942.0	2943.7	w	2941.96 Ti I (1)		
2943.0	2944.7	m		2944.57 V II (10)	
2943.2	2944.9	w		2945.10 He I (11)	
2944.0	2945.7	m		2945.47 Ti II (26)	*
2945.7	2947.4	m		2947.30 Ne I (11)	*
				2947.88 Fe I (1)	
2947.3	2948.9	m	2947.88 Fe I (1)	2949.20 Mn II (5)	*
				2941.37 V II (10)	
2952.0	2953.7	m		2953.77 Fe II (60)	78
				2953.94 Fe I (1)	
2952.5	2954.2	w		2954.76 Ti II (34)	
2956.0	2957.7	w		2957.37 Fe I (1)	
2956.5	2958.2	w	2956.80 Ti I (1)		
2957.5	2959.2	w	2957.37 Fe I (1)	2958.98 Ti II (34)	
2963.9	2965.6	s		2965.19 Mg II (7)	
				2965.26 Fe I (1)	
				2965.86 Sc I (11)	
2966.5	2968.2	w	2965.86 Sc I (11)	2967.87 Mg II (7)	
			2966.90 Fe I (1)	2968.23 Ti I (29)	
2967.9	2969.6	w	2967.22 Ti I (1)	2969.02 Mg II (6)	
2968.3	2970.0	m	2968.23 Ti I (29)		
2968.6	2970.3	m		2970.11 Fe I (1)	
				2970.35 Si I (42)	
				2970.37 Ti I (29)	
				2970.51 Fe II (60)	
2969.7	2971.4	m		2971.70 Mg II (6)	
2970.8	2972.5	m		2970.11 Fe I (1)	
			2970.37 Ti I (29)		
2971.7	2973.4	m		2973.19 Fe I (1)	
2972.6	2974.3	w		2974.01 Sc I (11)	
				2974.71 Ne I (10)	
2973.8	2975.5	w	2973.19 Fe I (1)	2975.52 Ne I	
2974.2	2975.9	w	2974.01 Sc I (11)		
2978.9	2980.6	m		2980.75 Sc I (11)	
2980.0	2981.7	m		2981.65 Ni I (24)	
2980.6	2982.3	m	2980.75 Sc I (11)	2982.66 Ne I (9)	
2982.2	2983.9	m	2981.65 Ni I (24)	2983.57 Fe I (9)	
2983.3	2985.0	s	2983.29 Ti I (29)		*
			2983.57 Fe I (9)		
2984.6	2986.3	m		2986.47 Cr I (11)	77
2985.9	2987.6	m	2985.46 Ti I (29)		*
2987.4	2989.1	w		2988.95 Sc I (11)	
2988.1	2989.8	w	2988.95 Sc I (11)		
2990.6	2992.3	m		2992.43 Ne I (8)	
2992.7	2994.4	m	2992.60 Ni I (25)	2994.43 Fe I (9)	
2999.0	3000.7	w		3000.38 Cr I (11)	
				3000.95 Fe I (9)	
3000.6	3002.3	s	3000.89 Ti I (29)	3002.49 Ni I (24)	

REST	STAR	I	I.S. ID	STELLAR ID	ORDR
			3000.95 Fe I (9)		
3002.3	3004.0	m	3002.49 Ni I (24)		
			3002.73 Ti I (29)		
3005.1	3006.8	w		3006.83 N II (18)	
3006.4	3008.1	w		3008.14 Fe I (9)	
3007.8	3009.5	w	3008.14 Fe I (9)		
3011.4	3013.1	m		3012.96 Ne I	
3013.5	3015.2	m		3015.36 Sc I (10)	
3015.6	3017.3	w	3015.36 Sc I (10)	3017.35 Ne I	
3016.1	3017.8	m		3017.63 Fe I (9)	
3017.8	3019.5	m	3017.63 Fe I (9)	3019.35 Sc I (10)	
3019.2	3020.9	w	3019.35 Sc I (10)	3020.75 Fe I (9)	
3019.8	3021.5	m		3021.56 Cr I (27)	
3020.7	3022.4	m	3020.75 Fe I (9)		
3022.2	3023.9	m		3023.67 N II (35)	*
3024.7	3026.4	m		3025.84 Fe I (9)	*
3026.2	3027.9	m	3025.84 Fe I (9)		76
3029.0	3030.7	m		3030.77 Sc I (10)	
3030.7	3032.4	w	3030.77 Sc I (10)	3032.44 Ni II (3)	
3036.2	3037.9	m		3037.39 Fe I (9)	
3037.4	3039.1	m	3037.39 Fe I (9)		
3043.3	3045.0	w	3043.34 V I (17)		
3044.0	3045.7	w		3045.95 Ne I	
3044.9	3046.6	w	3044.94 V I (17)		
3045.6	3047.3	w		3047.61 Fe I (9)	
3051.1	3052.8	m	3050.82 Ni I (25)		
3051.6	3053.3	w	3052.19 V I (15)		
3053.7	3055.4	m	3053.65 V I (17)		
3054.5	3056.2	m	3054.32 Ni I (25)		
3057.4	3059.1	w	3057.40 Ti I (5)	3059.09 Fe I (9)	
			3057.64 Ni I (24)		
3060.1	3061.8	s	3059.09 Fe I (9)		
			3059.74 Ti II (5)		
			3060.93 V I (15)		
3063.2	3064.9	w		3064.62 Ni I (24)	
3064.6	3066.3	m	3064.46 V I (17)	3066.27 Ti II (5)	
			3064.62 Ni I (24)		
3066.5	3068.3	m	3066.27 Ti II (5)		75
			3066.40 V I (15)		
3069.6	3071.4	m	3069.65 V I (15)		
3070.7	3072.5	m		3072.60 Ti II (5)	
3073.1	3074.9	m	3072.60 Ti II (5)	3075.23 Ti II (5)	
			3073.82 V I (15)		
3075.3	3077.1	m	3075.23 Ti II (5)	3076.97 Ne I	
3076.6	3078.4	m		3078.65 Ti II (5)	
3078.3	3080.1	m	3078.65 Ti II (5)		
3081.4	3083.2	m	3080.15 V I (15)		
			3080.76 Ni I (24)		
3085.9	3087.7	m		3088.03 Ti II (5)	
3087.5	3089.1	w	3088.03 Ti II (5)		

REST	STAR	I	I.S. ID	STELLAR ID	ORDR
3090.9	3092.7	m	3090.40 V I (15)		
3091.4	3093.2	m	3091.45 V I (15)		
3095.3	3097.1	w		3096.77 Sc II (6)	
3101.4	3103.2	m	3101.55 Ni I (25)		
3103.6	3105.4	s		3104.76 Mg II (6)	
3108.1	3109.9	m		3109.92 Ti II (55)	74
3109.8	3111.6	w		3111.61 Fe III (8)	
3112.5	3114.3	s		3114.49 Fe II (82)	
3113.5	3115.3	m		3115.65 Cr II (46)	
3114.5	3116.3	s		3116.59 Fe II (82)	
3116.6	3118.4	m		3118.65 Cr II (5)	
3118.1	3119.9	m	3118.25 Co I (11)	3119.80 Ti II (67)	
				3020.37 Cr II (5)	
3121.8	3123.6	m	3121.57 Co I (11)	3123.29 Ca II (10)	
			3121.60 Ti II (4)		
3122.8	3124.6	m		3124.98 Cr II (5)	
3127.0	3128.8	w		3128.70 Cr II (5)	
3128.5	3130.3	m		3130.80 Ti II (4)	
3129.8	3131.6	m		3131.54 Cr II (53,55)	
3131.1	3132.9	m	3130.63 Be II (1)	3133.10 Sc II (39)	
			3130.80 Ti II (4)		
3134.6	3136.4	m	3134.11 Co I (25)	3136.68 Cr II (5)	
3138.0	3139.8	m		3139.91 Cr II (54)	
3143.4	3145.2	m	3143.76 Ti II (4)		
3150.4	3152.2	m		3152.25 Ti II (10)	73
3151.9	3153.7	s		3154.20 Ti II (10)	
3153.8	3155.6	m		3155.67 Ti II (10)	
3155.4	3157.2	m		3157.52 Cr II (93)	
3156.6	3158.4	m	3157.40 Ti II (4)	3158.03 Cr II (70)	
				3158.87 Ca II (4)	
3160.0	3161.8	w		3161.95 Fe II (7)	
3160.6	3162.4	m		3162.57 Ti II (10)	
3161.8	3163.6	m		3163.09 Fe II (7)	
3163.6	3165.4	w		3165.62 C II (9)	
3164.2	3166.0	m		3166.22 Fe II (79)	
3165.7	3167.5	w		3167.85 Fe II (66)	
3166.4	3168.2	m		3168.52 Ti II (10)	
3167.5	3169.3	w		3169.20 Cr II (123)	
3168.4	3170.2	w		3170.34 Fe II (6)	
3170.8	3172.6	m		3172.79 Mg II (13)	
3174.9	3176.7	m		3176.27 He I	
3175.6	3177.4	m		3177.53 Fe II (82)	
3179.5	3181.3	s		3181.43 Cr II (9)	
3180.8	3182.6	m		3182.57 Ti II (122)	
3183.0	3184.8	s		3184.09 Ti II (3)	
				3185.29 He I	
3184.7	3186.5	m	3184.09 Ti II (3)	3186.74 Fe II (6)	
3185.2	3187.0	s	3185.40 V I (14)		
3186.0	3187.8	s	3186.45 Ti I (27)	3187.74 He I (3)	
3194.4	3196.2	m		3196.07 Fe II (7)	72

REST	STAR	I	I.S. ID	STELLAR ID	ORDR
3195.2	3197.0	s		3196.74 He I	
				3197.04 Cr II (9)	
3198.3	3200.1	s	3198.01 V I (14)		
3198.7	3200.5	s		3200.45 Cr II (114)	
3200.6	3202.4	s	3199.92 Ti I (27)	3203.44 Ti II (3)	
3201.9	3203.7	m		3203.87 Si II (7)	
3203.3	3205.1	m	3203.44 Ti II (3)	3205.11 Cr II (114)	
			3203.83 Ti I (27)		
3208.1	3209.9	s		3210.03 Si II (7)	
3209.5	3211.3	w		3211.57 He I	
3211.4	3213.2	w		3213.31 Fe II (6)	
3213.1	3214.9	w	3213.15 Ti II (3)	3214.75 Ti II (3)	
3214.0	3215.8	w	3214.20 Ti I (27)		
			3214.75 Ti II (3)		
3215.2	3217.0	m		3217.06 Ti II (2)	
3217.6	3219.4	m	3217.06 Ti II (2)		
			3217.12 V I (14)		
3218.1	3219.9	m		3219.79 Cr II (63)	
3218.8	3220.6	m		3220.47 Ti II (9)	
3219.7	3221.5	w		3221.76 Ti II (46)	
3220.4	3222.2	w		3222.83 Ti II (2)	
3222.3	3224.1	s	3222.83 Ti II (2)	3224.24 Ti II (84)	
3225.8	3227.6	s		3227.73 Fe II (6)	
3226.7	3228.5	m	3226.11 V I (14)	3228.61 Ti II (24)	
			3226.27 Ti I (27)		
			3226.77 Ti II (3)		
3227.7	3229.5	w		3229.19 Ti II (2)	
3229.1	3230.9	m	3229.19 Ti II (2)	3231.27 He I	
3230.3	3232.1	s		3231.64 Cr II (122)	
3231.0	3232.8	s		3232.79 Fe II (119)	

Notes to table 4.2

* denotes that the line is common to both orders

Strength of lines (I) s - strong

m - medium

w - weak

Apart from the stellar lines expected, there is evidence of a cool outer atmosphere to HD 168476, suggested by the lines of Si I, Ca I, Ti I, Cr I and Fe I. Resonance lines of atoms in a higher stage of ionisation are also visible both in the interstellar medium and in the star. The line profiles show no evidence of asymmetry or P Cygni profiles, which would be expected if there were mass loss. This confirms the finding of Lynas-Gray, Walker & Hill (1979) from the low dispersion spectra. The spectrum was considered generally to be too weakly exposed for the measurement of equivalent widths to have any useful value, hence the rough indication of the strength of the line in table 4.2. The wavelengths were measured to an accuracy of $\pm$0.2 A by inspection of the overlap regions. The line identifications suggested that some wavelengths may have larger errors due to the weakness of the lines, but the possibility of line shifts cannot be excluded. Hopefully a more exposed spectrum will clarify this problem.

Some of the interstellar lines, notably Mg II and Fe II, appeared to be very strong and for these an estimate of the equivalent width was made using a planimeter (see table 4.3). Equivalent widths for the Na I D lines were taken from table 5.5. The doublet ratio method of Strömgren (1948) gave a value for the abundance of Na I as a column density from the lines at 5890A and 5896A (Lynas-Gray, 1979). In that paper Strömgren gave a formula

for the column density calculated from an unsaturated line.

$$N = \frac{8\pi c}{\lambda^4} \frac{q_l}{q_k} \frac{1}{a_{lk}} w(\lambda)$$

where q_l, q_k are the statistical weights and a_{lk} is the transition probability for the line.

This is equivalent to the formula given by Morton (1967) using the oscillator strength 'f'.

$$N = \frac{m_e c^2}{\pi e^2} \frac{w(\lambda)}{\lambda^2 f}$$

The statistical weights, transition probabilities and oscillator strengths were taken from Morton (1979). Where more than one line of an ion was measured the individual column densities are shown in table 4.3 as well as the mean value. Also shown in table 4.3 are the column densities found by Morton (1975) for ζ Oph.. These data were obtained from high resolution scans with the ultraviolet spectrometer on the Copernicus satellite. Morton found column densities for 21 elements in various stages of ionisation, and put upper limits on a further 5 elements and 11 molecules. Using Hobb's (1974) relationship between E(B-V) and log N(Na I) it was found

for HD 168476 E(B-V) = 0.13 log N(Na I) = 13.0

for ζ Oph. E(B-V) =0.32 log N(Na I) = 13.7

These values agree well with those shown in table 4.3, so that the values shown there for other ions are taken as representative of the interstellar medium.

Table 4.3 Interstellar column densities derived from ultraviolet lines

Ion	λ (A)	$w(\lambda)$ (A)	log N (cm^{-2}) HD 168476	log N (cm^{-2}) ζ Oph.
Na I	5890/96	0.655/0.327	12.5	13.9
Mg I	2852.13	0.307	12.4	14.2
Mg II	2795.53	1.00	13.4	
	2802.70	1.00	13.7	
mean			13.6	15.0
Si I	2506.90	0.136	13.6	
	2514.32	0.128	13.2	
mean			13.4	$\leq$12.6
Ti II	3078.65	0.126	13.1	11.5
V I	3069.65	0.182	14.2	
	3090.40	0.148	13.4	
mean			13.8	$<$11.1
Mn II	2576.11	0.328	13.3	
	2593.73	0.223	13.2	
	2605.70	0.384	13.6	
mean			13.4	13.3
Fe II	2585.88	0.382	14.1	14.6

Inspection of the results shows that although the answers must be regarded as very uncertain due to the poor quality of the spectrum, it would appear that neutral sodium and magnesium are normally abundant, but that the other ions examined are overabundant when allowance is made for the lower interstellar reddening of HD 168476. This may be evidence of mass loss in the star at some time in its past, since these lines are not shifted from the rest wavelength.

5 EQUIVALENT WIDTHS FROM THE VISIBLE SPECTRUM

5.1 Introduction

As noted in chapter 1, Hill (1965) made a coarse analysis of HD 168476, and Schönberner & Wolf (1974) did a differential analysis on HD 168476 relative to HD 124448. The temperature they determined was very similar to that found by Hill, but the surface gravity was a factor of ten different. Spectra were obtained for a fine analysis from several different sources. The tracings of four Coudé spectra, taken on the 1.5m ESO telescope, were kindly loaned to the writer by Prof. K. Hunger and Dr. J. P. Kaufmann (Kiel and West Berlin Universities respectively). Several spectra were given to the writer by Dr. P. W. Hill. These spectra had been used in his 1965 analysis and were takem with the Radcliffe 1.9m telescope. In addition, spectra of several wavelength regions of HD 168476 were obtained with the 3.9m Anglo-Australian telescope (AAT) by Dr. A. E. Lynas-Gray and the writer. The stellar lines were identified using Moore (1945) with the wavelength revision for Si II and Si III lines from Moore (1965), for C II lines from Moore (1970) and for N II lines from Moore (1975). Some Ne I lines were taken from Harrison (1969) and some He I lines were taken from Hill (1964). The wavelength scales on the spectra were corrected for the star's radial velocity.

5.2 AAT spectra

Of the three nights allocated in 1977 June to Drs Lynas-Gray, Hill and the writer, only seven hours were usable. Prior to the observing, a set of the copper-argon arc spectra was obtained

from Dr. R. Fosbury and the wavelengths identified in the region from 3200A to 8000A. Dr. Fosbury had already identified most of the lines in the region between 3200A and 4500A, and these were confirmed. This identification was essential for the repeated scans of certain wavelength regions to examine any variation in the lines. A graph and list of central wavelength against grating angle position and collimator focus was prepared to facilitate moving to a new wavelength region whilst allowing for some overlap with the old.

The Royal Greenwich Observatory (RGO) spectrograph with the 82cm camera was used with the Image Photon Counting System (IPCS) to make the observations (AAT Observers Guide, 1976; IPCS Operating Notes, 1977). Grating 1 was used; blaze at 5000A and dispersion 10 A/mm. Two data windows (A and B) were set up (see figure 5.1). The star was observed through one window and sky through the other. The counts received could be displayed on a video terminal. When sufficient counts were accumulated, the scan was terminated and the star was moved to the other data window using the telescope beamswitching facility. Observations were made in the one-dimensional mode so that lines across the data window were added up to give a single spectrum. A sequence of five spectra were taken at each grating angle, alternating the data windows. This sequence was preceded and followed by an arc exposure. About 300A was visible at each grating angle position.

Ten spectra were obtained covering the wavelength regions 3610A to 4262A, 4275A to 4693A and 5485A to 6583A. Three scans of the region between 4352A and 4617A were obtained and two scans of the region between 3919A and 4253A. Initial reductions were

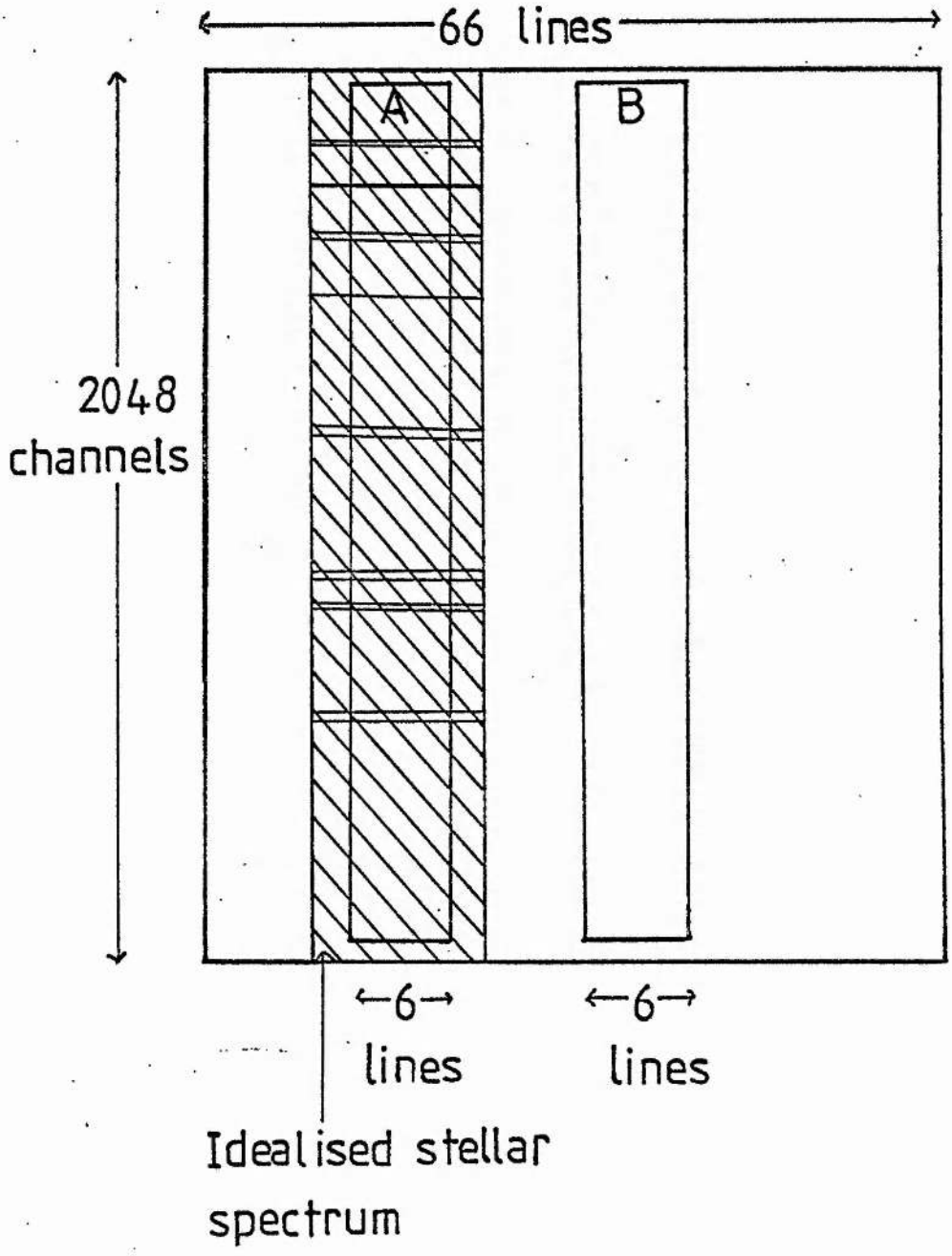

Figure 5·1 Sketch of VDU showing data windows A and B

made at the Anglo-Australian Observatory (AAO). A correction for the variation in cathode response was made using observations of a tungsten lamp emitting continuous radiation. The sky counts were removed from each channel and then the spectra from each set of five scans added up. The quantum noise obtained in the superimposed spectrum was about 3%.

A program for use with the University of St. Andrews IBM 360/44 computer was developed by Dr. A. E. Lynas-Gray. This removed the high frequency noise using the Fourier-Transform technique described in Gray (1976) and the instrumental profile. An unblended arc line, which was symmetrical and unsaturated, near the middle of the wavelength region observed was used as an approximation to the instrumental profile. The arc lines were identified so that the stellar spectrum could be linearised in wavelength. The continuum was drawn in on the spectrum plot and then sufficient points digitized for use with a spline-function so that equivalent widths could be calculated for lines with no wings. It was possible to put in profiles for the strong helium lines in a similar manner, so that more accurate values for their equivalent widths, and those of the lines affected by them, could be obtained.

5.3 ESO and Radcliffe Coudé spectra

5.3a ESO

Four spectra of HD 168476 were taken on the ESO 1.5m telescope at La Silla, Chile by Dr. J. P. Kaufmann as part of Prof. K. Hunger's observing programme. The emulsion used was IIaO and the dispersion was 20 A/mm. Details of the plates are shown in table 5.1.

Table 5.1 ESO Coudé spectra used

Plate	Date	Start time (UT)	End time
F 753	6th May 1972	$30^h\ 52^m$	$32^h\ 16^m$
F 755	8th May 1972	$27^h\ 44^m$	$28^h\ 53^m$
F 1288	12th Sept 1973	$26^h\ 54^m$	$28^h\ 34^m$
F 1297	15th Sept 1973	$26^h\ 44^m$	$28^h\ 44^m$

Reductions

The plates were calibrated and the spectra converted to intensity in the manner desribed by Schönberner & Wolf (1974). The four spectra were then superimposed and plotted, with the resulting chart being loaned to the writer for analysis. The spectral region covered was between 3610A and 4925A, with equivalent widths measured from 3730A to 4760A. As in the fine analysis of HD 124448 (Schönberner & Wolf, 1974) and BD-9°4395 (Kaufmann & Schönberner, 1977) the equivalent widths were measured with a planimeter. The planimeter was checked for accuracy by measuring several prepared areas plotted on the University of St. Andrews IBM 360/44 machine. Each spectral line was measured in both the clockwise and anti-clockwise direction with the areas checked to ensure agreement.

5.3b Radcliffe

Several of the plates taken with the 1.9m Radcliffe telescope and used by Hill (1964, 1965) in his coarse analysis of HD 168476 were used by the writer in the analysis. The plates are listed in table 5.2.

Table 5.2 Radcliffe Coudé spectra used

Plate	Date	Emulsion	Observer
DZ 49	9th June 1960	103aO	A.D. Thackeray
DZ 135	7th Sept 1960	103aO	A.D. Thackeray
DZ 332	25th July 1961	IIaO	P.W. Hill
DZ 336	26th July 1961	IIaO	P.W. Hill
DZ 341	25th Aug 1961	IIaO	P.W. Hill

Reductions

These plates were scanned on the RGO PDS microdensitometer, a very quick and efficient system under the control of a minicomputer. Dr. J. Pilkington (RGO) instructed the writer in the use of the instrument, which was set up to record density as a function of position on the plate, data being stored on a 7-track magnetic tape. A sequence of upper arc spectrum, clear plate, star spectrum, lower arc spectrum was used, with any calibration spots or step wedge associated with the star spectrum being scanned as well. A check of upper and lower arc spectra showed that the equipment compensated completely for backlash. Each plate was individually focused and adjustments made so that the clear plate gave a reading of about 20 on the density scale, to avoid any negative numbers occuring in the scan.

The 7-track tape was converted to a 9-track tape suitable for use with the University of St. Andrews IBM 360/44 computer by the University Computing Advisory Service. It transpired that the tape had a variable block length and so a subroutine prepared by Mrs. E. MacCormick was used to read the tape. A set of programs

was written to read the tape files and reduce the data. RG01 read and plotted a 'calibration spot' file followed by a 'clear plate' file, so that the appropriate conversion from density to intensity could be made. RG02 read and plotted as density values the 'stellar spectrum' file and 'clear plate' file so that noise, plate faults etc. on the stellar spectrum could be noted. RG03 used the prepared calibration from density to log(intensity), input on cards, to convert the stellar spectrum file, after removal of an averaged clear plate density, and plot the spectrum out as intensity verses wavelength. A linear interpolation was used in the conversion subroutine since the step size between points on the calibration could be as small as desired.

Two additional programs, RGOU1 and RGOU2, used consecutively were able to take several files of the star spectrum from the magnetic tape, convert each spectrum via its own calibration from density to intensity and add them together, since the dispersions were identical, to give one stellar spectrum with improved signal-to-noise. In this case the wavelength shift, found from the C II line at 4267A, was input so that the spectra would be added together correctly. The positiom of the start and end of the spectra could be found relative to each other, and the portion where the stellar spectrum was not significantly above the clear plate level was removed. A modification to RGOU2 produced RGOEL, in which the 'superimposed' spectrum was reformatted to be compatible with the format used in the AAT tape, and was stored on a temporary disc file in the computer to be operated on by the program package mentioned in section 5.2. The addition of the spectra was checked by repeating the process with arc spectra but no doubling or broadening of the arc lines

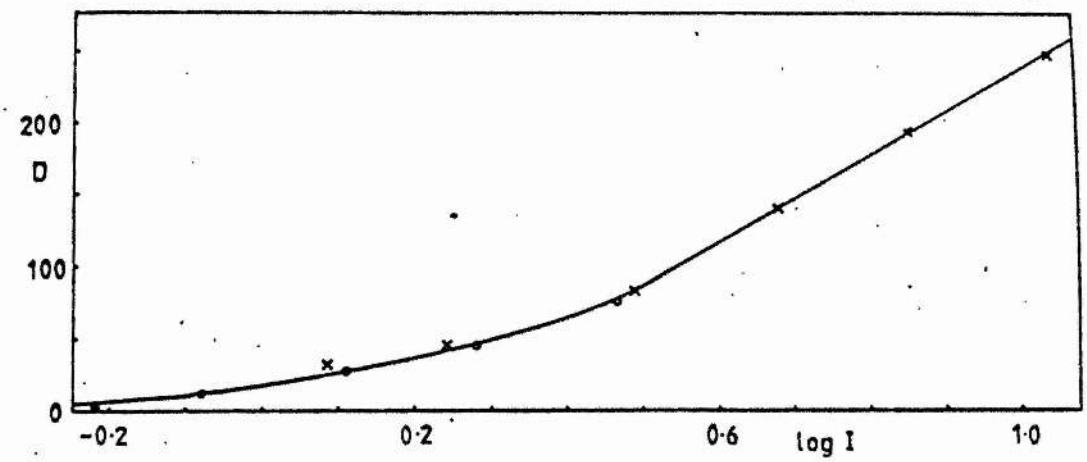

Figure 5·2 H-D curve for DZ 49

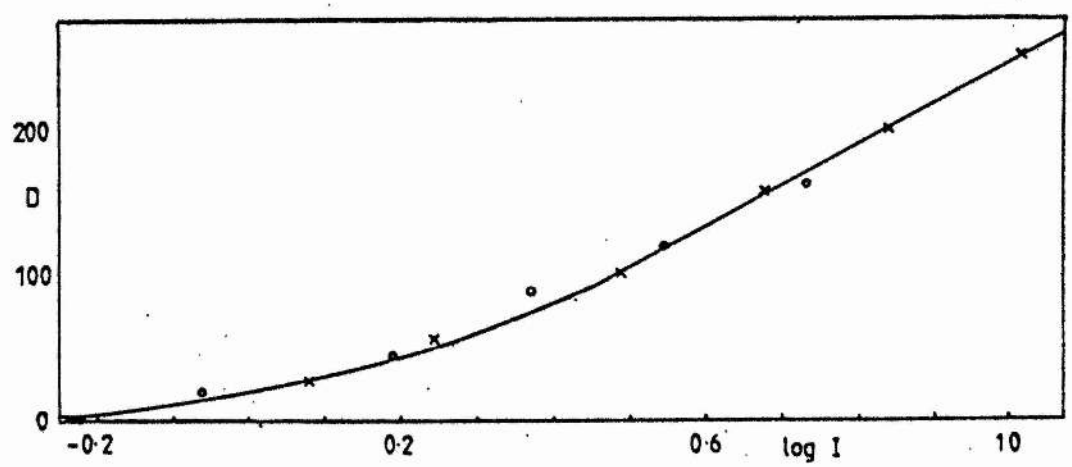

Figure 5·3 H-D curve for DZ 135

x - represents darker set of spots

o - represents fainter set of spots

was seen over the whole range used.

For the spectra DZ 49 and DZ 135, the H and D curve (Mees, 1954) was used to give the calibration from density to intensity. This method was used initially, since there were twelve calibration spots impressed on the plate, six taken for time 't' and six for time approximately '4t'. It was a simple matter to overlay the H and D curve for the fainter spots on that for the darker spots, giving a good calibration from very low to high densities (see figures 5.2 and 5.3). These two plates were well exposed and so in the useful range of the spectrum the calibration was on the linear section of the H and D curve. DZ 49 and DZ 135 were added together and plotted out for visual identification of lines and the measurement of equivalent widths was made using a planimeter. In addition to this the superimposed spectrum was treated with a fast-Fourier-transform, the instrumental profile removed and the spectrum wavelength scale linearised by the computer program developed by Dr. A. E. Lynas-Gray, mentioned in section 5.2. Equivalent widths were obtained from that spectrum by the computer. The results from the two techniques agree well (see figure 5.11).

Three plates DZ 332, DZ 336 and DZ 341 were on a different emulsion (see table 5.2) and so it was decided that they should not be added to DZ 49 and DZ 135 without the removal of the plate response. This was not easily obtainable since the plates had no wavelength calibration of response, only calibration spots. These plates were less well exposed and so the conversion from density to intensity would be on the toe of the H and D curve, where a small change in density results in a large change in intensity, causing the possible amplification of grain noise on

the photographic plate. For this reason it was decided to use the Baker density relation as described by de Vaucouleurs (1968). The main problem with this technique was that the numbers produced from the PDS microdensitometer were not absolute densities. In this case the Baker relation could be expressed as :-

$$\log I = n\log\left(10^{(D/a)} + b + 1\right) + \log A$$

It was found that 'b' = 0, i.e. there was no zero point shift in the system, but for each plate 'a' had a different value due to the adjustments made before each scan. For each spectrum a range of values of 'a' were tried with the computer, which plotted the results, so that a fit to a straight line could be found by inspection. The final value of 'a' in each case was found from all twelve spots using a least squares fit. Table 5.3 shows the values found, and figures 5.4, 5.5, 5.6, 5.7 the graphs.

Table 5.3 Baker relations found for DZ 332, DZ 336, DZ 341 & DZ 49

Plate	a	Equation of line n (se)	log A (se)
DZ 332	170	0.530 (07)	0.205 (06)
DZ 336	420	0.788 (17)	0.635 (10)
DZ 341	315	0.302 (16)	0.389 (08)
DZ 49	235	0.621 (23)	0.391 (13)

DZ 49 was reduced using the Baker relation for comparison with the reduction using the H and D curve. No noticable changes in the useful spectrum were found in the two plots of intensity

x - represents darker set of spots: o - represents fainter set of spots

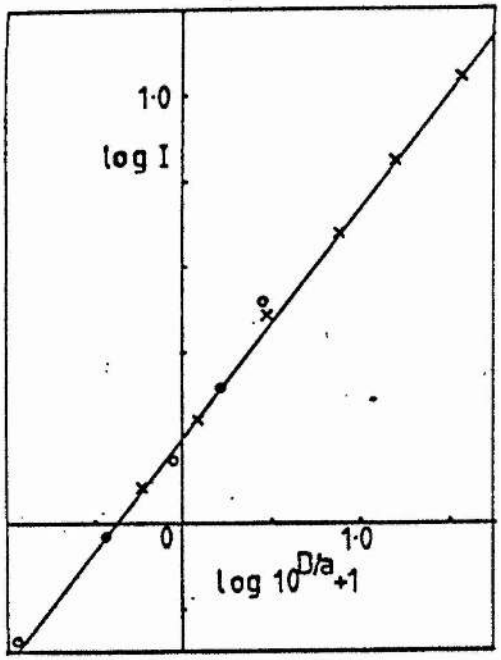

Figure 5·4 Baker relation for DZ 332

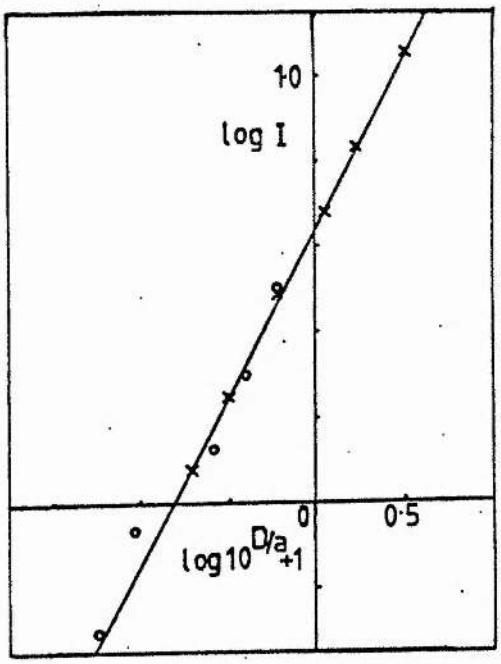

Figure 5·5 Baker relation for DZ 336

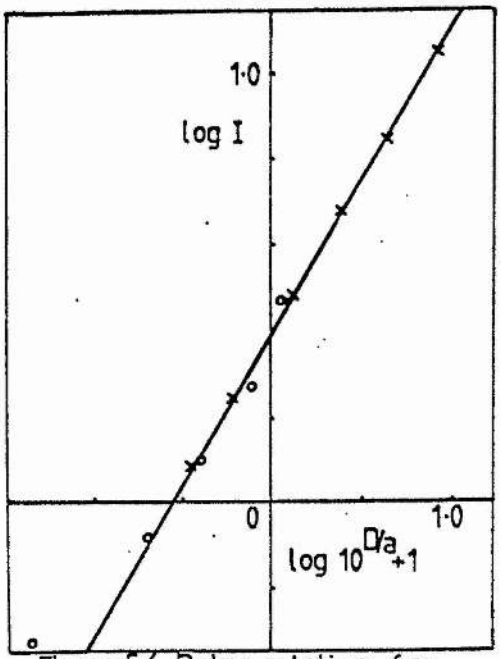

Figure 5·6 Baker relation for DZ 341

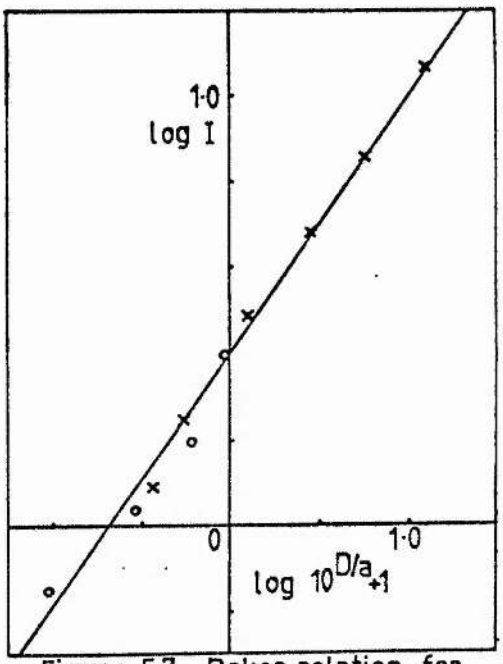

Figure 5·7 Baker relation for DZ 49

against wavelength.

In RG01, RG02 and RG03, smoothing was accomplished by taking the mean of four points to give one point. In addition to removing some noise it also reduced the density and position arrays to a size easily manageable by the computer. For the superimposed spectrum a more useful smoothing was obtained by taking half of the central channel and adding to it a quarter each of the channel before and after. This meant that the full number of points (about 19000) obtained from the PDS scans could be utilised in the final plot of the spectrum. Since the AAT package of computer programs (see section 5.2) contained its own technique of noise removal no smoothing was done on the data before it was stored to be reduced using those programs.

For the superposition of DZ 49 and DZ 135 the wavelength region usefully covered was between 3100A and 4400A. Equivalent widths between 3255A and 4295A were measured with a planimeter. The region covered by DZ 332, DZ 336 and DZ 341 was between 3500A and 4775A. This superimposed spectrum was still considerably weaker than the former, and so the lines were identified but no equivalent widths were measured.

5.3c Estimate of errors in the equivalent widths from ESO and Radcliffe spectra

The errors in the equivalent widths were determined as follows

$$\text{equivalent width } (w) = \frac{\text{area measured } (A) \times \text{dispersion}}{\text{continuum height } (h)}$$

If Δw is the error in w

ΔA is the error in A

and Δh is the error in h

$$\text{then} \quad \left(\frac{\Delta w}{w^2}\right)^2 = \frac{\Delta A^2}{A^2} + \frac{\Delta h^2}{h^2}$$

(Lynas-Gray, 1979)

$$A = A \pm 0.1 \text{ sq. cm.}$$

For the Radcliffe spectrum the areas measured ranged from 0.25 sq cm to 26 sq cm, and the continuum height from 7.0 cm to 17.4 cm. Areas as small as 0.25 sq cm were not measured at the smaller continuum height, although it is included for completeness. For the ESO spectrum the areas measured ranged from 0.35 sq cm to 28 sq cm, and the continuum height varied from 15.4 cm to 28.7 cm.

$$h = h \pm 0.5 \text{ cm}$$

For the Radcliffe spectrum at small continuum height

$$h = h \pm 0.3 \text{ cm}$$

Table 5.4 shows the error in equivalent width derived, and it is displayed graphically in figure 5.8.

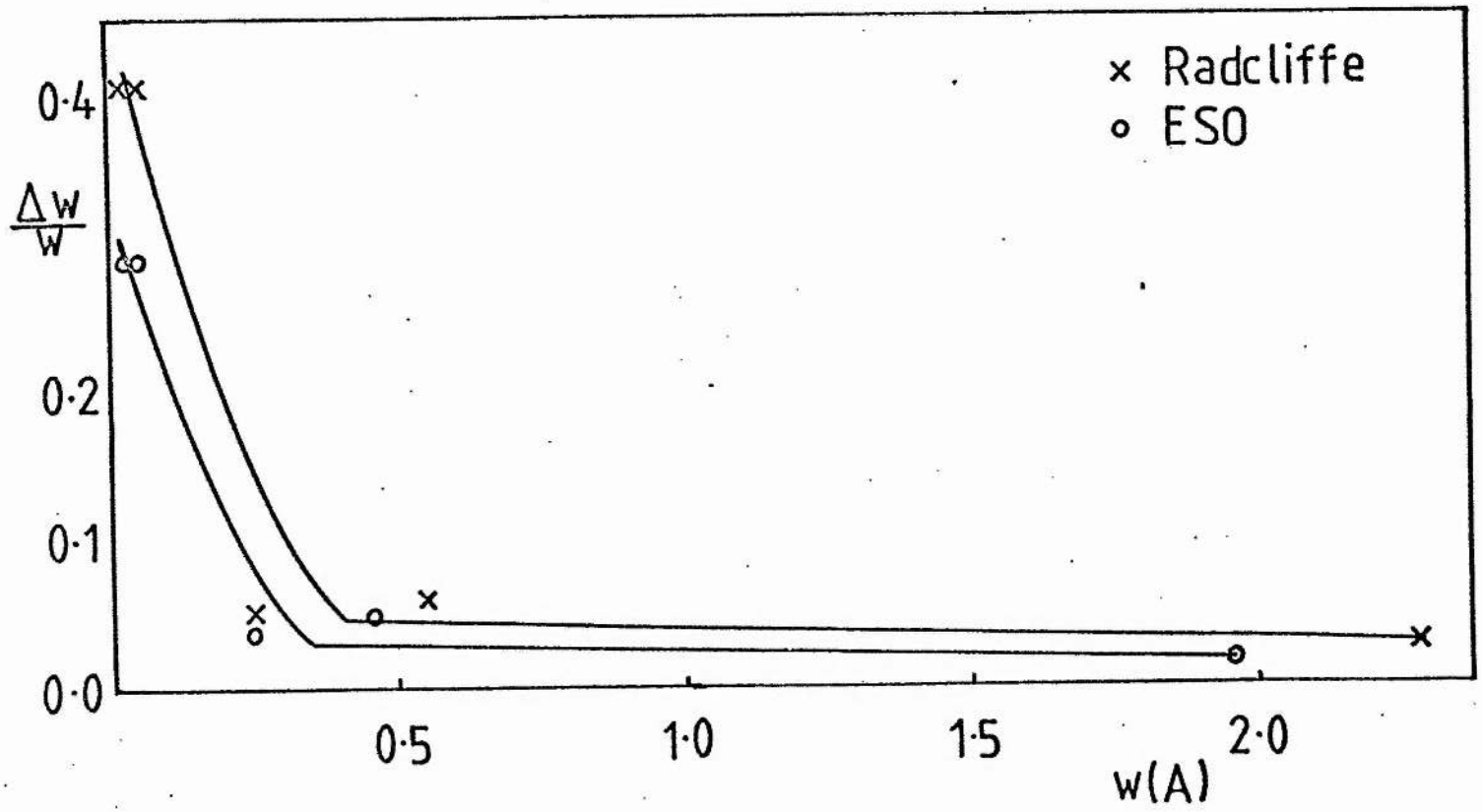

Figure 5·8 Error in equivalent width for Radcliffe & ESO spectra

Table 5.4 Errors in equivalent width for Radcliffe and ESO spectra

Radcliffe			ESO		
h (cm)	w (cm)	$\sqrt{\frac{\Delta w^2}{w^2}}$	h (cm)	w (cm)	$\sqrt{\frac{\Delta w^2}{w^2}}$
7.0	0.056	0.402	15.4	0.046	0.288
	0.557	0.059		0.455	0.043
17.4	0.022	0.401	28.7	0.024	0.286
	0.224	0.049		0.244	0.033
	2.331	0.029		1.951	0.018

5.4 Results

The line identifications and equivalent widths are listed in table 5.5. Values of the equivalent widths are given for the Radcliffe spectrum DZ49 + DZ 135 measured by planimeter and measured by computer, for the ESO spectrum measured by planimeter, and the mean equivalent widths from the ESO, Radcliffe and AAT spectra, as given in Lynas-Gray, Walker, Hill & Kaufmann (1979). The computed Radcliffe equivalent widths were obtained from the program of Dr. A. E. Lynas-Gray. A 'p' indicates that the line was present but no equivalent width measured. The columns are as follows :-

column 1 - LAMBDA - wavelength of line from multiplet table

column 2,3- ION M.N.- give ion and multiplet number (if available) for the line

column 4 - RAD:P - equivalent width of line measured by planimeter on DZ 49 + DZ 135 spectrum plot

column 5 - RAD:C - equivalent width of line computed on DZ 49 + DZ 135 spectrum

column 6 - RAD - indicates presence of line on DZ 332, 336, 341 spectrum plot

column 7 - ESO:P - equivalent width of line measured by planimeter on ESO spectrum plot

column 8 - MEAN - average equivalent width including AAT measurements if available

column 9 - R - remarks

column 10 - A - asterisk indicates line used in abundance analysis

As in Lynas-Gray, Walker, Hill & Kaufmann (1979) a colon or double colon beside the equivalent width indicates that the standard deviation for the equivalent width exceeds the expected error by a factor of two or three respectively. An asterisk in the remarks column indicates a note at the end of the table. The numbers in the remarks column are as follows :-

1 - not identified on 1 AAT spectrum

2 - not identified on 2 AAT spectra

3 - only identified on AAT spectra/um

4 - only identified om 1 AAT spectrum

5 - only identified on 2 AAT spectra

6 - identified on available AAT spectra/um

7 - identified on available AAT spetcra/um, but no equivalent width measured

All the lines from 5495A onwards are measured only on the AAT spectra and no remark is entered concerning that fact. The helium lines which have (H) in the multiplet number column are taken from Hill (1964). In all 1460 wavelengths are listed in table 5.5, with 1196 equivalent widths. There are 146 lines with

no identification at present. Hill (1964) listed 594 wavelengths, with 409 equivalent widths.

Table 5.5

ABSORPTION LINE WAVELENGTHS AND EQUIVALENT WIDTHS

LAMBDA A	ION	M.N.	RAD:P mA	RAD:C mA	RAD ESO:P mA	MEAN mA	R	A
3104.76	Mg II	6	p	132		132		
3105.08	Ti II	67		247		247		*
3105.55	Fe II	82		161		161		
3106.23	Ti II	67						
3106.56	Fe II	68	p	266		266		
3107.58	Cr II	125	p	138		138		
3107.95	Fe III	29		45		45		*
3108.66	Cr II	55	p	151		151		*
3109.92	Ti II	58		44		44		
3110.62	Ti II	67		68		68		*
3111.61	Fe III	8		48		48		*
3112.31	Cr II	125		36		36		*
3114.49	Fe II	82	p	374		374		
3115.65	Cr II	46	p	207		207		
3116.59	Fe II	82	p	176		176		*
3116.76	Cr II	126		84		84		*
3117.67	Ti II	67	p	136		136		*
3118.14	Cr II	55		66		66		*
3118.65	Cr II	5	p	350		350		
3119.80	Ti II	67	p	94		94		*
3120.37	Cr II	5	p	173		173		*
3121.05	Cr II	72		82		82		*
3121.60	Ti II	4		101		101		
3122.95	Sc II	39		156		156		
3124.98	Cr II	5	p	310		310		
3125.46	Cr II	55		p				
3126.02	Sc II	39		115		115		
3127.88	Ti II	121	p	91		91		
3128.70	Cr II	5	p	280		280		
3130.80	Ti II	4		133		133		*
3131.54	Cr II	53,55		68		68		*
3132.06	Cr II	5	p	319		319		
3133.10	Sc II	39		93		93		
3134.33	Cr II	94		111		111		*
3134.82	Mn II	15		165		165		
3135.36	Fe II	82						
3135.51	Mn II	15	p	216		216		
3135.74	Cr II	94		183		183		*
3136.32	Mn II	15						
3136.68	Cr II	5	p	261		261		
3137.55	Cr II	54		249		249		
3138.21	Fe II	227		91		91		*
3138.46	Sc II	39		72		72		
3139.91	Cr II	54	p	116		116		
3140.21	Cr II	124						

LAMBDA A	ION		M.N.	RAD:P mA	RAD:C mA	RAD ESO:P mA	MEAN mA	R	A
3141.80	Cr	II	175	p	p				
3142.22	Fe	II	7		92		92		
3142.74	Cr	II	85		71		71		*
3144.74	Ti	II	10	p	169		169		
3145.77	Cr	II	85		68		68		*
3147.19	Cr	II	54						
3147.23	Cr	II	5	p	68		68		
3148.03	Ti	II	4		67		67		*
3149.12	Cr	II	84		46		46		*
3149.33	Cr	II	54	p	32		32		*
3150.11	Cr	II	54	p	45		45		*
3152.25	Ti	II	10	p	83		83		*
3154.20	Ti	II	10	p	139		139		
3154.20	Fe	II	66						
3154.66	Cr	II	54	p	276		276		
3155.67	Ti	II	10		121		121		*
3157.52	Cr	II	93	p	121		121		*
3158.03	Cr	II	70		184		184		
3158.87	Ca	II	4	p	60		60		
3159.10	Cr	II	5	p	225		225		
3161.95	Fe	II	7	p	195		195		
3162.57	Ti	II	10						
3163.09	Fe	II	7	p	226		226		
3165.62	C	II	9		28		28		
3166.22	Fe	II	79		132		132		
3166.67	Fe	II	6		150		150		*
3167.85	Fe	II	66						
3167.93	C	II	9						
3168.52	Ti	II	10	p	235		235		
3169.20	Cr	II	123		143		143		*
3170.34	Fe	II	6		98		98		*
3172.08	Cr	II	71	p	p				
3172.79	Mg	II	13	p	90		90		
3175.08	Fe	II	157		68		68		*
3175.84	Mg	II	13		93		93		
3177.53	Fe	II	82	p	321		321		
3179.33	Ca	II	4	p	452		452		
3181.43	Cr	II	9	p	231		231		
3181.84	Ti	II	122						
3182.57	Ti	II	122	p	45		45		
3183.12	Fe	II	7	p	371		371		
3183.33	Cr	II	82						
3185.13	Si	III	8						
3185.32	Fe	II	7	p	111		111		
3186.74	Fe	II	6						
3187.74	He	I	3	p	254		254		
3190.87	Ti	II	26	p	211		211		
3192.92	Fe	II	6	p	162		162		*
3193.81	Fe	II	6	p	187		187		*

LAMBDA A	ION		M.N.	RAD:P mA	RAD:C mA	RAD ESO:P mA	MEAN mA	R	A
3194.26	Ti	II	120		240		240		
3194.63	Cr	II	70		77		77		*
3195.72	Ti	II	25	p	128		128		
3196.00	Ti	II	46						
3196.07	Fe	II	7	p	342-		342		
3196.96	Cr	II	9	p	p				
3197.12	Cr	II	9		243		243		*
3197.52	Ti	II	3		121		121		
3199.51	Si	II	13	p	81		81		*
3200.45	Cr	II	114		102		102		*
3201.26	Cr	II	114	p	86		86		*
3201.90	Fe	III	6		147		147		
3203.87	Si	II	7	p	162		162		*
3205.11	Cr	II	114		112		112		*
3208.02	Cr	II	114		68		68		
3208.62	Cr	II	9	p	93		93		*
3209.21	Cr	II	9	p	132		132		*
3210.03	Si	II	7	p	416		416		
3211.7				p					
3213.15	Ti	II	3						
3213.31	Fe	II	6	p	296		296		
3214.75	Ti	II	3	p	103		103		*
3217.06	Ti	II	2		21		21		
3217.44	Cr	II	9	p	52		52		*
3219.79	Cr	II	63		36		36		*
3220.47	Ti	II	9		55		55		
3221.76	Ti	II	46	p	p				
3222.84	Ti	II	2	p	209		209		
3224.24	Ti	II	84	p	120		120		*
3226.77	Ti	II	3		43		43		*
3227.73	Fe	II	6	p	403		403		
3228.61	Ti	II	24	p	99		99		*
3229.19	Ti	II	2	p	124		124		*
3231.27	He	I	(H)						
3231.32	Ti	II	9						
3231.64	Cr	II	122	p	148		148		
3232.79	Fe	II	119	p	199		199		*
3234.06	Cr	II	63		94		94		*
3234.52	Ti	II	2	p	295		295		
3234.92	Fe	II	1						
3236.12	Ti	II	24	p	92		92		*
3237.66	Fe	II	81	p	129		129		*
3238.77	Cr	II	63	p	81		81		*
3240.71	Ti	II	9		42		42		
3241.98	Ti	II	2	p	224		224		
3243.72	Fe	II	119	p	112		112		*
3247.17	Fe	II	81	p	234		234		*
3248.60	Ti	II	66						
3248.70	Ti	II	9	p	181		181		

LAMBDA A	ION	M.N.	RAD:P mA	RAD:C mA	RAD ESO:P mA	MEAN mA	R	A
3249.65	Fe II	81						
3249.91	Fe II	78	p	270		270		
3250.79	Cr II	61	p	89		89		*
3251.7			p					
3251.91	Ti II	2	p	191		191		*
3252.91	Ti II	2	p	146		146		
3252.94	Ti II	23						
3254.25	Ti II	2	p	71		71		*
3255.88	Fe II	1	122	193		158		*
3257.83	S II	17	p	146		146		
3258.28	He I	(H)	483	p		483		
3258.77	Fe II	81	p	200		200		*
3259.05	Fe II	81	p	11		11		
3261.60	Ti II	66,89	165	p		165		*
3266.25	Cr II	121		30		30		*
3266.94	Fe II	65	p	84		84		
3267.04	Fe II	80						
3268.48	Cr II	62		30		30		*
3269.77	Ti II	57	p	52		52		
3271.37	Ti II	66	p	77		77		*
3273.53	Fe III	7		65		65		
3274.90	Ni II	1		p				
3276.08	Fe III	7	p	116		116		*
3276.61	Fe II	92						
3276.77	Ti II	45	p	132		132		
3277.35	Fe II	1	99	158		129		*
3278.29	Ti II	66		63		63		*
3279.54	Cr II	121		97		97		*
3280.58	Fe III	7		84		84		
3281.29	Fe II	1	196	227		212		*
3282.33	Ti II	66	167	137		152		*
3283.75	Fe III	7		34		34		
3285.43	Fe II	1		43		43		
3287.37	Al III	10	p					
3287.66	Ti II	89	p	94		94		*
3289.35	Fe II	65	p	140		140		*
3290.54	Ni II	5		27		27		*
3290.69	Ni II	1						
3291.75	Cr II	68		123		123		*
3293.48	Ti II	57		35		35		
3295.06	Fe II	93		54		54		
3295.24	Fe II	79						
3295.43	Cr II	51	147	178		163		
3295.81	Fe II	1						
3296.79	He I	9	187	178		183		
3297.89	Fe II	91		123		123		*
3298.21	Ti II	44	93	42		68		
3299.44	Ti II	8		38		38		
3302.86	Fe II	1	p	65		65		*

LAMBDA A	ION	M.N.	RAD:P mA	RAD:C mA	RAD ESO:P mA	MEAN mA	R	A
3303.47	Fe II	1		37		37		*
3305.22	Fe III	7	p	87		87		*
3305.63	Fe II	79		56		56		*
3306.05	Ti II	44		63		63		
3307.04	Cr II	51	p	p				
3307.57	Fe II	65		48		48		*
3308.81	Ti II	7	p	86		86		*
3310.65	Cr II	120,158	p					
3311.96	Cr II	51	p	124		124		*
3314.2			p					
3315.29	Cr II	51		89		89		*
3315.53	Fe II	93		72		72		
3317.70	S II	42		34		34		
3318.02	Ti II	7	p	74		74		*
3321.70	Ti II	65	87	60		74		*
3322.94	Ti II	7	210	212		211		*
3324.06	Cr II	4	136	159		148		*
3324.57	N II	22		84		84		
3326.76	Ti II	7	98	63		81		*
3328.35	Cr II	4	122	88		105		*
3329.46	Ti II	7	158	161		160		*
3332.11	Ti II	65	85	55		70		*
3333.14	Si II	6	49	54		52		*
3335.19	Ti II	7	181	153		167		*
3336.16	Cr II	14	p	204		204		
3337.5			p					
3338.19	Fe II	5	120	161		141		
3339.36	Fe III	7	156	158		157		*
3339.80	Cr II	4	p	158		158		
3339.82	Si II	6						
3341.88	Ti II	16	226	168		197		*
3342.51	Cr II	4	p	97		97		*
3346.72	Ti II	7	p	84		84		
3346.91	Ti II	43						
3346.99	Ca II	9						
3347.84	Cr II	4	94	159		127		*
3349.40	Ti II	1	399	481		440		
3350.42	Ni II	1		125		125		
3351.46	Al II	26		58		58		
3353.12	Cr II	4		93		93		*
3353.73	Sc II	12		90		90		*
3354.55	He I	8	140	149		145		
3357.07	Fe III	19		p				
3358.25	Fe II	77						
3358.50	Cr II	4	138	203		171		
3360.16	Ti II	54	p	52		52		
3360.30	Cr II	21	p	116		116		*
3360.89	C II	7	p	88		88		
3361.05	C II	7	p	167		167		

LAMBDA A	ION		M.N.	RAD:P mA	RAD:C mA	RAD ESO:P mA	MEAN mA	R	A
3361.72	C	II	7	p	131		131		
3364.90	Ti	II	124		71		71		
3365.64	Fe	II	194		76		76		*
3367.42	Cr	II	79		135		135		*
3368.05	Cr	II	4	204	274		239		*
3369.05	Cr	II	68	113	145		129		*
3369.67	Ti	II	124		83		83		
3369.91	Ne	I	2						
3370.7				p					
3372.13	Cr	II	91		128		128		*
3372.80	Ti	II	1	268	228		248		
3373.98	Ni	II	1	179	169		174		*
3374.95	Cr	II	4		34		34		*
3376.27	Cr	II	78	78	115		97		
3378.34	Cr	II	21	p	114		114		*
3379.37	Cr	II	21	p	100		100		*
3379.83	Cr	II	21						
3379.93	Ti	II	64	p	151		151		
3380.28	Ti	II	1	p	141		141		*
3382.68	Cr	II	3	110	83		97		*
3383.76	Ti	II	1	198	241		220		*
3385.31	S	II		88	91		90		
3386.72	Fe	II			84		84		
3387.83	Ti	II	1	261	189		225		
3388.13	Fe	II	77		171		171		
3391.1				p					
3391.30	Fe	II	117		189		189		
3393.00	Cr	II	21	87	129		108		*
3394.32	Cr	II	21	p	120		120		*
3394.57	Ti	II	1	p	191		191		*
3395.34	Fe	II	117		130		130		*
3397.82	Ni	II	8	p					
3401.76	Ni	II	4		130		130		*
3403.32	Cr	II	3	148	222		185		*
3406.4				p					
3407.21	Ti	II	1	137	163		150		
3407.30	Ni	II	4						
3408.77	Cr	II	3	232	195		214		*
3409.81	Ti	II	1	p	79		79		*
3410.74	Fe	III	61,62	p	20		20		
3414.14	Fe	II	91	p	59		59		*
3416.02	Fe	II	16	95	147		121		*
3420.18	Fe	II	89	52	27		40		*
3421.20	Cr	II	3	115	p		115		*
3422.74	Cr	II	3	229	200		215		*
3425.09	Cr	II	8		48		48		
3425.58	Fe	II	5	p	84		84		*
3428.64	Fe	II	90	p	77		77		*
3430.15	Fe	II	89		45		45		*

LAMUDA A	ION		M.N.	RAD:P mA	RAD:C mA	RAD ESO:P mA	MEAN mA	R	A
3433.30	Cr	II	3	165	136		151		*
3434.3				p					
3436.11	Fe	II	91	p	96		96		*
3441.98	Mn	II	3	308	372		340		*
3443.39	Ti	II	99		95		95		*
3444.31	Ti	II	6	p	150		150		*
3446.2				p					
3447.59	He	I	7	276	358		317		
3448.43	Fe	II	90	p	94		94		
3449.28	Cr	II	111		55		55		
3450.23	He	I	(H)	p	37		37		
3450.34	Cr	II	60	p	99		99		*
3451.61	Fe	II	207	p	122		122		
3453.21	He	I	(H)	272	p		272		
3454.16	Ni	II	1	p	183		183		*
3456.00	Fe	II	4	p	135		135		
3456.79	He	I	(H)	322	p		322		
3456.93	Fe	II	76						
3457.81	Mn	II	9		95		95		
3459.29	Cr	II	136		73		73		*
3460.31	Mn	II	3	377	403		390		*
3460.95	He	I	(H)						
3461.50	Ti	II	6	254	243		249		
3462.73	Cr	II	2		60		60		*
3463.97	Fe	II	4		71		71		*
3464.50	Fe	II	114	130	131		131		*
3465.91	He	I	(H)	591	p		591		
3468.68	Fe	II	114	195	226		211		*
3470.24	Fe	II	89		101		101		*
3471.80	He	I	44	559	p		559		
3472.57	Ne	I	2	239	p		239		*
3474.04	Mn	II	3	323	327		325		*
3474.12	Mn	II	3						
3475.13	Cr	II	2		67		67		*
3477.18	Ti	II	6	p	157		157		*
3478.97	He	I	43	609	p		609		
3479.91	Fe	II	4	132	p		132		
3482.06	Mn	II	9		51		51		*
3482.91	Mn	II	3	254	237		246		*
3484.15	Cr	II	2		6		6		*
3486.08	Fe	II	102	p	p				
3486.91	Si	III	8.06	p	p				
3487.72	He	I	42	803	p		803		
3488.68	Mn	II	3	222	p		222		*
3489.74	Ti	II	6	p	p				
3490.62	He	I	41	246	p		246		
3491.05	Ti	II	6	p	p				
3493.16	V	II	6	250			250		
3493.47	Fe	II	114		265		265		*

LAMBDA A	ION	M.N.	RAD:P mA	RAD:C mA	RAD	ESO:P mA	MEAN mA	R	A
3495.37	Cr II	2	235				235		*
3497.54	Mn II	3	181	p			181		*
3498.64	He I	40	1012	p			1012		
3499.57	Fe III	26	p	p					
3501.32	Fe III	48	p	67			67		
3501.75	Fe III	26,48	200	221			211		*
3502.38	He I	39	126	112			119		
3503.00	P II	2		73			73		*
3504.40	Fe III	48	140	p			140		
3504.89	Ti II	88		155			155		*
3505.90	Ti II	88		17			17		*
3506.93	Fe III	48	p	50			50		*
3507.39	Fe II	16	p	90			90		*
3509.97	Mn II	9		55			55		*
3510.84	Ti II	88	143	p			143		*
3511.6			66				66		
3511.84	Cr II	2	p	p					
3511.93	Fe III	26	p	p					
3512.51	He I	38	1196	p			1196		
3513.09	Ti II	6	p	p					
3513.93	Ni II	1	232	p			232		*
3514.87	Fe III	26	67	p			67		
3515.82	Fe II	208	87	p			87		*
3517.33	He I	37	298	254			276		
3520.25	Ti II	98	71	p			71		*
3520.47	Ne I	7	71				71		*
3523.4			140				140		
3524.87	Ti II	118		49			49		
3526.5			153				153		
3528.23	Cr II	109		96			96		
3529.73	Cr II	89	p	p	p				
3530.49	He I	36	1337	p	p		1337		
3532.0			57				57		
3532.69	Fe II	75	78	p			78		*
3535.04	Mg II	12	153	215			184		*
3535.73	Sc II	11	90				90		*
3536.82	He I	35	243	261	p		252		
3538.80	Mg II	12	83	92	p		88		*
3540.28	Cr II	89		56			56.		
3545.19	V II	5		79			79		*
3549.61	Mg II	11		63			63		*
3551.7			90				90		
3553.51	Mg II	11	93		p		93		*
3554.46	He I	34	1100		p		1100		
3555.7			30				30		
3556.49	P II	21		188	p		188		
3556.80	V II	5	80				80		*
3557.55	Fe II	176	119				119		
3559.93	P II	21		58			58		*

LAMBDA A	ION	M.N.	RAD:P mA	RAD:C mA	RAD	ESO:P mA	MEAN mA	R	A
3561.58	Ti II	15	130	57			94		
3562.95	He I	33	287	p	p		287		
3564.54	Fe II	113	123	101	p		112		*
3566.37	Cr II	76	144	213	p		179		
3567.17	S II	56	68	105			87		*
3567.70	Sc II	3	62	98			80		*
3568.97	Fe II	113		35			35		*
3570.57	Cr II	89		40			40.		
3571.37	Cr II	107		45			45		*
3572.52	Sc II	3	88	109	p		99		*
3573.74	Ti II	15	48	79			64		*
3576.34	Sc II	3							
3576.38	Ti II	76	p	131	p		131		
3576.76	Ni II	4	p	277	p		277		*
3577.86	V II	78	67				67		
3584.01	Cr II	107	84	p			84		
3584.98	C II	23							
3585.54	Cr II	13	129	p	p		129		*
3585.81	C II	23	64		p		64		
3587.16	[He I]	32							
3587.25	He I	31	1694	p	p		1694		
3587.66	C II	23							
3588.92	C II	23	p	p					
3589.66	C II	23	80	p			80		
3590.47	Si III	7	116	p	p		116		*
3590.86	C II	23	99	p	p		99		
3594.46	S II	16	164	148			156		
3595.99	S II	4							
3596.05	Ti II	15	164	164	p		164		
3599.37	He I	30	299	317	p		308		
3600.7			117				117		
3601.62	Al III	1	175	203	p		189		*
3601.90	Al III	1							
3603.77	Cr II	13	239	248	p		244		*
3605.7					p				
3606.18	Fe II	175		53			53		*
3607.05	Fe II	101	58	89			74		
3608.70	Ni II	4	179	213	p		196		*
3610.33	Fe II	112	70	134	p		102		*
3612.35	Al III	1	75	p	p		75		
3613.23	Cr II	13	p	p	p				
3613.64	He I	6	887	p	p		887		
3613.80	Mg II	2							
3614.87	Fe II	112	104	p			104		*
3616.92	S II	56	51	66			52:	6	*
3617.32	Cr II	147	114	135			125		*
3620.27	Fe III	25					39	3	
3621.27	Fe II	144	221	243	p	p	232	6	*
3622.81	Fe II	175					63		

LAMBDA A	ION	M.N.	RAD:P mA	RAD:C mA	RAD	ESO:P mA	MEAN mA	R	A
3624.89	Fe II	144		201	p	p	201		*
3625.30	Cr II	98	117	70			94		
3627.17	Fe II	193		129			82::	6	*
3627.71	Ti II	62	69				69		
3630.74	Sc II	2	225	p	p		225	7	*
3631.49	Cr II	12	219	p	p	p	219	7	*
3631.72	Cr II	12	178	p	p	p	178		*
3632.02	S III	1	114		p		114	7	
3632.29	Fe II	112	p	p	p				
3633.16	Cr II	147	158	p		p	158		
3634.10	[He I]	29							
3634.30	He I	28	1326	p	p	p	1326	7	
3636.90	Fe II	112					134	3	
3639.0			154				154		
3641.33	Ti II	52	154	p	p		116::	6	*
3642.79	Sc II	2	104	128			116	7	*
3643.22	Cr II	1		41			41		*
3644.70	Cr II	1	110	112	p		111		*
3647.40	Cr II	1		19			19		*
3648.86	Ti II	83					75	3	
3649.01	Ti II	14	128	100	p		114		
3651.97	He I	27	435	508	p	p	209	*	
3652.12	He I	27					207		
3652.81	Ti II	116		69		p	69		
3654.51	S II	4	102	140			85::	6	
3655.00	Al II	12							
3656.61	S III	6	84	80	p		82	*	
3657.5			60				60		
3658.19	Cr II	98,146	90	93			72	6	*
3659.77	Ti II	75	96	p	p		82	6	*
3661.17	Fe II	111					57	3	
3662.24	Ti II	75		181			134::	6	*
3662.62	Cr II	1	161	32	p		97		
3663.47	S II	16					21	3	
3664.95	Cr II	156					69	3	*
3666.59	Ti II	116					51	3	
3669.05	S II	16	66	68	p		74	6	
3669.69	Cr II	1	95	47	p		58	6	
3671.12	Cr II	6			p				
3672.14	S II	4	36	59	p		48		
3672.6			42				42		
3673.77	Fe II	131					35	3	*
3676.50	Cr II	1					47	3	*
3677.82	Cr II	12	173	p	p	p	167	6	*
3678.8			83				83		
3681.4			72				72		
3684.25	Cr II	145					58	3	*
3685.19	Ti II	14	298	311	p	p	231::	6	*
3686.67	Cr II	118					58	3	*

LAMBDA A	ION	M.N.	RAD:P mA	RAD:C mA	RAD	ESO:P mA	MEAN mA	R	A
3688.01	Cr II	1					44	3	
3688.71	Fe III	93					50	3	
3696.39	Ti II	73					101	3	
3698.00	Cr II	118					89	3	*
3700.14	Fe III	84					79	3	
3700.42	Cr II	1					80	3	
3702.09	Al III	4	101	122			112		*
3703.22	Al II	18					143	6	*
3704.79	[He I]	26							
3705.04	He I	25	1524	p	p	p	1278::	6	
3706.03	Ca II	3	122	p	p	p	163:	6	
3706.5			119				119		
3708.06	Mn II	8					203	3	
3709.25	Cr II	6					233	3	
3709.88	Mn II	8					95	3	
3710.42	S III	1					175	*	
3711.97	Fe II	192					81	3	*
3712.99	Cr II	12	p	165	p		159	6	*
3713.10	Al III	4	p	150			150		*
3715.45	Cr II	145	137	159			120:	6	*
3720.17	Fe II	23					129	3	
3721.63	Ti II	13		86			69	6	*
3723.63	Ti II	72					60	3	
3724.81	Mn II	8					70	3	*
3725.2	He I	(H)	125	169	p	p	147		
3725.30	Fe II	130							
3725.7						p			
3727.37	Cr II	117	131	p	p	p	101:	6	*
3730.64	S II								
3730.8	He I	(H)	71	113	p		92		
3731.95	Al II	11							
3732.5			p						
3732.93	He I	24	362	p	p	344	353	6	
3733.91	Al II	11					24	3	*
3736.90	Ca II	3	358	p	p	361	360	7	*
3737.7	He I	(H)	208	194	p	167	190		
3738.00	Al II	11	190	193	p		192		*
3738.38	Cr II	20	119	p	p	96	108		*
3739.6	Ti II	107				51	51		
3741.63	Ti II	72	215	p	p	p	189	6	*
3745.36	Fe II	131				p			
3745.9	He I	(H)	791	p	p	p	791	7	
3746.3			p						
3746.56	Fe II	14	45	p		p	45		*
3747.90	S III	1		p		p			
3748.49	Fe II	154	285	p	p	351	301	6	*
3750.74	S III	1	76	p		93	81	6	
3751.22	V II	100	109			98	104		
3753.10	Al II	39						7	

LAMBDA A	ION	M.N.	RAD:P mA	RAD:C mA	RAD	ESO:P mA	MEAN mA	R	A
3754.59	Cr II	20	83	p	p	p	92	6	*
3755.13	Cr II	20	77	p	p		77		
3755.5o	Fe II	154	50	p	p		68	6	
3755.61	Ca II	8							
3756.10	He I	66	1174	p	p	995	1085::	7	
3757.68	Ti II	72	68	p	p	p	68	7	*
3758.36	Ca II	8	83	p	p		79	6	
3759.29	Ti II	13	444	p	p	392	370::	6	
3759.46	Fe II	154						7	
3761.32	Ti II	13	p	285	p	p	273	6	*
3761.69	Cr II	11	p	189	p	p	189		
3762.89	Fe II	192	167	p	p	131	118:	6	*
3764.09	Fe II	29	91	p	p	79	85		*
3764.3			132				132		
3765.62	Cr II	20					79	3	*
3767.18	Cr II	20	53	p			53		
3767.9			140	177	p		159		
3768.81	He I	65	1167	p	p	1494	1331::	7	
3769.46	Ni II	4		p				7	
3770.41	Ti II	107	76	p	p		76	7	
3773.30	Fe III	34		65			45	6	
3774.52	S III	10	25	37		71	39	6	
3774.52	Al II	33							
3776.06	Ti II	72		57	p		57		*
3776.80	S II	51		78			62	6	*
3781.51	Fe II	130			p		121	3	*
3783.16	S II	41							
3783.35	Fe II	14	333	p	p	p	280::	6	
3784.89	He I	64	924	p	p	1344	1014::	6	
3786.33	Ti II	12	119	p	p		93:	6	
3786.37	Fe II	15							
3786.94	Fe III	71					120	3	
3787.5			139	144	p	243	193		
3787.89	Cr II	6	143	161			137	6	
3791.41	Si III	5	35	33	p	96	71	6	*
3792.46	S II	50		39			39		*
3793.52	Fe III	71	64	p			56	6	*
3795.41	Si II	7.08	118	p	p	67	74::	6	*
3796.11	Si III	5	p	115	p	114	118	6	*
3798.36	Fe II	14		64			51	6	*
3799.81	Ti II	13					37	3	
3800.43	Fe III	47	49	89			69		
3801.21	Cr II			59			59		
3801.63	Mn II	14	54	p	p		60	6	*
3802.65	S II	50	171	p	p	76	107::	6	*
3803.38	Mn II	14		p					
3804.48	Mn II	14	71	p	p		71		
3804.8			679			p	679		
3805.3					p	p			

LAMBDA A	ION	M.N.	RAD:P mA	RAD:C mA	RAD	ESO:P mA	MEAN mA	R	A
3805.77	He I	63	1410	p	p	1442	1287::	6	
3806.54	Si III	5	p	p	p	p	151	6	*
3806.82	Fe II	153	101		p		101		
3808.6			69	p			69		
3809.5			180			168	174		
3809.67	S II	50	p	p	p	p	246	*	
3813.39	Ti II	12		97			84		*
3814.12	Fe II	153	p	180	p		183	6	*
3814.58	Ti II	12	155	161	p	102	139		*
3815.3						89	89		
3817.7			74		p	p	74		
3818.3			101				101		
3819.25	[He I]	23							
3819.64	He I	22	2132	p	p	2294	2031::	6	
3821.3						p			
3821.92	Fe II	14	109	p	p		97	6	*
3824.91	Fe II	29	196	261	p		216	6	
3827.08	Fe II	153	119	172	p		148	6	*
3828.44	Fe III	70,95		103			98	6	
3829.47	[He I]	21	110	p	p	118	156::	6	
3829.79	N II	30	114	p	p	p	114		*
3831.02	V II	3			p	p			
3831.41	S II								
3831.74	C II	13	150	p	p	161	156	7	
3832.5			136		p		136		
3833.57	He I	62	1621	p	p	2313	1727	6	
3834.81	Fe II	129	62	p	p	p	62		*
3835.73	C II	13	171	p	p	p	213::	6	
3836.68	C II	13	168	p	p		173	6	
3838.09	He I	61	293	p	p	186	256:	6	
3838.39	N II	30							
3839.0			80				80		
3840.9			66				66		
3842.18	N II	30	52	82		36	80:	6	*
3843.00	Sc II	1		82			80	o	
3844.48	V II	20	127				127		
3845.21	S II	22	103	161	p	108	131	6	
3847.41	N II	30	p	70		78	75	6	*
3848.24	Mg II	5	188	p	p	172	197	6	*
3849.58	Ni II	11	266	285	p	202	238	6	
3850.40	Mg II	5	p	196	p	163	187	6	*
3850.93	S II	50	89	147	p	p	118		*
3852.4			51				51		
3853.09	S II	50	p			p			
3853.66	Si II	1	358	468	p	277	359:	6	*
3856.02	Si II	1	547	603	p	538	555	6	*
3856.06	N II	30							
3857.2			33		p		33		
3858.32	Al III	5	14	32			24	o	

LAMBDA A	ION		M.N.	RAD:P mA	RAD:C mA	RAD	ESO:P mA	MEAN mA	R	A
3859.26	S	II	30	9		p		25	6	
3859.33	Al	II	38							
3859.8				23				23		
3860.15	S	II	41	92		p	63	78	6	
3860.64	S	II	50	p		p	p	98	6	*
3860.92	Fe	II					101	101		
3862.60	Si	II	1	501		p	420	450	6	*
3863.41	Fe	II	152					123	3	*
3863.95	Fe	II	127,152	110		p		84:	6	*
3865.59	Cr	II	167	64			73	69		
3865.72	V	II	20							
3866.01	Cr	II	130	55		p		55:		*
3866.16	Al	II	17	69		p		132	6	*
3866.54	Cr	II	130	64				64		*
3867.53	He	I	20	632		p	390	504::	6	
3870.06	Al	II	74	67				67		*
3870.7				57		p	p	57		
3871.32	He	I	60	1579		p	1824	1583::	6	
3872.76	Fe	II	29	p						
3874.41	Cr	II	143	41				64	6	*
3874.76	Cr	II	143							
3876.35	C	II	33	392		p	393	394	6	*
3877.2				p						
3878.03	C	II	33							
3878.18	He	I	59	159		p	361	295::	6	
3880.59	C	II	33			p		251	3	
3881.6				82				82		
3883.82	C	II	33					29	3	
3887.5				69		p	90	80		
3887.7							90	90		
3888.65	He	I	2	862		p	704	780:	6	
3892.14	Cr	II	167							
3892.32	S	II	50	108		p	134	131	6	*
3892.5				p						
3900.55	Ti	II	34	275		p	176	212:	6	*
3900.68	Al	II	1	p	90			90		
3902.09	Sc	II	9				60	60		
3902.7				108				108		
3903.9							p			
3905.64	Cr	II	167	p	101	p		101		*
3906.04	Fe	II	173	p	p	p	137	140	6	*
3906.95	S	II	3	58	99		84	64:	6	
3909.25	Cr	II	129			p				
3910.4				63				63		
3911.32	S	II				p				
3911.32	Cr	II	129							
3913.46	Ti	II	34	211	p	p	131	159:	6	*
3914.48	Fe	II	3			p	67	67	6	*
3914.8				54	24			39		

LAMBDA A	ION		M.N.	RAD:P mA	RAD:C mA	RAD	ESO:P mA	MEAN mA	R	A
3918.19	S	II	29	143	184			164		
3918.98	C	II	4	574	p	p	421	492:	4	
3919.00	N	II	17							
3920.69	C	II	4	578	p	p	545	565	6	*
3921.5				114				114		
3923.48	S	II	55	183	p	p	118	153	6	*
3924.05	S	II	33	59	p	p	p	59		
3924.8				38			110	74		
3925.5				43				43		
3926.53	He	I	58	2092	p	p	1698	1723::	6	
3928.4						p	p			
3929.4				90		p		90		
3930.31	Fe	II	3	95	p	p		95		*
3931.94	S	II	29	242	p	p	p	190:	6	
3932.01	Ti	II	34							
3932.30	S	II	30	p		p	73	73		
3933.29	S	II	55		p					
3933.66	Ca	II	1	833	642	p	796	776:	6	*
3935.91	He	I	57	502	612	p	456	449::	6	
3935.94	Fe	II	173							
3938.29	Fe	II	3	90	146	p	101	107	6	*
3938.97	Fe	II	190	103	177	p		73::	1	
3939.49	S	II	45	58	89	p		67	*	*
3939.8				90				90		
3942.4				63		p	81	72		
3944.19	C	II	32	49	128			89		
3945.00	C	II	32	36	120	p		78		
3945.06	S	II	33			p	62	85:	6	
3945.20	C	II	32	p		p				
3946.28	C	II	32	27	104	p		55:	1	
3946.43	C	II	31							
3946.98	S	II	45	p	52		92	65	6	*
3947.72	C	II	32	72	75	p		74	2	
3948.35	C	II	32	45	70	p		58		
3949.37	C	II	31							
3949.53	C	II	31	31	13			14	1	
3950.42	S	II	45		35		58	35	6	*
3952.06	C	II	32	76	94	p		109	6	
3952.4				67				67		
3953.8					11		61	36		
3954.38	Fe	III	120	72	105	p	73	81		
3954.8				76				76		
3955.85	N	II	6	99	108	p	111	112::	6	*
3956.4				76				76		
3960.90	Fe	II	212	67	131	p	65	87:	6	*
3961.4				72			73	73		
3961.55	S	III	8	85	271			178		
3963.13	S	II	45		95	p	88	109	6	*
3963.7				86				86		

LAMBDA A	ION		M.N.	RAD:P mA	RAD:C mA	RAD	ESO:P mA	MEAN mA	R	A
3964.73	He	I	5	649	779	p	620	674	6	
3966.43	Fe	II	3	36	90			63		
3968.47	Ca	II	1	773	919	p	600	691::		*
3969.52	C	II	37	p						
3970.39	C	II	37	41				41		
3970.69	S	II	45	149	218	p	163	144::		*
3972.44	C	II	37	32	56	p	42	43		
3973.76	C	II	37	95	162			129		
3974.16	Fe	II	29	p				101	3	*
3974.5					124		72	98		
3974.8				54		p		54		
3975.03	Fe	II	191					4	*	
3977.27	C	II	37	18	75	p		60:	1	
3978.76	C	II	37	32	109	p		61	1	
3979.86	S	II	59	77	p	p	72	69	1	*
3980.32	C	II	37	82	67	p	79	92	1	*
3982.00	Ti	II	11		89			89		
3983.3				68				68		
3983.70	Al	II	32						7	
3985.91	Cr	II	10		169	p	p	169		
3986.3				110				110		
3987.2				46				46		
3990.94	S	II	45	55	105	p	52	75	6	*
3991.47	V	II	10	55				55		
3993.53	S	II	29	83	181	p	109	121:		
3995.00	N	II	12	354	415	p	317	314:	6	*
3998.79	S	II	59	152	218	p	108	131:	6	*
4002.07	Fe	II	29	69	114	p		115::	6	
4002.55	Fe	II	190	125	172	p	145	147		*
4003.89	S	II	45					88	6	*
4007.3				51				51		
4007.78	S	II	29							
4007.81	[He	I]	56	70	p	p	92	98:	6	
4009.27	He	I	55	1450	p	p	1437	1505		
4009.39	S	II	55							
4009.58	Al	II	37							
4009.88	C	II	27							
4010.5				64			38	51		
4010.6							38	38		
4011.6				65				65		
4012.37	Ti	II	11	118	p	p		99		
4012.47	Fe	II	126							
4013.80	Mg	II	22	111	167	p		146	6	
4015.3				149				149		
4015.50	Ni	II	12	125	198	p	221	191	7	*
4017.28	C	II	27	42	62	p		70	6	
4017.96	Cr	II	166		64			64		*
4018.9				60				60		
4019.45	P	II	30	70	94	p		82	7	

LAMBDA A	ION		M.N.	RAD:P mA	RAD:C mA	RAD	ESO:P mA	MEAN mA	R	A
4020.4				70				70		
4021.17	C	II	27			p		66	4	
4022.36	Cr	II	183			p	62	62		*
4023.99	He	I	54	256	p	p	199	270::	6	
4024.55	Fe	II	127	143	p	p	112	128		
4025.49	[He	I]	19	p		p	69	69		
4026.22	He	I	18	2433	p	p	2037	2229	6	
4026.5	Al	II	24							
4027.8				91		p		91		
4028.33	Ti	II	87	79	p			79	7	*
4028.79	S	II	45	92		p	81	87	7	*
4029.2				120				120		
4030.28	Cr	II	19			p				
4030.87	Al	II	72	52		p		52		*
4031.17	Al	II	72	57		p		58	1	*
4031.46	Fe	II	151						7	
4032.81	S	II	58	233	p	p	86	162:	6	
4032.95	Fe	II	126							
4035.08	N	II	39		76		85	81	6	*
4035.5					72		p	72		
4038.2							87	87		
4041.31	N	II	39	52	32		76	91:	1	*
4041.84	Fe	II	13				55	55		
4043.53	N	II	39					100	3	*
4044.49	P	II	30	71	193	p		132		*
4045.16	[He	I]	17	52	74	p		63		
4045.5				80				80		
4047.3				57				57		
4048.83	Fe	II	172	128	150	p		113	6	*
4050.11	S	II	45					14	3	*
4053.81	Ti	II	87	90	181			136		*
4054.11	Cr	II	19					72	3	*
4056.90	N	II	39	77	106	p	54	73:		*
4057.46	Fe	II	212					121	3	*
4057.7				96				96		
4058.70	S	II	54					85::	3	
4061.79	Fe	II	189	67	26			41	1	*
4062.08	P	II	17		73			73		*
4063.94	Cr	II	19	73	95			84		
4065.0				111		p		111		
4065.8							111	111		
4067.05	Ni	II	11	228	321	p		275::	6	*
4067.2							118	118		
4069.88	Fe	II	188		30			41	1	*
4072.56	Cr	II	26					232	4	
4073.04	N	II	38		82		79	113:	1	
4074.52	C	II	36	p	p	p	217	217		
4074.85	C	II	36	p	p	p	178	178		
4075.40	C	II	36							

LAMBDA A	ION		M.N.	RAD:P mA	RAD:C mA	RAD	ESO:P mA	MEAN mA	R	A
4075.45	Si	II	3.01	212		p	p	212	7	*
4075.85	C	II	36	335	269	p	317	327	6	
4076.14	C	II	35.01	p	115	p		115		
4076.78	Si	II	3.01	89	140	p	150	132		*
4076.87	Cr	II	19	p		p	p	120	3	
4077.50	Cr	II	19	p	69	p	p	69		
4077.63	C	II	36	94		p	p	94		
4077.79	C	II	35.01	45	28	p		37		
4078.3							128	128		
4080.04	P	III	1					51	3	
4081.21	Cr	II	165		23			23		
4082.27	N	II	38	p	p		p	96	1	*
4082.89	N	II	38	70	p		64	84	1	
4086.14	Cr	II	26					77	3	*
4086.9				80				80		
4087.63	Cr	II	19		8			33	6	
4088.90	Cr	II	19					61	4	
4089.49	Cr	II	164		19			19		
4091.2							39	39		
4093.90	Mg	II	29	76	89		43	74	6	
4094.8							32	32		
4095.90	N	II	38	41	18		39	34	7	*
4097.12	Ca	II	17				42	42		*
4097.3								51	4	
4097.8				51			39	45		
4099.1				66				66		
4099.94	N	I	10	46	97	p		106	6	
4100.5							53	53		
4109.83	Ca	II	41							
4109.95	N	I	10							
4110.04	N	II	44	274	p	p	137	249	6	*
4110.33	Ca	II	17							
4111.01	Cr	II	18,26					55	3	*
4111.90	Fe	II	188					93	4	*
4112.59	Cr	II	18		92			68:	1	
4113.24	Cr	II	18		53			53		
4117.09	P	II	17	73	116			95		
4119.53	Fe	II	21		116		39	78::		
4120.86	He	I	16	658	749	p	523	582::	6	
4122.64	Fe	II	28		152	p	53	118:	6	
4124.79	Fe	II	22			p		92	3	
4128.07	Si	II	3	o11	p	p	453	522:	6	*
4130.89	Si	II	3	732	p	p	438	616::	6	
4131.78	N	II	43.01	p		p				
4132.41	Cr	II	26	70	118	p	49	72:		*
4133.0							46	46		
4133.67	N	II	65	59	120			90		
4135.77	Cr	II	163	102	52			77	7	
4137.04	N	I	6		135		25	87:	6	

LAMBDA A	ION	M.N.	RAD:P mA	RAD:C mA	RAD	ESO:P mA	MEAN mA	R	A
4138.1			108				108		
4138.40	Fe II	39		143			121:	1	
4141.25	[Al III]	17		134	p	42	109::	1	
4141.6			82				82		
4142.29	S II	44	47	p	p	103	75:	7	*
4143.76	He I	53	1809	p	p	1594	1643	1	
4144.2			58				58		
4145.10	S II	44	p	p	p	37	73::	1	*
4145.78	N II	65	143	p	p	p	105::	1	*
4146.94	S II	65		p	p	34	65:	1	
4151.48	N I	6		133	p	80	105	6	
4152.5			126				126		
4153.10	S II	44	143	397	p	129	206::	6	*
4156.39	N II	50	170	225	p	66	157::	1	
4157.01	N II	50	p	99		73	86		
4159.31	Al II	71	94				94	7	*
4160.26	Al II	71	39				34	1	*
4160.50	N II	50	89	177	p		133		
4161.14	N II	50							
4161.52	Ti II	21					50	3	*
4162.70	S II	44,65	278	388	p	188	240::	6	*
4163.64	Ti II	105	134	161	p	188	98:	6	*
4165.11	S II	64		117		28	73	6	
4166.73	P II	16	67	158			65::	6	
4168.41	S II	44							
4168.66	Fe II	22							
4168.97	He I	52	466	660	p	369	441::	6	
4171.61	N II	43	57	70		p	92:	1	*
4171.90	Ti II	105							
4171.92	Cr II	18	40	67	p	101	96	1	
4173.45	Fe II	27							
4173.54	Ti II	21	306	304	p	209	216::	1	
4173.57	N II	50							
4173.8						p			
4174.04	S II	64	p	144	p		245::	6	
4174.09	Ti II	105							
4176.16	N II	43	114	25		49	54	6	*
4177.70	Fe II	21	97	115	p	84	95	7	*
4178.86	Fe II	28	418	431	p	275	316::	0	
4179.67	N II	50	40	64			52		*
4180.70	S II	64				35	39	6	
4183.35	Si II	7.26					42	3	
4184.09	Fe III	22					15	3	
4184.33	Ti II	21		66			59	1	
4185.95	S II			31			31		
4186.8			99		p		99		
4187.14	Si II	7.17	p	181	p	91	136::		*
4188.0			99		p		99		
4189.71	S II	44,64	93	190	p	87	115::	1	*

LAMBDA A	ION		M.N.	RAD:P mA	RAD:C mA	RAD	ESO:P mA	MEAN mA	R	A
4190.29	Ti	II	21	64	125	p	p	115	1	
4190.72	Si	II	7.26	p	67	p	63	79	1	
4192.5				88				88		
4193.44	Mg	II	28	88	137	p	98	97	6	*
4195.97	N	II	49	24	42			33	7	*
4196.42	Ne	I		65	50		38	48	7	
4196.64	Ti	II	21	p	84			84		
4198.13	Si	II	7.26	77	99		52	70	6	
4199.98	N	II	49	48	95			72		*
4200.79	Si	II	7.06	113	188	p	129	149	6	*
4206.21	Ca	II	16	108	46			50	1	
4206.38	Mn	II	7							
4207.35	Cr	II	26					29	4	*
4211.1							84	84		
4211.80	Fe	II	21	169	104		98	117		
4213.50	S	II	44		21		32	36	6	*
4215.77	Cr	II	18					39	4	
4217.23	S	II	44		57		49	67	1	*
4223.3				117				117		
4224.85	Cr	II	162	74	83			79		*
4226.5				68				68		
4227.49	Al	II	46	98	96	p		97		*
4227.74	N	II	33	111	97	p	35	70::		*
4227.99	Al	II	46	74		p	p	74		*
4228.2							113	113		
4229.81	Cr	II	26		16			21	6	
4230.2				80				80		
4230.98	S	II	67		5	p	39	22	7	*
4233.17	Fe	II	27	378	371	p	240	330::	1	
4233.25	Cr	II	31							
4236.33	Cr	II	17		77			77		
4236.98	N	II	48	112	103	p	67	87		*
4237.05	N	II	48							
4237.9				63				63		
4238.69	Cr	II	17		111	p		111		
4238.79	Mn	II	2	100				100		
4240.75	Al	II	36						7	
4241.78	N	II	48	88	121	p	p	105		*
4242.38	Cr	II	31	p	176	p		155	6	*
4242.47	Mg	II	20	283	190	p	141	189		*
4246.41	Cr	II	31					83	3	
4246.83	Sc	II	7	145	185	p		165		*
4251.49	Fe	II	12	63	12			38		
4252.62	Cr	II	31							
4253.02	Mn	II	7	96	113	p	46	75::		*
4253.59	S	III	4	19	25		23	23		*
4256.16	Cr	II	192		96			96		*
4257.42	S	II	66		56	p	53	55		
4258.16	Fe	II	23	116	212		57	111::		*

LAMBDA A	ION	M.N.	RAD:P mA	RAD:C mA	RAD	ESO:P mA	MEAN mA	R	A
4259.18	S II	66	71	84		85	81		*
4261.92	Cr II	31	116	101			109		*
4263.49	Cr II	17		42			42		
4264.0			75				75		
4264.19	Cr II	17		101			101		
4267.14	C II	6	982	1046	p	801	908::		*
4269.28	Cr II	31	150	176	p	78	121::		*
4269.76	S II	49	137	86		p	112		*
4271.1			72				72		
4271.94	Ti II	95		59			59		
4273.32	Fe II	27	85	173	p	64	97::		*
4275.57	Cr II	31	172	131	p	79	115:		*
4278.54	S II	49	132	155	p	71	107::		*
4279.93	Sc II	15		87			87		
4281.03	Cr II	17		10			10		
4282.63	S II	49		82	p	39	61		*
4283.77	Mn II	6	67	98			83		
4284.21	Cr II	31	67				58	6	*
4284.43	Mn II	6		58		25	42		*
4284.99	S III	4		52		39	54	6	*
4285.70	C II	42		46	p		65	6	
4287.89	Ti II	20		72			72	*	*
4290.22	Ti II	41	88	136	p	68	90::	*	*
4291.45	S II	49		75	p	p	97:	6	*
4291.82	C II	41,42		80	p	p	80		
4292.25	Mn II	6	136	185	p	100	117::	6	
4294.10	Ti II	20					250	3	
4294.43	S II	49	149	175	p	158	160	*	*
4295.37	Cr II	37		84			84		
4295.92	C II	41		127	p	72	100:	*	
4296.57	Fe II	28	p		p	36	36	6	*
4300.05	Ti II	41	p		p	57	57		*
4300.20	Mn II	6			p	p		*	
4301.93	Ti II	41	p			47	66	6	*
4303.17	Fe II	27	p		p	93	74	6	*
4305.72	Sc II	15						7	
4307.17	C II	12.02					62	3	
4307.90	Ti II	41	p			101	101		*
4312.86	Ti II	41			p	p	66	6	*
4313.10	C II	28	p			83	83	*	*
4314.08	Sc II	15						7	
4314.29	Fe II	32	p		p	65	65		
4314.98	Ti II	41	p		p	65	57	6	*
4316.81	Ti II	94				65	65	7	
4317.26	C II	28	p		p	32	32	*	
4318.22	Fe II	220				61	61		*
4318.60	C II	28	p		p	40	49	6	*
4318.68	S II	49							
4320.1			p						

LAMBDA A	ION	M.N.	RAD:P mA	RAD:C mA	RAD	ESO:P mA	MEAN mA	R	A
4321.34	Fe II	220				108	108		*
4321.65	C II	23					24	3	
4323.10	C II	28					28	3	
4323.81	Fe III	32					16	3	
4324.36	Fe II	147				90	90		
4325.10	Mn II	6			p	101	101		
4325.83	C II	28	p				113	6	
4326.16	C II	28	p				91	6	
4328.91	Cr II	37						7	
4329.7					p	83	83		
4330.26	Ti II	94	p			108	108	6	
4331.53	Fe II						69	3	
4331.93	Mg II	27			p		113	3	*
4332.00	Al II	31							
4332.4						76	76		
4337.33	Ti II	94	p						
4337.92	Ti II	20	p		p	68	53	6	*
4338.50	Si III	3	p						
4338.70	Fe II	32						7	
4340.30	S III	4			p	32	29	6	*
4340.7			p			61	61		
4341.37	Ti II	32					71	3	*
4342.84	S II	43						7	
4343.99	Mn II	6						7	
4344.7			p						
4350.83	Ti II	94					48	3	*
4351.76	Fe II	27	p		p	169	192:	6	*
4352.70	Fe III	4	p				125	1	
4354.36	Fe II	213							
4354.56	S III	7			p	54	81:	6	
4355.4			p						
4357.57	Fe II				p	54	50	1	
4361.53	S III	4	p		p	25	43	1	*
4362.10	Ni II	9					68	6	*
4362.4						33	33		
4363.4			p						
4364.73	S III	7					33	5	*
4365.56	Fe III	4					43	3	*
4367.66	Ti II	104				58	47	5	*
4368.26	C II	45,46	p		p	p	89:	5	
4369.40	Fe II	28					39	4	*
4370.0			p						
4370.13	C II	45					56	4	
4371.10	Fe III	4					155::	5	
4371.59			p		p	73	73	*	
4372.0			p						
4372.35	C II	45,46	p						
4372.49	C II	45	p		p	116	116		*
4374.27	C II	45	p		p	105	140:	6	*

LAMBDA A	ION	M.N.	RAD:P mA	RAD:C mA	RAD	ESO:P mA	MEAN mA	R	A
4374.98	N II	16			p	p			
4375.01	C II	45	p						
4376.56	C II	45	p		p	87	91	6	
4379.3						47	47		
4379.59	N II	16			p	33	33		*
4382.31	Fe III	4					90	5	*
4383.1					p	34	34		
4384.0			p						
4384.33	Fe II	32				134	134::		*
4384.64	Mg II	10	p		p	124	185	6	*
4385.38	Fe II	27	p		p	107	88	6	*
4386.57	Fe II	26			p	21	21	7	*
4387.93	He I	51	p		p	1223	1322	6	
4390.59	Mg II	10	p		p	206	190	6	*
4391.84	S II	43				45	58	6	*
4394.7						70	70		
4395.03	Ti II	19	p		p	81	106:	6	*
4395.78	Fe III	4							
4395.85	Ti II	61			p	88	122::	1	
4399.77	Ti II	51				62	47	6	*
4399.86	Fe II	20							
4400.63	Ti II	93					31	3	
4402.86	S II	43				55	50	6	*
4409.22	Ti II	61							
4409.52	Ti II	61			p	85	85:		
4409.98	C II	40			p	37	80	6	
4410.7						48	48		
4411.16	C II	39							
4411.51	C II	39			p	p	181:	6	
4411.94	Ti II	61							
4413.26	C II	39					15	5	
4413.60	Fe II	32					11	4	*
4415.37	S II	53					26	5	*
4416.82	Fe II	27			p	154	140	1	*
4417.72	Ti II	40			p	52	74	6	*
4418.84	S III	4					60	5	
4419.59	Fe III	4				66	94:	6	*
4420.3						66	66		
4420.9						63	63		
4427.24	N II	55							
4427.90	Ti II	61							
4427.96	N II	55							
4428.00	Mg II	9			p	59	129:	6	*
4428.6						70	70		
4430.8					p	33	33		
4430.95	Fe III	4					89	5	*
4431.02	S II	32				30	30		
4431.82	N II	55				52	52		*
4432.41	S II	43					102	3	*

LAMBDA A	ION	M.N.	RAD:P mA	RAD:C mA	RAD	ESO:P mA	MEAN mA	R	A
4432.74	N II	55				89	89		*
4433.99	Mg II	9			p	155	150	6	*
4436.48	Mg II	19			p	107	174:	6	*
4437.55	He I	50			p	380	362	6	
4439.87	S III	7					23	4	
4442.02	N II	55				44	44		*
4443.80	Ti II	19			p	74	79	6	*
4444.56	Ti II	31					93	1	
4445.26	Fe II	9					44	4	
4446.25	Fe II	187			p		55:	5	*
4447.03	N II	15			p	114	117	6	
4450.49	Ti II	19			p		34	5	*
4455.0						67	67		
4456.43	S II	43			p		67	5	*
4459.93	N II	21				56	56		
4460.4					p				
4463.58	S II	43			p	126	106	6	*
4464.43	S II				p	p			
4464.46	Ti II	40			p	66	83	1	
4466.50	Ne I				p	51	51	7	
4468.49	Ti II	31			p	87	86	6	*
4469.16	Ti II	18			p	73	87	2	
4469.92	[He I]	15			p	106	100	6	
4471.51	He I	14			p	2063	2166	6	
4472.92	Fe II	37				p	17	1	*
4475.66	Ne I				p	40	40	7	
4477.69	N II	21							
4478.48	S III	7			p	66	66	7	
4481.23	Mg II	4			p	824	755	o	*
4483.42	S II	43				94	104	6	*
4486.66	S II	43					63	3	*
4487.2						p			
4489.19	Fe II	37					84	3	*
4491.40	Fe II	37			p	174	179:	6	*
4492.30	S II	58				68	60	6	*
4493.53	Ti II	18					35	3	*
4495.90	S II	48				42	42		*
4496.99	Mn II	17					37	3	*
4497.88	S II	53					17	3	*
4501.27	Ti II	31			p	87	87	6	*
4507.20	Fe II	213					7	4	*
4507.56	N II	21					42	4	*
4508.28	Fe II	38			p	159	198:	6	*
4510.21	Mn II	17					48	5	*
4512.54	Al III	3						7	
4515.34	Fe II	37			p	160	144:	6	*
4517.43	[He I]	13			p		11	3	
4520.23	Fe II	37			p	84	123	6	
4520.37	Ti II	30							

LAMBDA A	ION	M.N.	RAD:P mA	RAD:C mA	RAD	ESO:P mA	MEAN mA	R	A
4522.63	Fe II	38			p	180	169	6	*
4524.68	S II	40							
4524.95	S II	40			p	207	198	6	*
4529.15	Al III	3			p	127	127		*
4530.41	N II	58			p	62	62	7	*
4534.17	Fe II	37			p	204	245	6	
4534.26	Mg II	26							
4534.7						p			
4537.75	Ne I	11					61:	6	
4539.62	Cr II	39					33	6	
4540.38	Ne I	17					49	5	
4541.52	Fe II	38			p		92:	3	*
4545.14	Ti II	30					29	5	
4549.21	Fe II	186							
4549.47	Fe II	38			p	346	343	6	
4549.62	Ti II	82							
4552.62	Si III	2			p	196	245	6	*
4555.02	Cr II	44			p	94	76:	1	*
4555.89	Fe II	37			p	118	160::	6	*
4558.66	Cr II	44			p	177	168:	6	*
4558.83	Cr II	44							
4563.76	Ti II	50				99	101	2	*
4565.78	Cr II	39			p		57	3	
4566.5					p				
4567.82	Si III	2			p	136	113	6	*
4571.24	Cr II	16					54:	4	
4571.97	Ti II	82			p	153	118	1	*
4574.76	Si III	2			p	64	94:	6	*
4576.33	Fe II	38			p	89	78	6	*
4577.78	Fe II	54					62::	5	
4579.52	Fe II						54	5	
4580.06	Fe II	26			p		62	5	*
4582.12	Fe II	19					77	4	
4582.84	Fe II	37			p	p	80	1	*
4583.83	Fe II	38			p	269	241:	*	*
4583.99	Fe II	26					227	4	
4585.82	Al II	45					66	3	*
4588.22	Cr II	44			p	165	159	6	
4588.22	Al II	45							
4588.40	Cr II	16							
4589.75	Al II	45							
4589.96	Ti II	50				123	91:	2	*
4592.09	Cr II	44			p	58	55	6	
4593.6					p				
4595.68	Fe II	38					60	5	*
4601.34	Fe II	43				96	96		
4601.48	N II	5				188	176	6	*
4606.3						55	55		
4607.16	N II	5				101	131::	6	*

LAMBDA A	ION		M.N.	RAD:P mA	RAD:C mA	RAD	ESO:P mA	MEAN mA	R	A
4612.84	P	II	9					14	4	
4613.87	N	II	5				119	139:	6	*
4616.64	Cr	II	44					74	3	*
4618.83	Cr	II	44					207	3	*
4620.51	Fe	II	38			p	150	175	6	*
4621.39	N	II	5			p	172	246:	6	*
4621.41	Cr	II	25							
4625.91	Fe	II	186			p		158	4	
4626.3							117	117		
4629.29	Ti	II	38							
4629.34	Fe	II	37			p	196	209	6	
4629.70	Al	II	35							
4630.54	N	II	5			p	205	280::	6	
4634.11	Cr	II	44			p	123	108	6	*
4635.33	Fe	II	186			p		140::	3	*
4635.5							127	127		
4636.35	Ti	II	38			p				
4637.63	C	II	12.01					120:	3	
4638.91	C	II	12.01					160	3	
4640.64						p		26	4	
4641.81	O	II	1			p		29	4	*
4643.09	N	II	5			p	164	199:	6	*
4645.8						p				
4648.17	S	II	36					5	4	*
4648.93	Fe	II	25					93::	3	
4654.53	N	II				p				
4656.74	S	II	9			p	104	104		*
4656.97	Fe	II	43			p	109	109	7	
4660.93	Fe	II	146			p				
4661.19	Fe	II	170							
4662.71	Ti	II	38							
4662.74	Ti	II	38							
4663.09	Ne	I				p	307	307	7	
4663.70	Fe	II	44					57	4	
4666.75	Fe	II	37			p	97	92	1	*
4667.21	N	II	11			p				
4668.58	S	II	36			p	116	90	6	
4670.17	Fe	II	25			p		100	4	*
4674.2						p				
4674.91	N	II	11			p				
4681.32	S	II	8			p	52	52		
4683.36	Si	III	13			p				
4685.95	Fe	II	50			p				
4697.62	Cr	II	177			p				
4700.30	P	II	14			p				
4701.65	Al	III	6			p				
4712.00	Ne	I	10			p	p			
4713.20	He	I	12			p	606	606		
4715.34	Ne	I	16			p	96	90		

LAMBDA A	ION		M.N.	RAD:P mA	RAD:C mA	RAD	ESO:P mA	MEAN mA	R	A
4716.23	S	II	9			p	244	244		*
4729.45	S	II	46			p				
4730.36	Mn	II	5			p				
4731.44	Fe	II	43			p				
4737.97	C	II	1			p	188	188		
4739.59	Mg	II	18			p	220	220		*
4744.77	C	II	1			p	153	153		
4751.7						p				
4752.73	Ne	I	21			p	200	200		
4755.12	S	II	35			p				
4756.5							185	185		
4769.0							p			
4771.2						p	p			
4775.3						p	p			
4802.36	Ne	I					p			
4803.27	N	II	20				p			
4815.52	S	II	9				p			
4824.07	S	II	52				p			
4824.13	Cr	II	30				p			
4851.10	Mg	II	25				p			
4921.93	He	I	48				p			
4923.92	Fe	II	42				p			
5495.67	N	II	29					72		*
5496.45	Si	II	32					82		
5499.72	P	II	6							
5507.15	P	II	23							
5509.67	S	II	6					177		*
5510.68	Cr	II	23					99		
5518.74	S	II	61					45		
5526.22	S	II	11					83		
5534.86	Fe	II	55					81		
5535.35	C	II	10							
5537.61	C	II	10							
5540.74	Si	II	9					54		
5541.19	P	II	23							
5556.01	S	II	6					122		*
5559.06	S	II	61							
5562.77	Ne	I	19					93		
5564.94	S	II	6					217		*
5573.30	Fe	III	68					20		*
5576.66	Si	II	9					69		
5578.85	S	II	11					128		*
5583.33	P	II	23							
5588.25	P	II	27							
5606.11	S	II	11					310		*
5616.63	S	II	11					95		*
5639.48	Si	II	9							
5639.96	S	II	14							
5640.32	S	II	11					658		

LAMBDA A	ION		M.N.	RAD:P mA	RAD:C mA	RAD ESO:P mA	MEAN mA	R	A
5640.55	C	II	15						
5645.62	S	II	6				199		*
5646.98	S	II	14						
5648.07	C	II	15				196		
5656.66	Ne	I	24				66		
5659.95	S	II	11				247		*
5662.47	C	II	15				285		
5664.73	S	II	11				136		*
5666.63	N	II	3				294		*
5676.02	N	II	3				170		*
5679.56	N	II	3				311		*
5686.21	N	II	3				153		*
5694.30	C	II	44.01				13		
5710.77	N	II	3				144		
5712.51	C	II	44.01						
5719.23	Ne	I	28				51:		
5739.73	Si	III	4				52	4	
5747.30	N	II	9				78:		*
5748.30	Ne	I	13				81		
5764.42	Ne	I	13				267		
5767.44	N	II	9				38:		*
5795.37	Fe	II	211				50		*
5800.47	Si	II	8				152		
5804.45	Ne	I	19				143		
5806.74	Si	II	8				151		
5813.67	Fe	II	163				66		*
5819.22	S	II	14				241		
5820.16	Ne	I	19				210		
5823.14	C	II	22						
5827.35	C	II	22				41		
5836.35	C	II	22				21		
5846.13	Si	II	8				88		
5852.49	Ne	I	6				360		*
5856.04	C	II	22						
5868.40	Si	II	8				134		
5872.83	Ne	I	31				185		
5875.67	He	I	11				1088		
5881.90	Ne	I	1				369		
5889.77	C	II	5				494		
5889.95	Na	I	1				371	*	
5891.38	Fe	II	211						
5891.59	C	II	5				232		
5895.89	S	II	20						
5895.92	Na	I	1				246	*	
5915.22	Si	II	8				45		
5927.15	S	II	21				61		
5927.81	N	II	28				60		*
5931.78	N	II	23				54		*
5940.24	N	II	28				19		*

LAMBDA A	ION		M.N.	RAD:P mA	RAD:C mA	RAD ESO:P mA	MEAN mA	R	A
5941.65	N	II	28				83		*
5944.83	Ne	I	1				400		
5951.30	S	II	21						
5952.39	N	II	28				99		*
5957.56	Si	II	4				222		
5965.47	Ne	I	39						
5974.63	Ne	I	28				134		
5975.53	Ne	I	1				155		*
5978.93	Si	II	4				265		*
5991.38	Fe	II	46				39		*
5996.16	S	II	13				54		
6024.15	P	II	5				242::		*
6030.00	Ne	I	3				187::		*
6034.01	P	II	5				152		*
6043.10	P	II	5				230		*
6045.50	Fe	II	200				53:		
6074.34	Ne	I	3				471		
6080.85	S	II	20				20		
6084.11	Fe	II	46				25		
6087.76	P	II	5				46		
6092.13	S	II	20				30		
6098.51	C	II	24				83		
6102.56	C	II	24				33		
6103.54	Fe	II	200				64		
6113.33	Fe	II	46				45		
6122.44	Mn	II	13				94		
6125.86	Mn	II	13				41		
6128.21	S	II	28				64		
6128.73	Mn	II	13						
6138.98	S	II	63				23		
6143.06	Ne	I	1				575		
6147.74	Fe	II	74				26		
6149.24	Fe	II	74				60		
6151.43	C	II	16.04				192		
6155.99	O	I	10				97		*
6156.78	O	I	10				164		
6158.19	O	I	10				165		*
6161.84	S	II	27				29		
6163.59	Ne	I	5				307		*
6165.56	P	II	5				85		*
6179.38	Fe	II	163				38		
6217.28	Ne	I	1				290		*
6238.38	Fe	II	74				121		
6239.63	Si	II	7.13				239		
6243.36	Al	II	10						
6247.56	Fe	II	74				94		
6250.74	C	II	38.03						
6253.34	C	II	43.03						
6266.50	Ne	I	5				433		

LAMBDA A	ION		M.N.	RAD:P mA	RAD:C mA	RAD ESO:P mA	MEAN mA	R	A
6274.34	S	II	19				50		
6275.79	C	II	43.03				57		
6286.35	S	II	19				119	4	
6287.06	S	II	26				150		
6290.01	C	II	43.03				40	4	
6305.32	Fe	II	200				382	4	
6305.51	S	II	19						
6312.68	S	II	26				66		*
6314.29	S	II	28				47	4	
6326.43	S	II	63				51		
6331.97	Fe	II	199				71	4	
6334.45	Ne	I	1				328::		*
6347.10	Si	II	2				889		
6369.34	S	II	19				106		
6369.45	Fe	II	40						
6371.36	Si	II	2				341		
6379.62	N	II	2				120		
6382.99	Ne	I	3				543		
6384.89	S	II	19				128		
6386.48	S	II	5				108		
6386.75	Fe	II	203						
6397.30	S	II	19				201		
6398.05	S	II	19				109		
6402.25	Ne	I	1				792		
6407.30	Fe	II	74				9		
6413.71	S	II	19						
6416.91	Fe	II	74				68		
6432.65	Fe	II	40				37		
6433.45	N	II	13.04				75		
6446.28	Mn	II	19						
6456.38	Fe	II	74				159		
6457.69	N	II	13.04				100		
6460.10	P	II	32						
6461.95	C	II	17.04				243		
6482.05	N	II	8				353		
6482.21	Fe	II	199						
6487.43	Fe	II	203				102		
6506.53	Ne	I	3				648		
6516.05	Fe	II	40				15		
6521.39	S	II	25				40		
6545.80	Mg	II	23				306		
6578.05	C	II	2				219		
6582.88	C	II	2						

Notes to table 5.5

3651.97 3652.12	The two components are resolved only in the AAT spectrum: for the Radcliffe spectrum the equivalent width given is for the blend.
3656.61	very weak in AAT spectrum
3710.42	identified in AAT spectrum only, and doubtful since 3709.37 S III (1) absent
3809.67	may be affected by 3809.5, present in AAT spectra
3939.49	very weak, and absent in 2 AAT spectra
3795.03	identified only on 1 AAT spectrum, and blended
4287.89	weak on AAT spectrum
4290.22	weak on AAT spectrum
4294.43	weak on AAT spectrum
4295.92	weak on AAT spectrum
4300.20	weak on ESO and AAT spectra
4313.10	very weak on AAT spectrum
4317.26	very weak on AAT spectrum
4371.59	identified in Moore (1945) as C II (45), but not confirmed in Moore (1970)
4583.83	appeared partially filled with emission on AAT spectra
5889.95	Interstellar
5895.92	Interstellar

Figure 5·9 Mean equivalent width against Hill Coudé

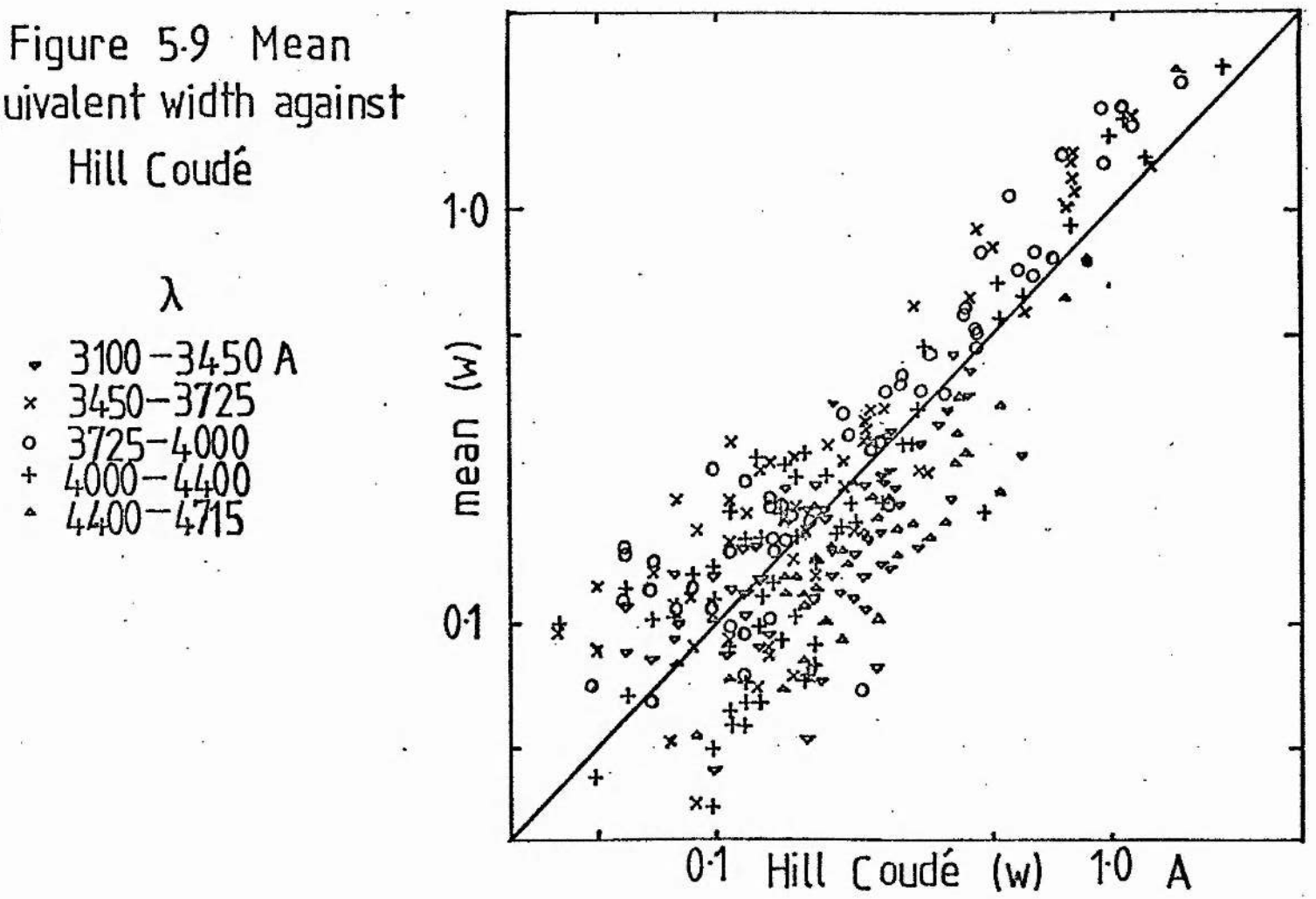

Figure 5·10

Radcliffe (planimeter) against Hill Coudé

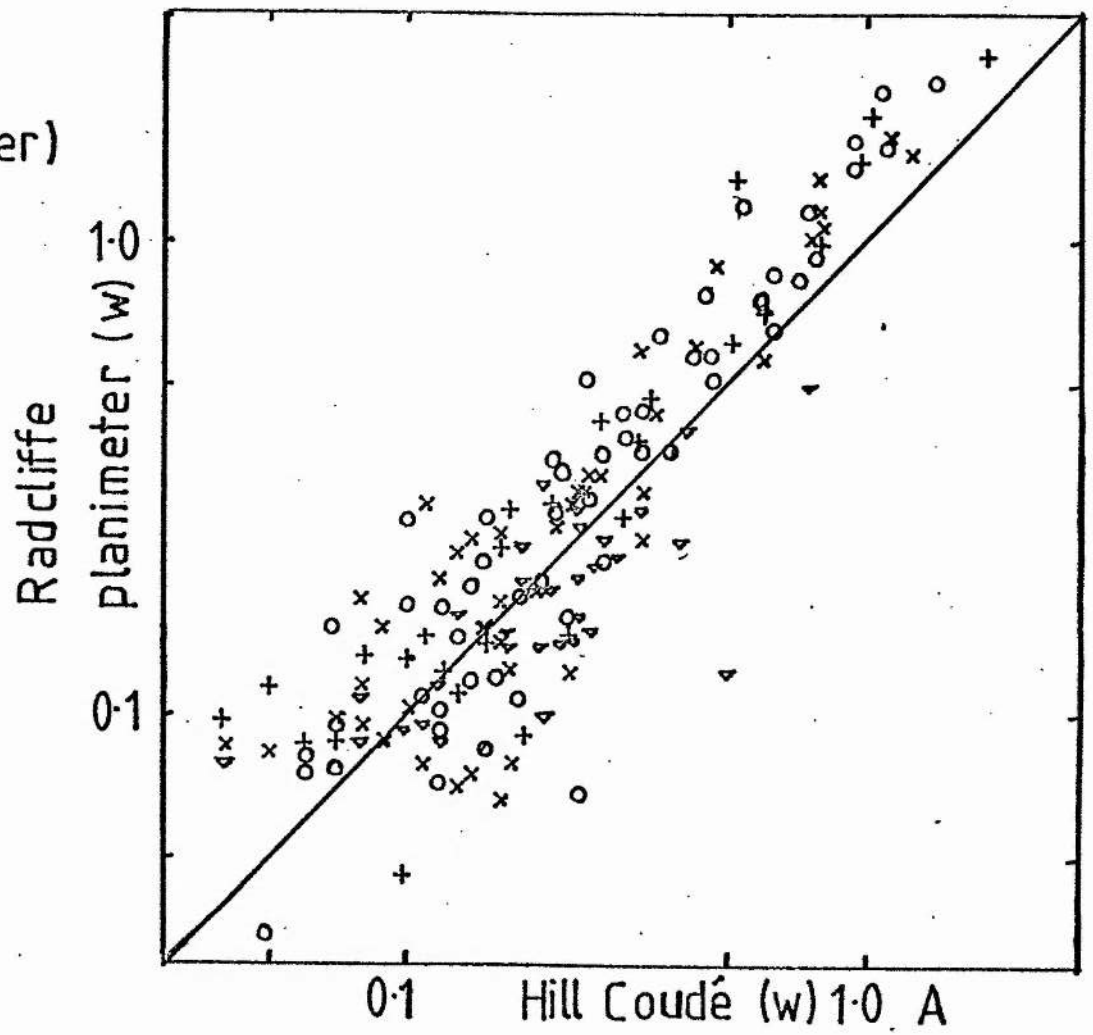

Comments as for figure 5·9

Figure 5·11
Radcliffe (planimeter) against (computed)

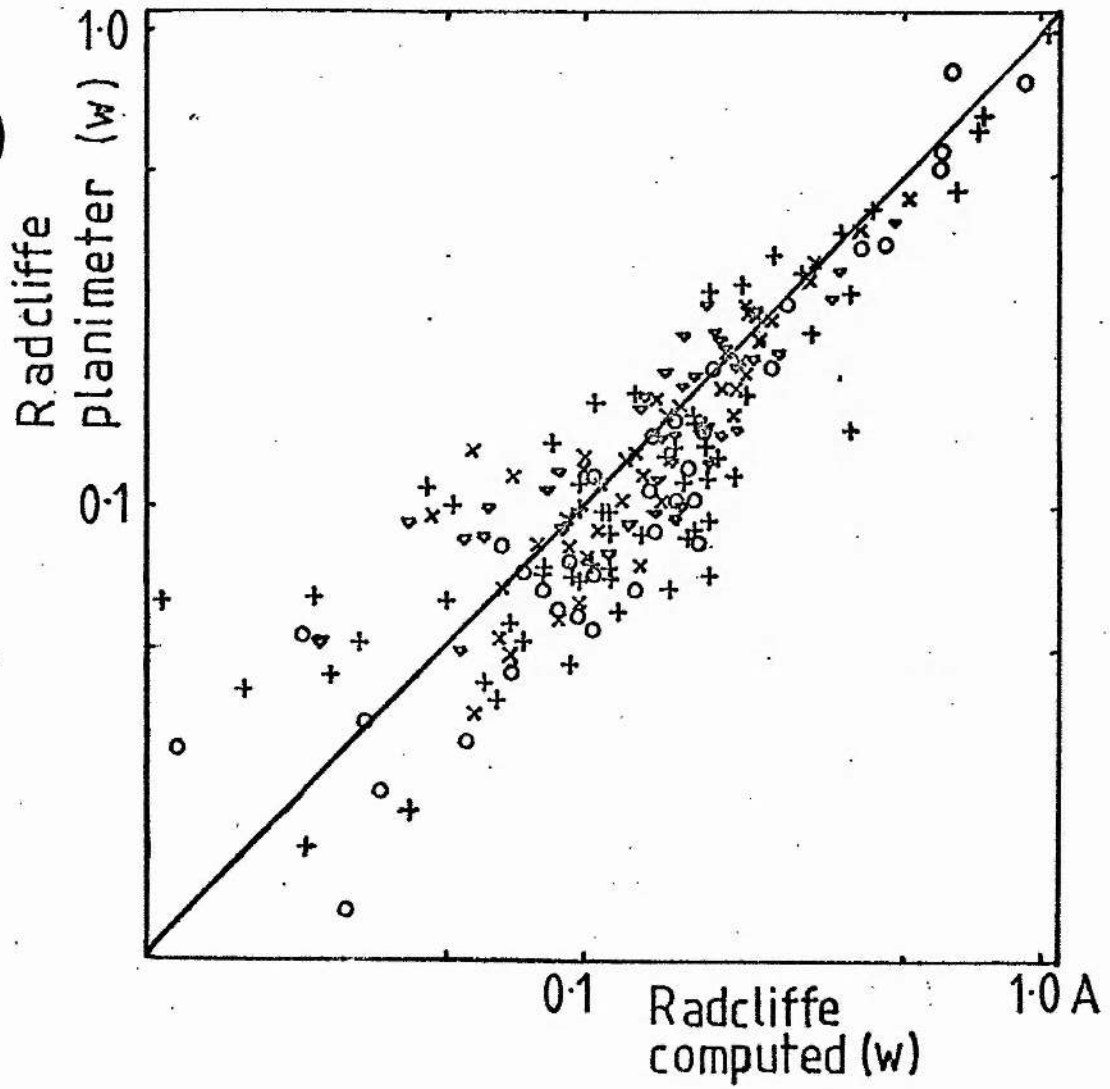

Comments as for figure 5·9

Figure 5·12 ESO (planimeter) against Radcliffe

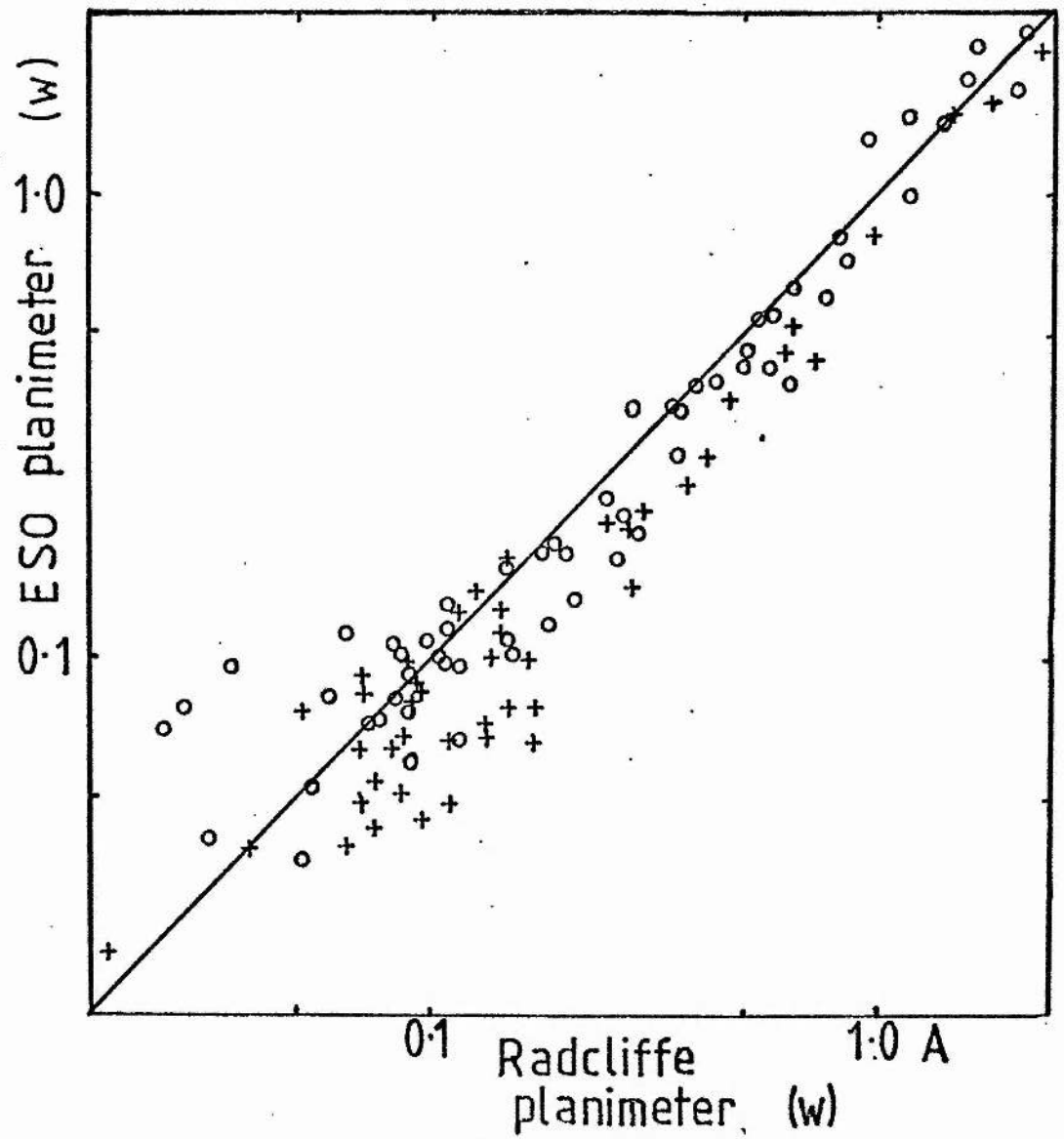

Comments as for figure 5·9

5.5 Discussion

In figures 5.9 to 5.12 the equivalent widths measured here and those determined by Hill (1965) on the Coudé spectrograph are compared. Figure 5.12 confirms the finding of Schönberner & Wolf (1974) that there are no significant differences between the ESO Coudé spectrograph and the Radcliffe Coudé spectrograph. Their technique of using log w for the graph was followed, since this relates directly to the abundance determination, and shows clearly that the smaller equivalent widths have 'larger' errors, and will give a poorer detrmination of abundance. There were slight differences between the measurements here but none were significant, except that it appeared that the equivalent widths of Hill were lower for the strongest lines. This might have been caused either by an underestimation of the strength of the wings of the He I lines, or a lower continuum, possibly caused by underestimating the number of weak lines in the spectrum. Due to the slight variation in individual equivalent widths from the various spectra, the mean equivalent width was used for the detrmination of abundances.

Some variation as shown in figure 5.13 (taken from Lynas-Gray, Walker, Hill & Kaufmann, 1979) is possibly due to intrinsic spectral variation. The lines displayed are shown in table 5.6. The error bar shown gives the quantum noise at the continuum level. There is an interval of approximately six hours between the first and second spectrum, with about one hour between the second and third. The variation in line 3 of figure 5.13 is particularly pronounced over the period of one hour. The cause for this variation, and that of the other lines with colons in table 5.5 is not known, but it seems unlikely that this can be

just an instrumental effect. The change in line profile could be caused by slight mass motion at certain phases of the star's variability, but this must be investigated. The phenomenon of equivalent width variation does not seem limited to any one ion or group of ions, and it does not affect all the lines in any ion, or even all the lines in one multiplet of the ion. These variations must be investigated further, so that their extent, nature and time-scale may eventually be understood.

Table 5.6 Lines displayed in figure 5.13

Line 1	4549.49	Fe II	(38)	main component
	4549.62	Ti II	(82)	
2	4552.62	Si III	(2)	
3	4555.02	Cr II	(44)	
	4555.89	Fe II	(37)	
4	4558.66	Cr II	(44)	main component
	4558.83	Cr II	(44)	

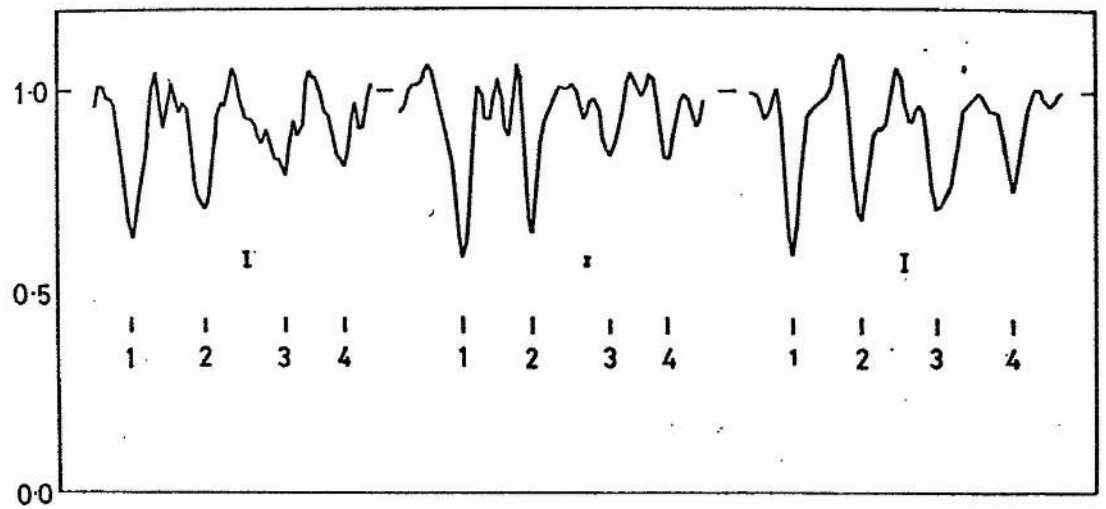

Figure 513 Line variation in AAT spectra

6 ATMOSPHERIC MODEL AND ABUNDANCE ANALYSIS

6.1 Theory of Hunger/Van Blerkom model

Hunger & Van Blerkom (1967) computed a pure helium model stellar atmosphere, for an effective temperature of 18000°K and log g = 3.5. The techniques used were discussed there and also the consequences of such an atmosphere. The main points are briefly summarised here, and equations taken from that paper are given the number in the paper preceded by HB. The usual assumptions were made for the model, i.e. that of local thermodynamic equilibrium (LTE), hydrostatic equilibrium, radiative equilibrium and a plane parallel atmosphere. The equation of hydrostatic equilibrium was as follows :-

$$\frac{dP_G}{d\bar{\tau}} = \frac{g}{\bar{\kappa}} - \frac{\sigma_R T_{eff}^4}{c} \qquad \text{HB 1}$$

where $\bar{\kappa}$ is the Rosseland mean opacity

σ_R is the Steffan-Boltzmann constant

It was solved using the Hammings predictor-corrector-method (Ralston & Wilf, 1960). For the radiative equilibrium (flux F constant with optical depth) the iteration schemes of Lucy (1964) and Unsöld (1955) were used for flux constancy.

The temperature correction was given by :-

$$\Delta B = \frac{\kappa_J}{\kappa_p} J - B - \frac{\kappa_J}{\kappa_p}\left\{\frac{1}{2}\Delta F(0) + \frac{3}{4}\int_0^{\bar{\tau}} \frac{\bar{\kappa}_F}{\bar{\kappa}} \Delta F \, d\bar{\tau}\right\} \qquad \text{HB 2}$$

where $$\kappa_J = \frac{1}{J}\int_0^\infty \kappa_\nu J_\nu \, d\nu \qquad \kappa_p = \frac{1}{B}\int_0^\infty \kappa_\nu B_\nu \, d\nu \qquad \text{HB 3}$$

$$\kappa_F = \frac{1}{F}\int_0^\infty (\kappa_\nu + \sigma) F_\nu \, d\nu \qquad \text{HB 3}$$

B, J, F were the integrated Planck function, mean intensity and flux.

Since $$B = \int_0^\infty F_\nu \, d\nu = \frac{\sigma}{\pi} T_{eff}^4$$

it can be seen that by calculating the flux, a trial solutiom of $B(\bar{\tau})$ can be corrected by HB 2. Hunger & Wan Blerkom noted that :-

$$\Delta F = \frac{\sigma}{\pi} T_{eff}^4 - \int_0^\infty F_\nu(\bar{\tau}) \, d\nu$$

is the difference between the postulated flux and the flux obtained by a trial solution with a given $B(\bar{\tau})$.

The Saha equations were used for the relationship between P and T, involving the mass fractions of helium X(He I), X(He II) and X(He III).

$$\frac{X(\text{He II}).P_e}{X(\text{He I})} = \left(\frac{2\pi m}{h^2}\right)^{3/2} (kT)^{5/2} \frac{2U_1}{U_0} e^{-\chi_{HeI}/kT} \qquad \text{HB 4}$$

$$\frac{X(\text{He III}).P_e}{X(\text{He II})} = \left(\frac{2\pi m}{h^2}\right)^{3/2} (kT)^{5/2} \frac{2U_2}{U_1} e^{-\chi_{HeII}/kT} \qquad \text{HB 5}$$

U_0, U_1, U_2 are the partition functions for neutral, singly and doubly ionised helium; χ_{HeI} and χ_{HeII} are the ionisation potentials and P_e is the electron pressure.

An iterative solution after Böhm & Deinzer (1965) was used, starting from the assumption that the electron pressure was due

only to electrons from He II, i.e. X(He III) = 0.

The source function was as follows :-

$$S_\nu = \frac{\kappa_\nu}{\kappa_\nu + \sigma} B_\nu + \frac{\sigma}{\kappa_\nu + \sigma} J_\nu \qquad \text{HB 6}$$

where σ is the scattering coefficient, B_ν and J_ν are the monochromatic Planck function and mean intensity respectively. Hunger & Van Blerkom noted that there was a well defined boundary ($\tau = \tau_\nu^*$) which separated the scattering dominated layers from the absorption dominated layers. In the uppermost layer the grey solution for the source function was a good approximation. In linear form this was :-

$$S_\nu = \frac{1}{2} F_\nu^* \left(1 + \frac{3}{2} \tau_\nu\right) \qquad \text{HB 7}$$

where F_ν^* is the flux at the bottom of the scattering layer, consisting of outgoing flux minus a proportion which is back-scattered. For the source function a lambda (Λ)- iteration method by Mihalas (1965) was used.

The most important problem with the helium atmosphere must be the opacity. In Hunger & Van Blerkom only the bound-free and free-free transitions of He I and He II were used, as well as electron scattering. The He I absorption cross-sections were shown in their table 3. They stated that for the bound-free transitions with terms n = 1 and n = 2 a simple interpolation formula was adopted. For n = 3 the transitions were computed from the quantum defects, using the method of Burgess & Seaton (1960). For He II they noted that the absorption coefficient will be hydrogenic. They used, for bound-free transitions, the

Gaunt factors of Gingerlich (1964) and for free-free transitions, those of Menzel & Pekeris (1935). Hunger & Van Blerkom's values for the opacity agree well with those values calculated by the Kyoto group (Ueno et al., 1954), see figure 2 of Hunger & Van Blerkom (1967).

It was found that the final model departed from the grey approximation at mean optical depths of less than one (HB figure 5). Hunger & Van Blerkom noted that the low opacity of the pure helium atmosphere resulted in a higher pressure than for a normal main sequence star (HB figure 6). In the visible region of the spectrum they found little difference in the emergent flux between the pure helium star and a main sequence star, but shortward of 2000A the flux in the main sequence star was higher until it reached the Lyman limit at 912A, where it was cut off, and the helium star flux continued to the helium limit at 504A. This resulted in the UBV colours and the bolometric correctiom being very nearly the same for a helium star as for a main sequence star with the same T_{eff} and log g.

Wolf (1973) noted that the model was modified to contain in addition to He I and He II, a contribution to the absorption coefficient from He^-, from free-free transitions (John, 1968), though the model was still essentially that of Hunger & Van Blerkom. Wolf used the method of Avrett & Loesser (1963) for the determination of the source function. Schönberner & Wolf (1974) modified the program to contain a contribution to the opacity from C I, C II, C III, N I, N II, N III (Peach, 1970).

Schönberner (1973) gave details of the line program used in the model. Most important were the lines due to He I, 4471A and 4388A, which had parameters obtained from Barnard et al.

(1969, 1970), with the forbidden components included. The 'f' values were taken from Green et al. (1966). For other helium lines (4121A, 4438A, 4713A) Schönberner used data from Jones, Benett & Griem (1971). In the metal lines he mainly used a Voigt profile for the line absorption coefficient.

All the necessary work for the theoretical model had thus been done. Several suitable models had been generated for the differential analysis of HD 168476 relative to HD 124448 (Schönberner & Wolf, 1974) so that it was necessary to generate very few new grid points. On one visit to the groups in Kiel and Berlin, Dr. A. E. Lynas-Gray accompanied the writer and assisted with the computing, with the aid and direction of Dr. D. Schönberner (Kiel). Dr. Schönberner then computed any new data that was necessary for the model determination. A further visit was made by the writer to Kiel, Dr. Schönberner and the writer produced curves of growth for all ions for the abundance analysis.

6.2 Fine analysis - Introduction

In order to perform a fine analysis for HD 168476 certain parameters must be determined, namely the effective temperature, the surface gravity, the microturbulent velocity, the rotational velocity and the helium and carbon abundances. The values determined in a coarse analysis (e.g. Hill, 1965) could be used as a first approximation, but since the technique of analysis (e.g. Hunger & Van Blerkom, 1967) has improved in recent years, it was decided to redetermine the parameters with the Schönberner & Wolf (1974) values as a starting point, and using mainly the ESO spectra. Schönberner & Wolf showed that in the case of HD 124448 there was no systematic difference in equivalent width

between the results obtained on the Radcliffe Coudé and the results obtained on the ESO Coudé; the results in section 5.5 confirmed this.

An element with many weak lines in the spectrum was used to determine the microturbulent velocity, in this case nitrogen. The profiles of the helium lines are indicators of temperature and gravity, as are ionisation equilibria, here those of silicon and sulphur were used. The carbon abundance is best determined from the weak lines which are more sensitive to changes in abundance than those lines on the saturation portion of the curve of growth. The strong lines of carbon are a useful indicator of the rotational velocity which will in the case of the ESO spectrum, contain a certain amount of broadening due to the instrumental profile, which is not removed.

6.3 N II lines - microturbulent velocity

All possible nitrogen lines were measured in the first instance, although not all the lines were computed theoretically. From those lines measured, any that were obviously blended were removed and for the rest curves of growth were plotted for several microturbulent velocities (v_t), at different temperatures. Figure 6.1 shows an example of the curves of growth for different microturbulent velocities. The microturbulent velocity is very nearly independent of gravity so that $\log g = 2.00$ was used throughout. At an effective temperature of 14000°K v_t of 0, 5, 10, 15, 20 km/s were used and at 16000°K only the first four were computed.

Originally twenty-four lines were measured but three were conspicuously blended and were not used. Of the remainder five

were suspected to be slightly blended from the difference in their abundances to those of the other lines and so were not used in the final derivation. The abundances from the remaining fifteen lines showed a minimum error in log(abundance) at 14000°K when the microturbulent velocity was 10 km/s and at 16000°K when the microturbulent velocity was 15 km/s. Table 6.1 shows the values obtained for the log n of each line at the various values of v_t used.

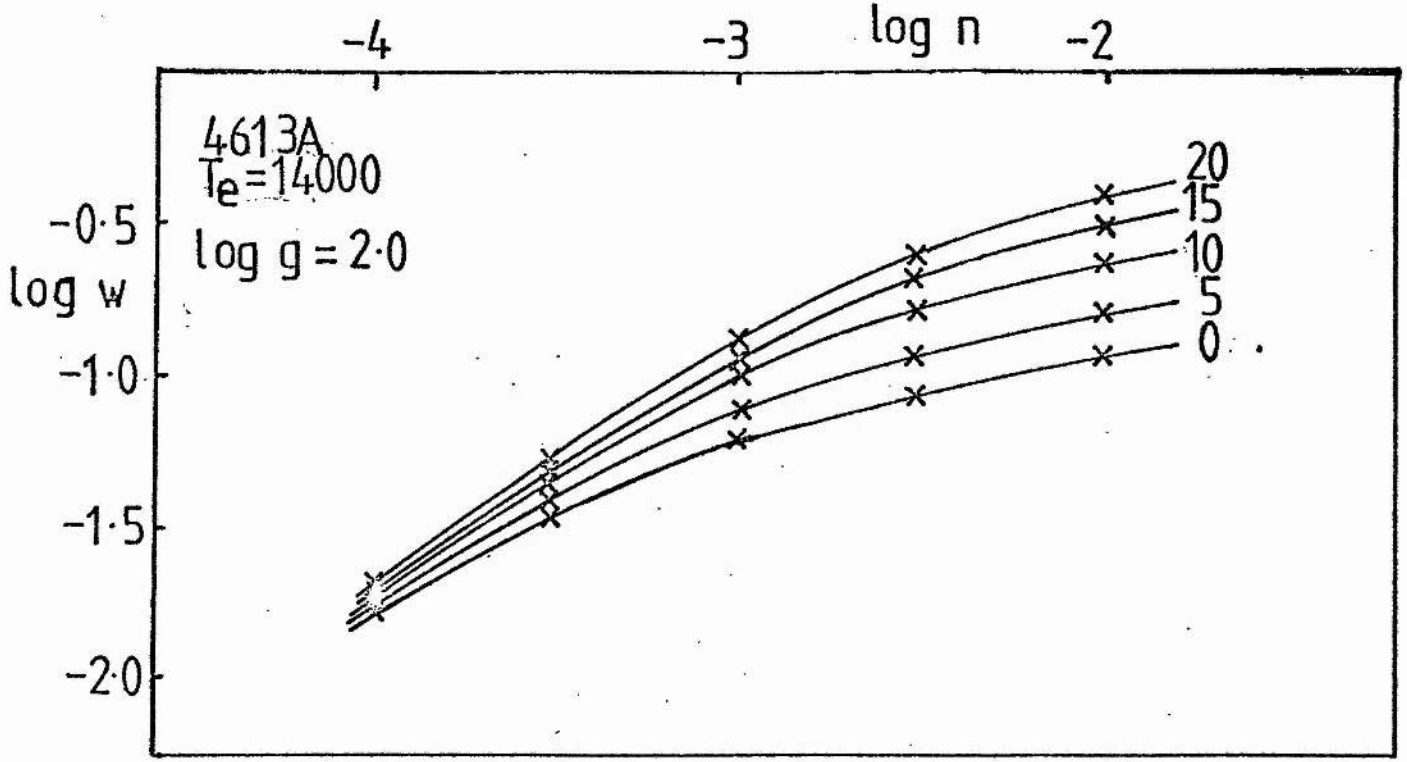

Figure 6·1 Curves of growth for N II at indicated v_t

Table 6.1 Determination of microturbulent velocity from N II lines from log n

	λ (A)	W_λ (mA)[b]	log n microturbulent velocity (km/s) 0	5	10	15	20
T_e=14000	3842.18	36	-2.52	-2.61	-2.76	-2.80	-2.86
	3995.00	317	-1.80	-1.94	-2.58	-3.07	-3.34
	4041.31	76	-2.67	-2.92	-3.12	-3.23	-3.31
	4095.90	39	-2.25	-2.41	-2.56	-2.63	-2.67
	4176.16	49	-2.84	-3.02	-3.16	-3.25	-3.29
	4227.74	35	-2.42	-2.54	-2.66	-2.71	-2.74
	4431.82	52	-1.94	-2.02	-2.25	-2.30	-2.37
	4432.74	89	-2.12	-2.39	-2.58	-2.71	-2.77
	4442.02	44	-2.56	-2.66	-2.80	-2.88	-2.92
	4447.03	114	-2.33	-2.83	-3.20	-3.33	-3.40
	4530.41	62	-2.48	-2.71	-2.88	-3.00	-3.04
	4607.16	101	-2.54	-2.97	-3.24	-3.35	-3.39
	4613.87	119	-1.92	-2.49	-2.84	-3.00	-3.08
	4630.54	205	-1.96	-2.42	-3.14	-3.43	-3.54
	4643.09	164	-1.88	-2.34	-2.91	-3.10	-3.21
15 lines							
log n			-2.28	-2.55	-2.85	-2.99	-3.06
ε			±0.33	±0.32	±0.29	±0.32	±0.33
T_e=16000	3842.18		-2.69	-2.90	-3.08	-3.18	
	3995.00		-1.86	-1.94	-2.31	-2.83	
	4041.31		-2.70	-3.07	-3.41	-3.60	
	4095.90		-2.50	-2.76	-2.95	-3.09	
	4176.16		-3.02	-3.25	-3.52	-3.67	
	4227.74		-2.62	-2.82	-3.00	-3.08	
	4431.82		-2.14	-2.36	-2.62	-2.75	
	4432.74		-2.23	-2.52	-2.89	-3.08	
	4442.02		-2.76	-3.00	-3.19	-3.33	
	4447.03		-2.30	-2.76	-3.22	-3.47	
	4530.41		-2.64	-2.94	-3.23	-3.39	
	4607.16		-2.38	-2.83	-3.23	-3.42	
	4613.87		-1.84	-2.31	-2.86	-3.10	
	4630.54		-1.97	-2.22	-2.88	-3.26	
	4643.09		-1.86	-2.13	-2.78	-3.08	
15 lines							
log n			-2.37	-2.65	-3.01	-3.22	
ε			±0.38	±0.38	±0.31	±0.26	

6.4 He I lines - effective temperature and surface gravity

The profiles of seven helium lines could be computed theoretically, those of the three strong helium lines 4471A, 4388A and 4026A, and those of four weak lines 4437A, 4120A, 3964A and 3888A. The profiles of the strong helium lines are a much better indicator of effective temperature and gravity, especially 4471A with its forbidden component at 4469A.

On the spectrum plot of the four plates taken at ESO the continuum was drawn in. Then the height of the line and the continuum at many points on the helium line profile was measured so that the profile could be plotted with a normalised continuum. Theoretical profiles were plotted on the same scale, with profiles of the same temperature on the same sheet of paper, so that an interpolation in log g could be made. Profiles were computed for the lines noted above with $13000^{\circ}K \leq T_{eff} \leq 16000^{\circ}K$, $1.0 \leq \log g \leq 2.0$. Several of the profiles are shown in figures 6.2 to 6.4, for the line 4471A. The helium line profiles all gave a good fit for $T_e = 13000^{\circ}K$ log $g = 1.0 \pm 0.2$; $T_e = 13500^{\circ}K$ log $g = 1.2 \pm 0.2$ and an excellent fit for $T_e = 14000^{\circ}K$ log $g = 1.5 \pm 0.2$. The profiles were not dependent on microturbulent velocity or rotational velocity and showed no noticable variation for a carbon abundance in the range 0.01 to 0.05 (by number). Figures 6.5 and 6.6 show the observed profiles for the AAT spectrum and the Radcliffe spectrum with the theoretical profile for $T_e = 14000^{\circ}K$, log $g = 1.5$. The line centre on the Radcliffe spectrum is deeper than the theoretical mainly due to noise, but in the AAT spectrum the line will be deeper than the ESO profile due to the removal of the instrumental profile.

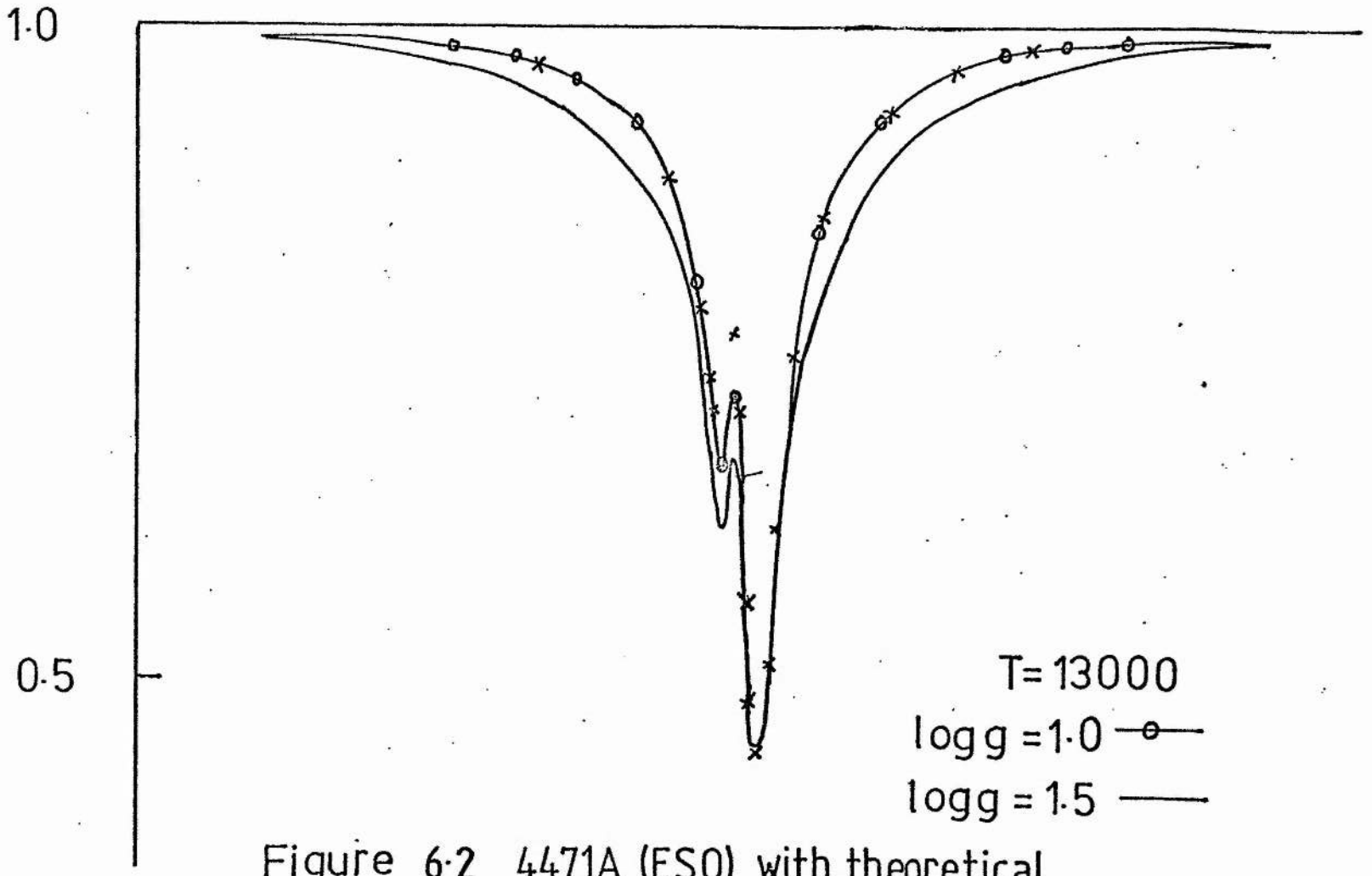

Figure 6·2 4471A (ESO) with theoretical profiles at 13000°K

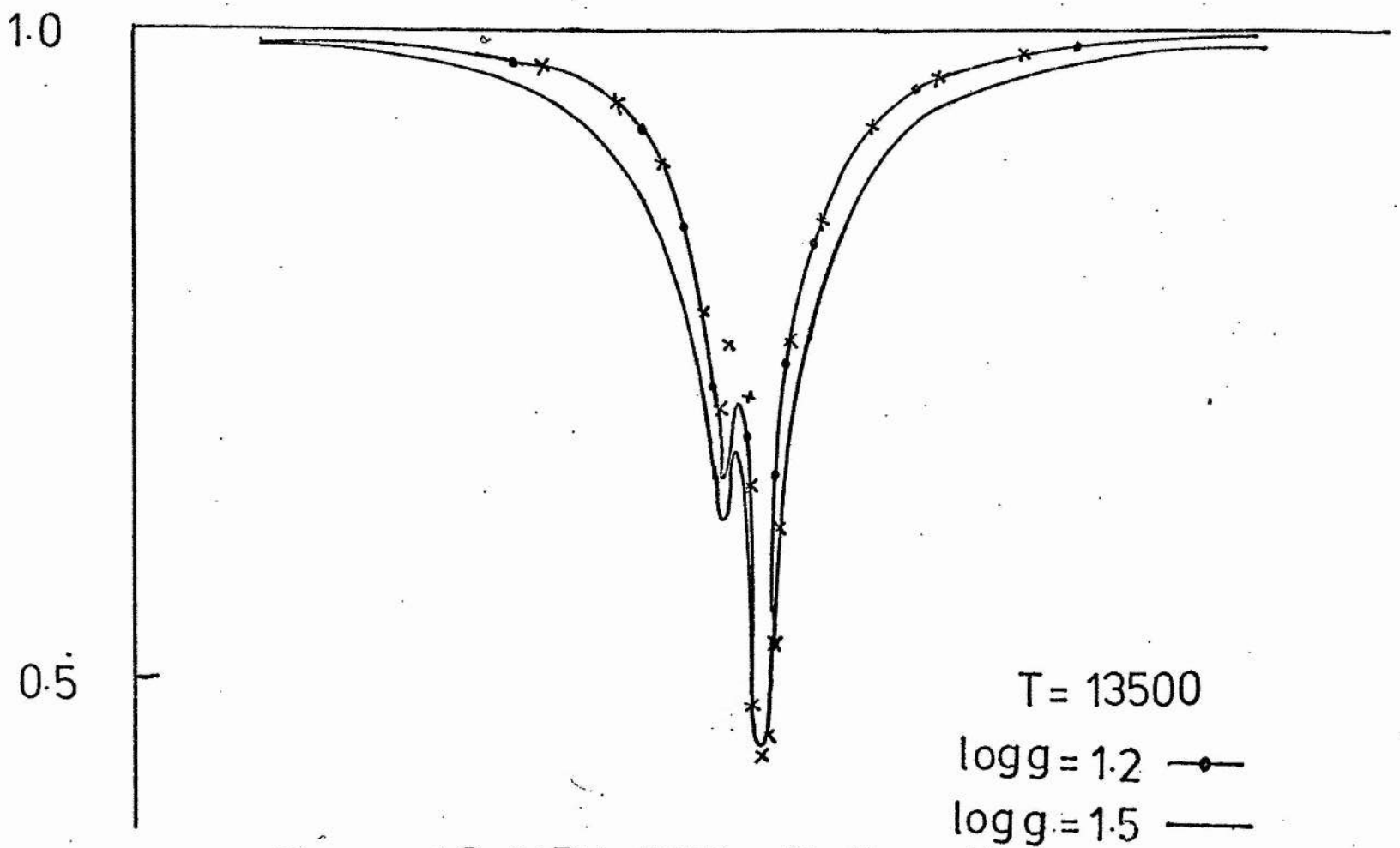

Figure 6·3 4471A (ESO) with theoretical profiles at 13500° K

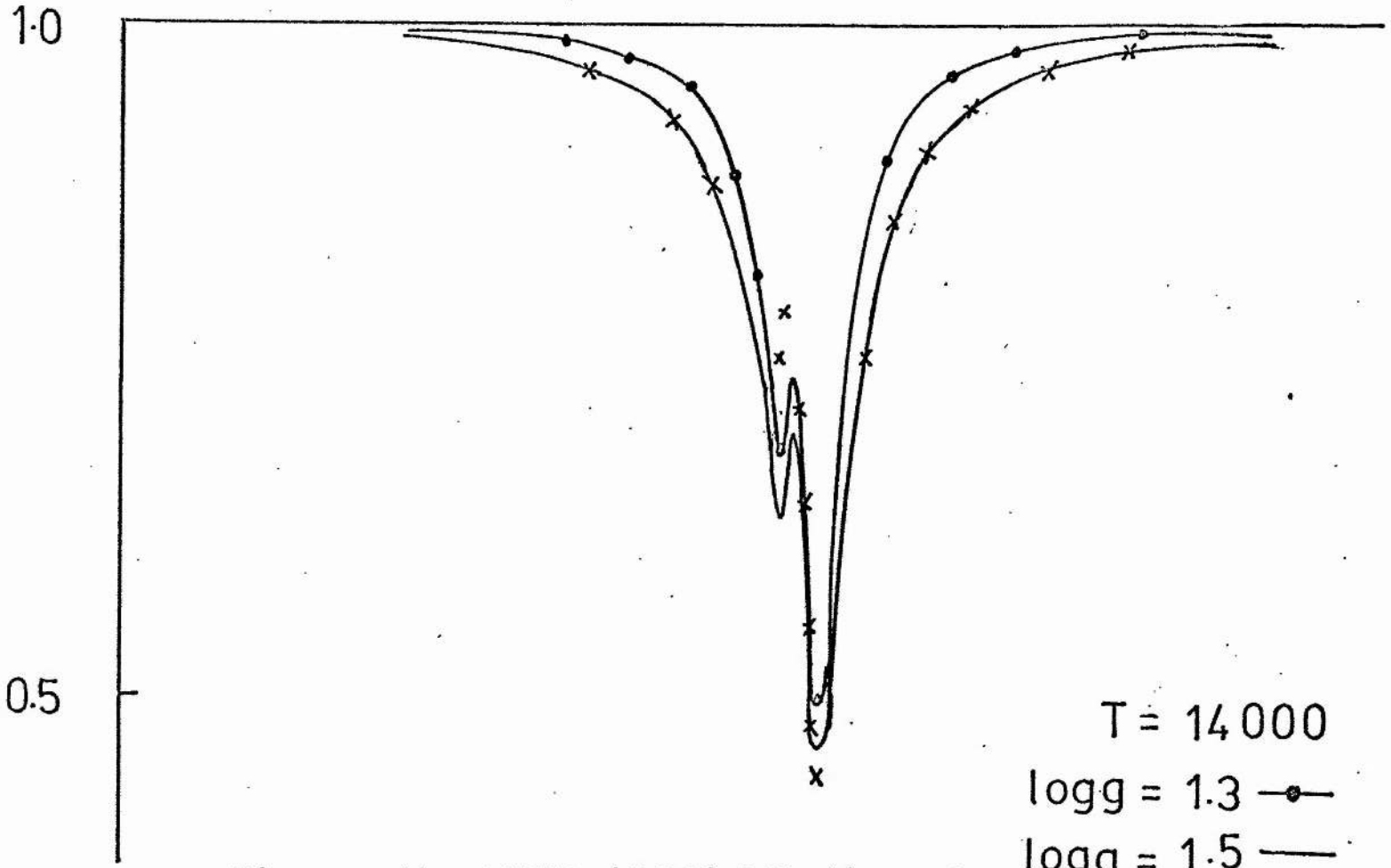

Figure 64 4471A (ESO) with theoretical profiles at 14000°K

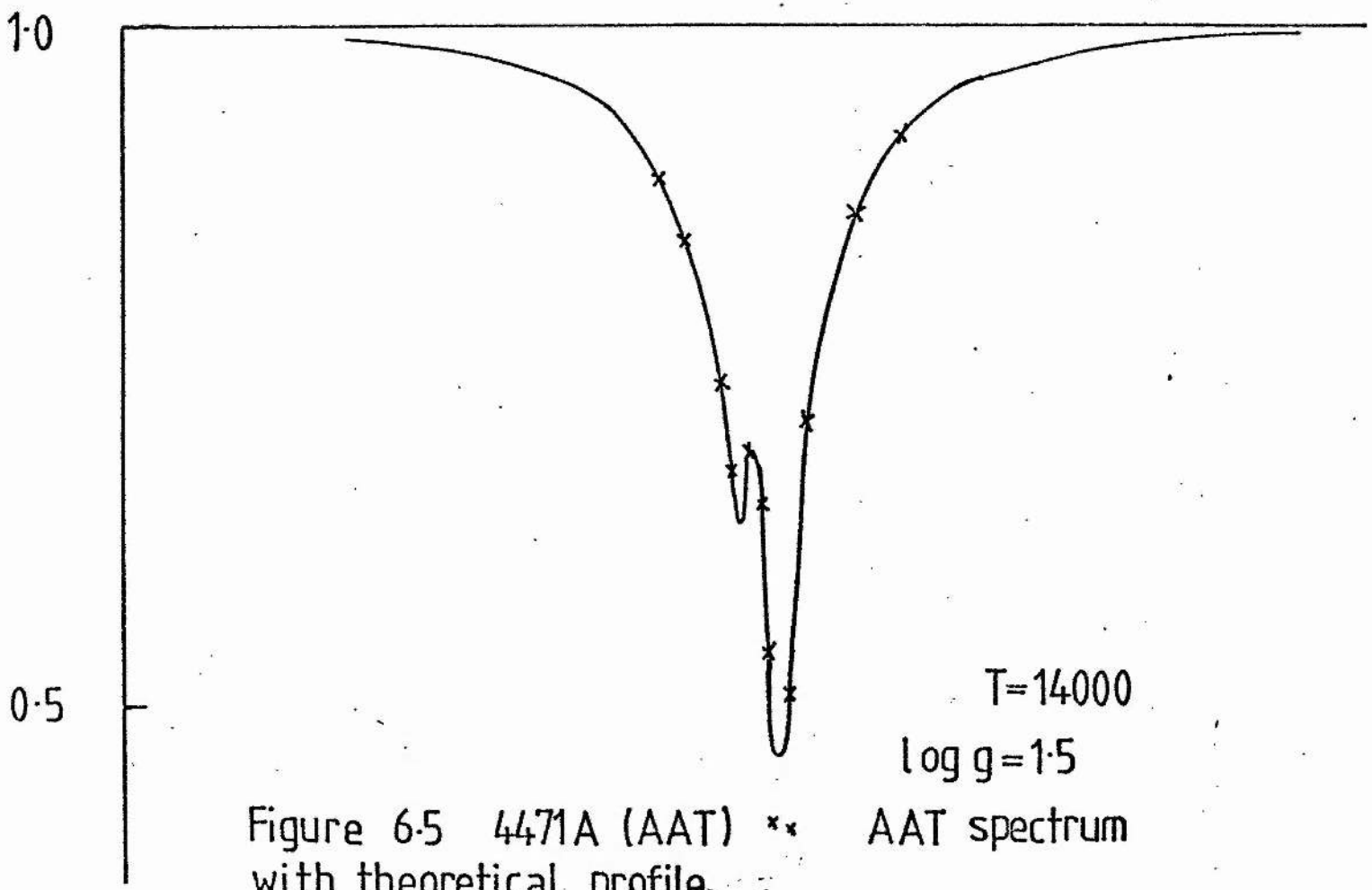

Figure 6·5 4471A (AAT) ×× with theoretical profile at 14000°K

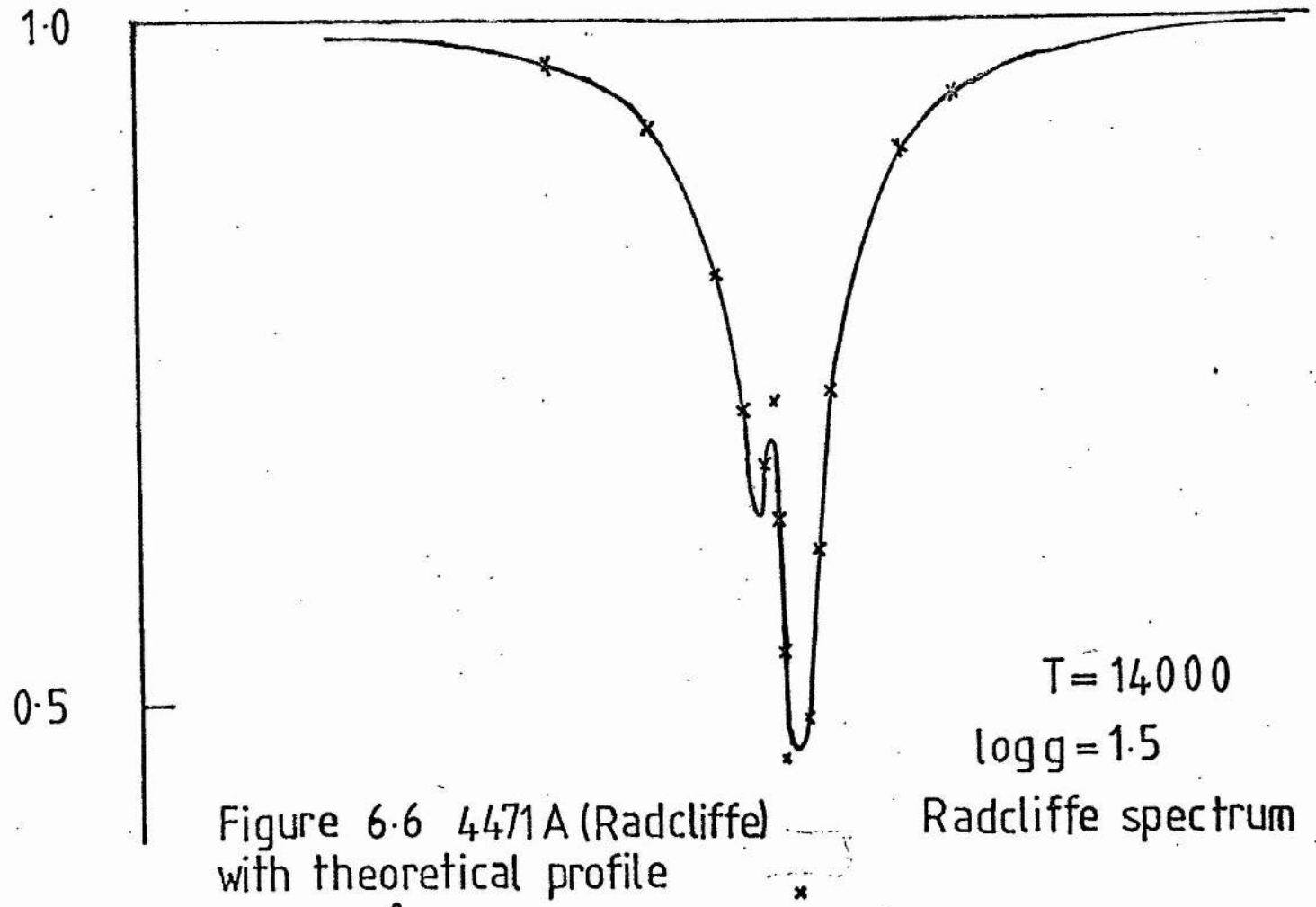

Figure 6·6 4471 A (Radcliffe) with theoretical profile at 14000°K

6.5 Ionisation equilibrium - effective temperature and surface gravity

At a given temperature and log g, the abundance of an element is found from its two stages of ionisation. At a given effective temperature, this is usually done for several different gravities so that plotting abundances against gravity for the two stages of ionisation gives more accurately the value of log g where the abundances are equal. This is done below for S II/S III and Si II/Si III.

6.5a S II/S III

Several weak lines of S III were found in the spectrum and the ionisation eqilibrium of this element was used to determine T_e and log g. The models were calculated for a carbon abundance of 0.01 by number and a microturbulent velocity of 5 km/s. The calculations were made before the microturbulent velocity was discovered to be 10 km/s, but since a small variation in v_t does not affect the line strengths (Schönberner, 1979) the values that had been obtained at 5 km/s were used, with half weight. A list of lines used, with the abundances found from the curves of growth for given effective temperature and log g are given in table 6.2. 35 S II lines were measured, from which a maximum of 30 were used, depending on the precise model program run. Seven S III lines were measured of which four proved unblended and suitable for the abundances from curves of growth to be obtained. From the resulting graphs (figure 6.7) it can be seen that at 13500°K agreement in log n is found at log g = 0.90 $\pm$ 0.2, and at 14000°K for log g = 1.38 $\pm$ 0.2.

Table 6.2 Abundances determined from S II and SIII lines

T_e / log g	λ (A)	w_{ob} (mA)	log n 13500 1.2	13500 1.5	13500 1.3	14000 1.5	14000 2.0
S II	3802.65	76	-4.36	-4.46	-4.09		
	3860.15	63	-4.80	-4.92	-4.55	-4.72	-4.85
	3892.32	134	-4.00	-4.11	-3.62		
	3923.48	118	-4.68	-4.77	-4.37		
	3946.98	92	-3.89	-4.02	-3.64	-3.85	-4.00
	3950.42	58	-4.46	-4.55	-4.20	-4.40	-4.54
	3963.13	88	-4.14	-4.27	-3.92	-4.09	-4.23
	3979.86	72	-4.57	-4.68	-4.32		
	3990.94	52	-4.92	-5.00	-4.66	-4.85	-5.00
	3998.79	108	-4.43	-4.54	-4.19		
	4028.79	81	-4.64	-4.96	-4.59	-4.77	-4.92
	4033.81	86	-4.89	-5.01	-4.70		
	4142.29	103	-4.82	-4.92	-4.52	-4.80	-4.92
	4153.10	129	-4.85	-4.92	-4.52	-4.77	-4.92
	4162.70	188	-4.09	-4.25	-4.66	-4.00	-4.23
	4165.11	28	-5.07		-4.82		
	4189.71	87	-4.89	-5.00	-4.62	-4.82	-4.96
	4213.5	32	-4.24	-4.32	-4.00	-4.15	-4.29
	4217.23	49	-5.08		-4.85	-5.02	-5.21
	4257.42	53	-4.92	-4.04	-4.70		
	4259.18	85	-4.66	-4.77	-4.46		
	4278.54	71	-4.77	-4.85	-4.54		
	4294.43	158	-4.19	-4.31	-4.89		
	4391.84	45	-4.75	-4.85	-4.51	-4.68	-4.82
	4402.86	55	-3.92	-4.02	-3.68	-3.82	-3.96
	4463.58	126	-4.18	-4.28	-3.85	-4.10	-4.28
	4483.42	94	-4.25	-4.33	-4.00	-4.17	-4.32
	4524.95	207	-4.39	-4.51	-4.08	-4.31	-4.43
	4656.74	104	-4.68	-4.75	-4.38	-4.55	-4.70
	4668.58	116	-4.42	-4.51	-4.12	-4.32	-4.48
$\overline{\log n}$			-4.53	-4.60	-4.27	-4.43	-4.58
ε			±0.35	±0.33	±0.37	±0.37	±0.37
N			30	28	30	19	19
S III	4253.59	28	-4.82	-4.57	-4.82	-4.77	-4.50
	4284.99	39	-4.17	-4.04	-4.28	-4.24	-4.00
	4340.30	32	-3.85	-3.72	-4.00	-3.92	-3.64
	4361.53	25	-4.02	-3.85	-4.25	-4.08	-3.82
$\overline{\log n}$			-4.22	-4.05	-4.34	-4.25	-3.99
ε			±0.43	±0.37	±0.35	±0.37	±0.37

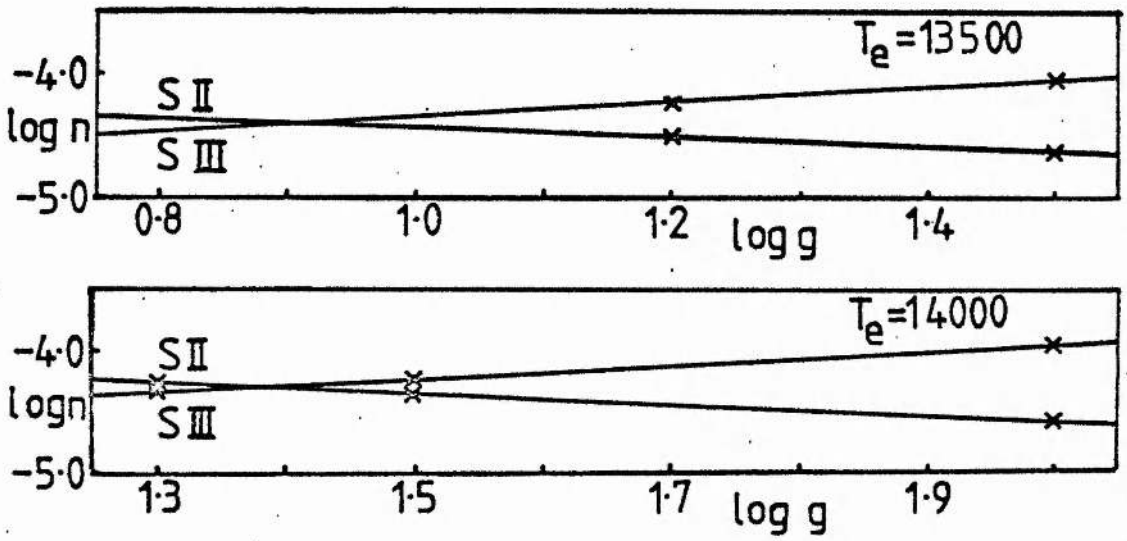

Figure 6·7 S II/S III ionisation equilibria

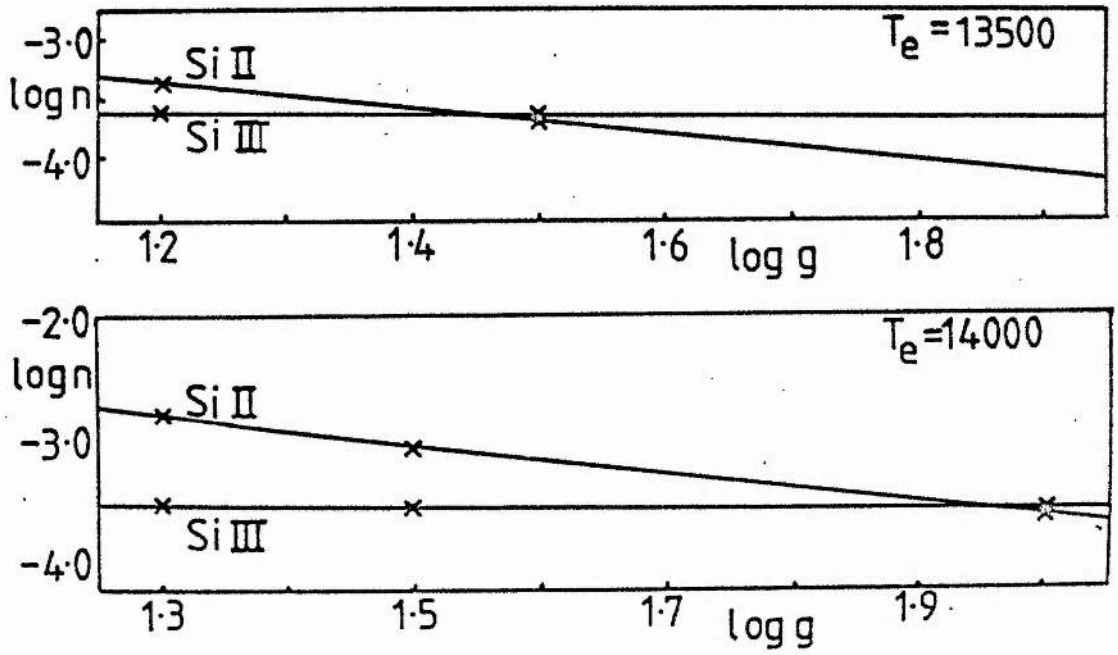

Figure 6·8 Si II/Si III ionisation equilibria

6.5b Si II/Si III

For this element two stages of ionisation were present, and models were calculated for a fixed carbon abundance of 0.01 by number and a microturbulent velocity of 5 km/s, as noted in section 6.5a. The microturbulence was later discovered to be too low and a value of 10 km/s more appropriate. However, Schönberner (1979) reported that a differential correction could be made by adding 400° to the temperature. The list of lines is given in table 6.3 together with the abundances determined from the curves of growth for the given effective temperatures and log g. Five lines of Si II and five lines of Si III were used, none of which were significantly affected by blending. It had been noted that the abundances for the lines of Si II 4128A and 4130A seemed to be lower than the others, but this was found to be a consequence only of the low microturbulent velocity (v_t = 10 km/s is shown for T_e = 13500°K, log g = 1.5 in table 6.3). Hence all the lines were used for the determination of the mean log n. From figure 6.8 it was found that at 13500°K there was agreement at log g = 1.42 $\pm$ 0.2 and at 14000°K for log g = 1.94 $\pm$ 0.2. With the differential correction for microturbulence applied this gives agreement at 13900°K, log g = 1.42 and at 14400°K, log g = 1.94.

6.6 C II lines - carbon abundance and rotational velocity

For the carbon abundance a maximum of eleven lines were suitable in the model calculations, although not all the lines were available on all the models. A range of models with 13000°K $\leq T_e \leq$ 16000°K and 1.0 $\leq$ log g $\leq$ 2.0 were used and the microturbulent velocity was either 5 km/s or 10 km/s. It was found that the abundances were almost independent of temperature

Table 6.3 Abundances determined from Si II and Si III lines

T_e / log g / v_t	λ (A)	W_{obs} (mA)	log n 13500 1.2	13500 1.5	14000 1.3	14000 1.5	14000 2.0	13500 1.5 10
Si II	3853.66	277	-3.11	-3.44	-2.50	-2.77	-3.48	-5.00
	3856.02	538	-3.07	-3.42	-2.54	-2.80	-3.48	-4.30
	3862.60	420	-2.85	-3.21	-2.32	-2.60	-3.27	-4.23
	4128.07	453	-3.75	-4.02	-3.25	-3.47	-4.01	-4.38
	4130.89	438	-4.01	-4.28	-4.54	-3.77	-4.28	-4.70
$\overline{\log n}$			-3.36	-3.68	-2.83	-3.08	-3.70	-4.52
			±0.49	±0.45	±0.53	±0.51	±0.42	±0.32
Si III	3971.41	96	-3.29	-3.34	-3.24	-3.27	-3.38	-3.70
	3976.11	114	-3.40	-3.44	-3.34	-3.42	-3.50	-3.89
	4552.62	196	-3.43	-3.39	-3.38	-3.38	-3.46	-4.06
	4567.82	136	-3.77	-3.80	-3.75	-3.75	-3.80	-4.26
	4574.76	64	-4.10	-4.20	-4.16	-4.18	-4.14	-4.36
$\overline{\log n}$			-3.60	-3.63	-3.57	-3.60	-3.65	-4.05
			±0.33	±0.36	±0.38	±0.37	±0.32	±0.27

Table 6.4 Abundances determined from C II lines

T_e / log g / v_t	λ (A)	W_{obs} (mA)	log n 13000 1.0 5	13000 1.0 10	13500 1.5 5	13500 1.5 10	14000 1.5 5	14000 1.5 10
C II	3876.3	393	-1.55	-1.89	-1.82	-2.03	-1.75	-2.01
	3920.69	545	-1.20	-1.68	-1.59	-1.82	-1.25	-1.68
	3980.35	79	-1.40	-1.66	-1.54	-1.77	-1.52	-1.77
	4267.13	801	-2.11	-2.25	-2.22	-2.33	-2.09	-2.19
	4313.10	83	-1.82	-1.72	-1.62	-1.82	-1.59	-1.82
	4318.60	40	-2.16	-2.30	-2.18	-2.28	-2.24	-2.39
	4372.49	116	-1.62	-1.89	-1.82	-2.01	-1.80	-2.03
	4374.27	105	-1.64	-2.11	-1.82	-2.16	-1.80	-2.22
$\overline{\log n}$			-1.69	-1.94	-1.83	-2.03	-1.75	-2.01
			±0.33	±0.26	±0.26	±0.22	±0.31	±0.25

over the range considered and most dependent on microturbulent velocity. At a log g of 1.5 for v_t = 10 km/s the log (abundance) of carbon was determined as -2.02 i.e. the abundance was 0.01 by number (see table 6.4). This value agrees with the value assumed for the model calculations made so far and so no correction is necessary for a different carbon abundance.

The profiles of the lines at 3918A, 3920A and 4267A can be used to determine the rotational velocity. Theoretical profiles were calculated for 0 km/s, 5 km/s, 12.5 km/s and 20 km/s. The observed lines were all slightly deeper than the theoretical lines due, it was suspected, to blending with other lines (3918A was not used to determine the abundance due to blending). The profile at 20 km/s fitted the observed profiles quite well in the middle range of the line profiles.

6.7 Results

The pairs of values of T_e and log g determined from the various elements are shown in figure 6.9. For log g, the error was taken from that determined for the ionisation equilibria and helium lines. For the temperature, the error was found from the coincidence of the sulphur ionisation equilibrium line and the helium profiles line. The final parameters for the adopted model are :-

$$T_e = 14000^{\circ}K \pm 300$$

$$\log g = 1.5 \pm 0.2$$

$$n_{He} = 0.99$$

$$n_C = 0.01 \; {}^{+0.007}_{-0.005}$$

$$v_t = 10 \text{ km/s} \pm 5$$

$$v_{rot} = 20 \text{ km/s} \pm 20$$

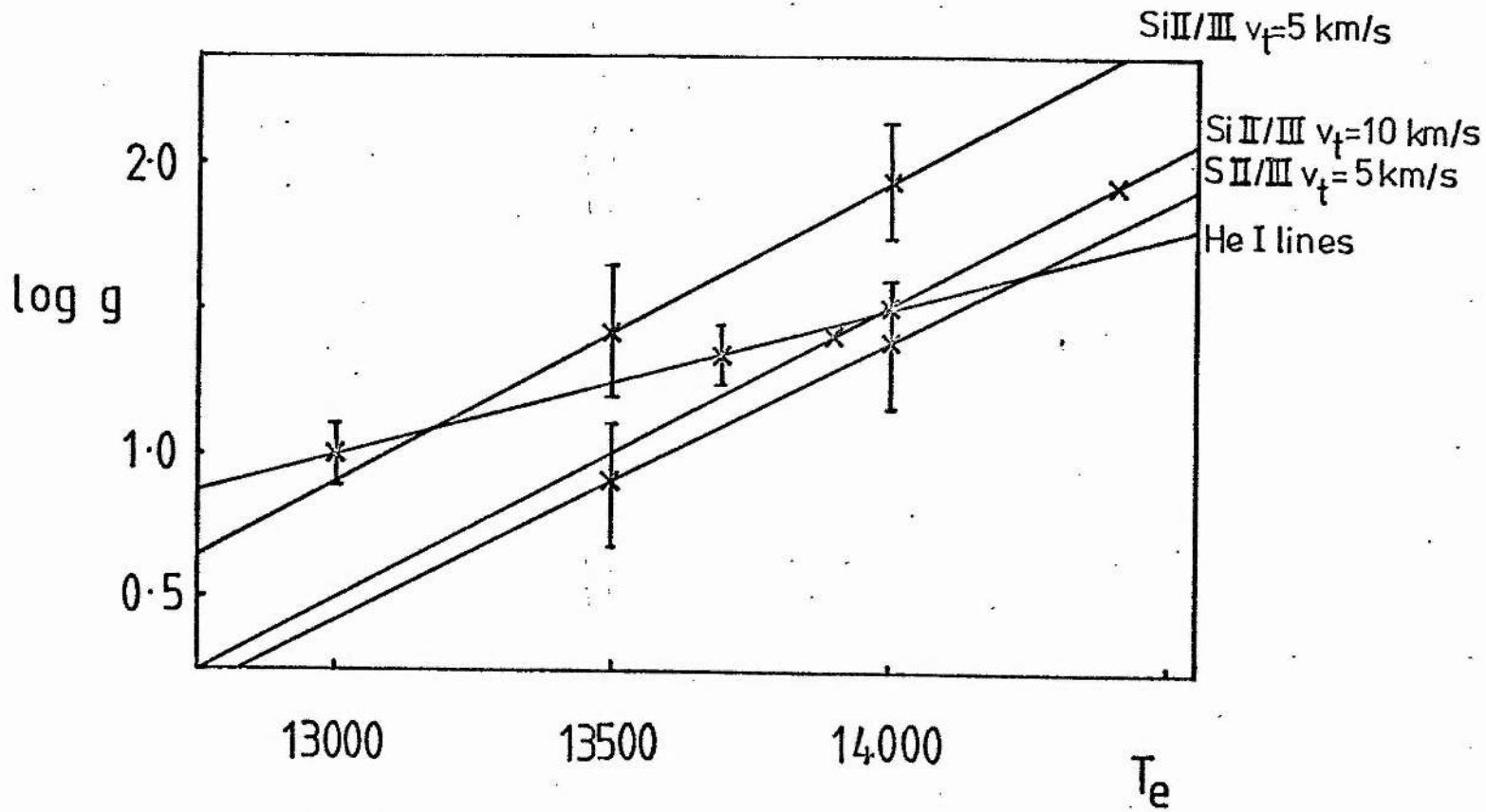

Figure 6·9 T_e – log g diagram for final model

6.8 The abundance determination

With the above atmospheric parameters, curves of growth were generated for the various ions. For two abundances, the equivalent widths of the lines of each ion were computed and the results plotted as log w/λ against log gf - $\theta_{eff}\chi$ + log m, where χ is the lower excitation potential of the line and m is the abundance. The opacity below the helium jump at 3450A was higher than that above the jump and so a different curve of growth was obtained for these lines. For red lines ($\lambda \gtrsim$ 5000A), the opacity was again higher and these curves of growth coincided with those for lines bluer than 3450A (see Hunger & Van Blerkom, 1967, figures 2 and 7). The two curves of growth prepared for Ti II are shown in figure 6.10. The shape of all the curves of growth are the same for all ions except in the region of largest equivalent width, the damping portion of the curve of growth which depends on the damping parameters used for the lines. For a few elements, notably S III more than two curves of growth were required (see figure 6.11) due to the opacity changing significantly over a small change in wavelength (about 200A).

In figure 6.10 the shoulder of the curve of growth is marked and for each ion the numerical value of this point on the curve for lines between 3450A and 5000A, is given in table 6.5. Also given in table 6.5 are the source of gf values used, number of lines used for the abundance determination and log(abundance) with the standard deviation from the mean for each element. The abundances were originally found relative to $n_{He} = 0.99$, but a constant was added to log n such that $\Sigma \log n_i \mu_i = 12.15$. The abundances determined by Schönberner & Wolf (1974) and Hill (1965) are also given, those by Hill being adjusted so that $\Sigma \log n_i \mu_i$

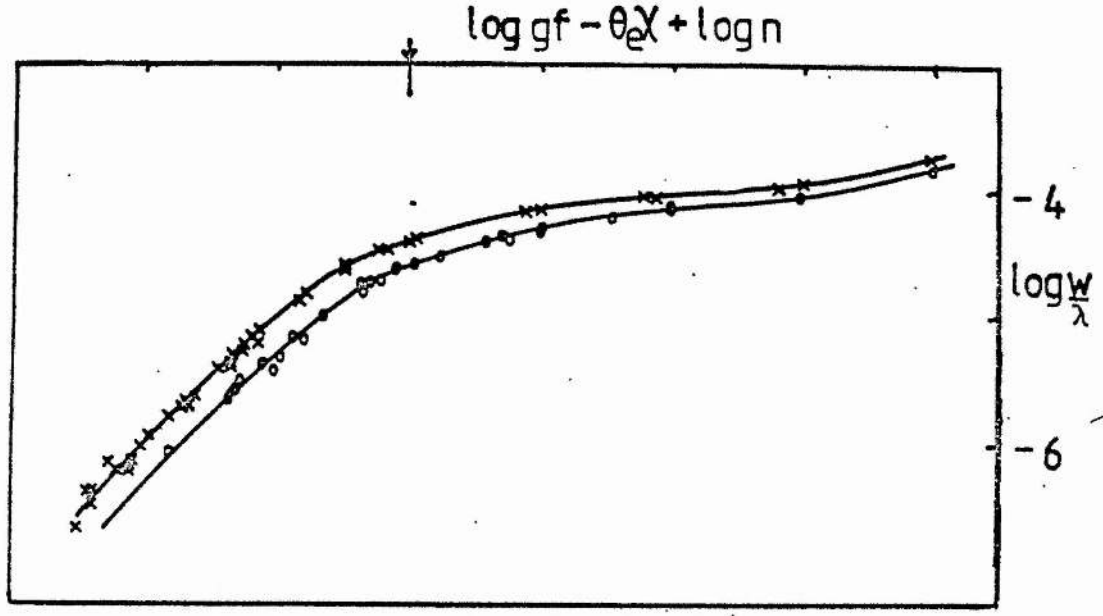

Figure 6·10 Curve of growth for Ti II ×- λ > 3450A ∘- λ < 3450A

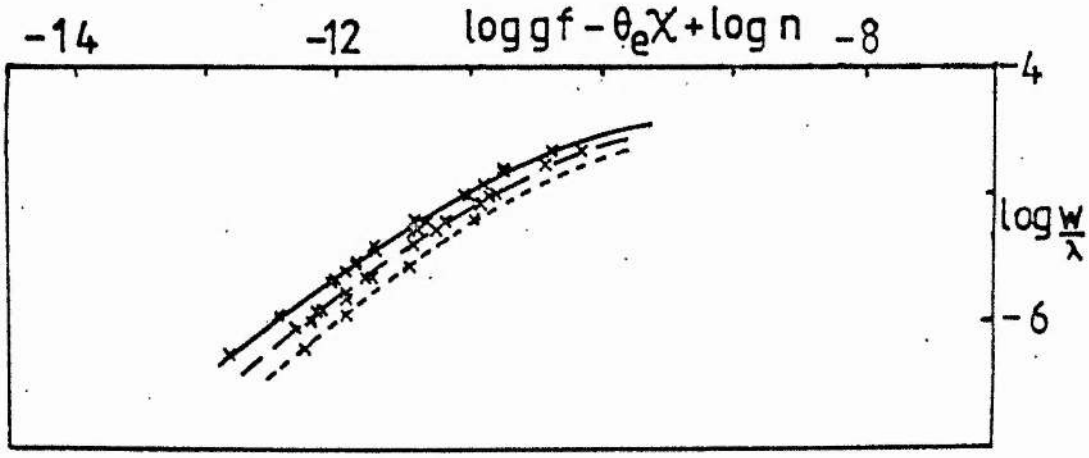

Figure 6·11 Curve of growth for S III

--- λ < 3700A
– – 4200A < λ < 4600A
—— 3700A < λ < 4200A

was 12.15 instead of 12.23.

The excitation potentials for the analysis came from Moore (1945) except in the case of N II, Si II/III which came from Moore (1975) and Moore (1965) respectively. For hydrogen the minimum equivalent width that would be detected in the spectral region of the line was used to decide a maximum abundance. For the transition elements the recommendations of Biémont (1978) were followed for log gf values.

Almost one thousand two hundred lines had equivalent widths measured from the various spectra available and of these 531 were judged to be unblended and had a log gf value published. The lines used are marked with an asterisk in the "A" column of table 5.5. Of 51 lines with single colons examined for use in the abundance analysis 9 were found to be blended. 39 lines with double colons were examined and 13 were found to be blended. Thus it would appear that although the different resolutions of the spectrographs may have an effect on the blending of the line and hence its equivalent width, this cannot explain all the variations noted (see also figure 5.13). The variation does not significantly alter the abundances, otherwise all the lines with colons would be rejected from the analysis. The abundances found in this analysis agree well with previous determinations except for some of the transition elements which will be affected significantly by the log gf values selected. Further discussion of the results is given in chapter 7.

Table 6.5 Abundances determined for HD 168476

Ion	gf values	shoulder pt.	no of lines		log n_i	sd	Hill log n_i	Sch.	Notes
H I	WSG	-7.45	3		<7.8	± 0.3	<7.0	<8.2	1
He I	GJK		7		11.5		11.5	11.5	
C II	KP		8		9.5	± 0.3	9.1	9.6	
N II	KP	-10.20	38		9.0	± 0.4	8.3	8.8	
O I	WSG	-7.45	2		8.3	± 0.4	<8.2	<8.4	
O II	WSG	-11.31	1						
Ne I	WSG	-10.30	8		9.4	± 0.5	9.0		
Mg II	WSM	-8.65	16		7.6	± 0.3	7.5	7.9	2
Al II	KP	-9.47	12	-4.1	7.3	± 0.4	6.1	5.8	
Al III	KP	-11.16	4	-4.8					
Si II	KP	-8.90	13	-3.8	7.6	± 0.4	7.0	7.4	3
Si III	KP	-11.50	7	-3.9					
P II	WSM	-9.50	8		6.4	± 0.4	6.0	6.1	4
S II	WSM	-10.19	53	-4.6	7.1	± 0.2	6.7	6.8	5
S III	WSM	-10.57	5	-4.2					
Ca II	WSM	-7.44	4		7.0	± 0.1	5.9	6.5	
Sc II	KP	-7.00	7		4.3	± 0.3	4.2		
Ti II	RAS	-7.00	80		5.7	± 0.4	5.9	4.8	6
V II	KP	-7.30	2		4.4	± 0.1	4.6		
Cr II	KP	-8.05	107		6.2	± 0.6	5.1		
Mn II	KP	-8.44	14		6.2	± 0.5	4.5		
Fe II	KP	-8.05	112	-4.0	7.6	± 0.4	7.4	7.6	
Fe III	KP	-9.50	13	-3.9					
Ni II	KP	-8.81	10		6.5	± 0.5	5.3		

Notes

1. Hγ w < 25mA, Hδ w < 30mA, Hε w < 20mA
2. 4193.44, 4242.47, 4331.93, 4436.48, 4739.59 used log gf from KP
3. 3856.00, 3862.60, 3853.65, 4128.05, 4075.45, 4076.78 used log gf from SG
4. 3559.93, 4044.49, 4062.08 used log gf from KP
5. 4230.98, 4415.37, 4492.30, 4497.88 used log gf from KP
6. 4350.83, 4493.53 used log gf from WB

GJL – Green, Johnson & Kolchin (1966)
KP – Kurucz & Peytremann (1975)
RAS – Roberts, Andersen & Sørensen (1973)
SG – Schulz-Gulde (1969)
WB – Wolnik & Berthel (1973)
WSG – Wiese, Smith & Glennon (1966)
WSM – Wiese, Smith & Miles (1966)

Unsöld (1955, page 416) showed a curve of growth derived from the central depth parameter $\bar{R}_c$. Following a suggestion by Prof. K. Hunger the Unsöld technique was used in attempt to reduce the curves of growth to a single one for each ion. Figure 6.12 shows a plot of log $\bar{R}_c$ against wavelength for the deep lines measured (see table 6.6). Figures 6.13 and 6.14 show the new curves of growth for Ti II and S III (respectively). Using this parameter so that log $w/\lambda\bar{R}_c$ is plotted against log gf - $\theta\chi$ + log n - log $\bar{R}_c$. For Ti II the separation between the two curves of growth is now zero. For S III it was found that log $\bar{R}_c$ was not sensitive enough to reduce the curves to a single one. Figure 6.12 does show that the central depth below the helium jump at 3450A is very similar to that around 5500A.

Another way of changing the curve of growth might be to explicitly include the excitation temperature rather than the effective temperature. An examination of the S III lines showed that the depth at which the line centre was formed (and hence the temperature) depended mostly upon the strength of the line and it was not noticably dependent on wavelength.

Table 6.6 Central depth of lines from all available spectra

λ	Ion	MN	Rad R_c	ESO R_c	AAT R_c	AAT R_c	AAT R_c	log R_c
3104	Mg II	4	0.474					-0.324
3179	Ca II	4	0.529					-0.276
3258	He I	H	0.493					-0.307
3349	Ti II	1	0.482					-0.317
3447	He I	7	0.406					-0.392
3471	He I	44	0.460					-0.338
3498	He I	40	0.521					-0.283
3587	He I	31	0.643					-0.192
3634	He I	28	0.632	0.650	0.557			-0.213
3705	He I	25	0.644	0.571	0.577			-0.224
3768	He I	65	0.574	0.474	0.391			-0.319
3819	He I	22	0.746	0.639	0.640			-0.171
3871	He I	60	0.680	0.589	0.559			-0.223
3888	He I	2	0.708	0.550	0.534			-0.224
3933	Ca II	1	0.740	0.650	0.577	0.528	0.534	-0.218
3968	Ca II	1	0.725	0.594		0.595	0.556	-0.209
4026	He I	18	0.748	0.615		0.680	0.653	-0.171
4143	He I	53	0.696	0.534		0.641	0.607	-0.208
4267	C II	6	0.627	0.523				-0.240
4387	He I	51		0.517	0.586	0.549		-0.259
4471	He I	14		0.556	0.630	0.602		-0.225
4481	Mg II	4		0.539	0.607	0.613		-0.232
4549	Fe II	38		0.343	0.362	0.405		-0.432
4662	Fe II	38		0.262				-0.581
4713	He I	12		0.389				-0.410
5564	S II	6			0.343			-0.465
5606	S II	11			0.378			-0.423
5640	S II	11			0.497			-0.303
5764	Ne I	13			0.299	0.247		-0.564
5875	He I	11				0.502		-0.299
5944	Ne I	1				0.363		-0.440
6074	Ne I	3			0.457			-0.340
6163	Ne I	5			0.420			-0.376
6266	Ne I	5			0.456	0.560		-0.294
6347	Si II	2			0.543	0.506		-0.284
6402	Ne I	1				0.600		-0.222
6506	Ne I	3				0.572		-0.243

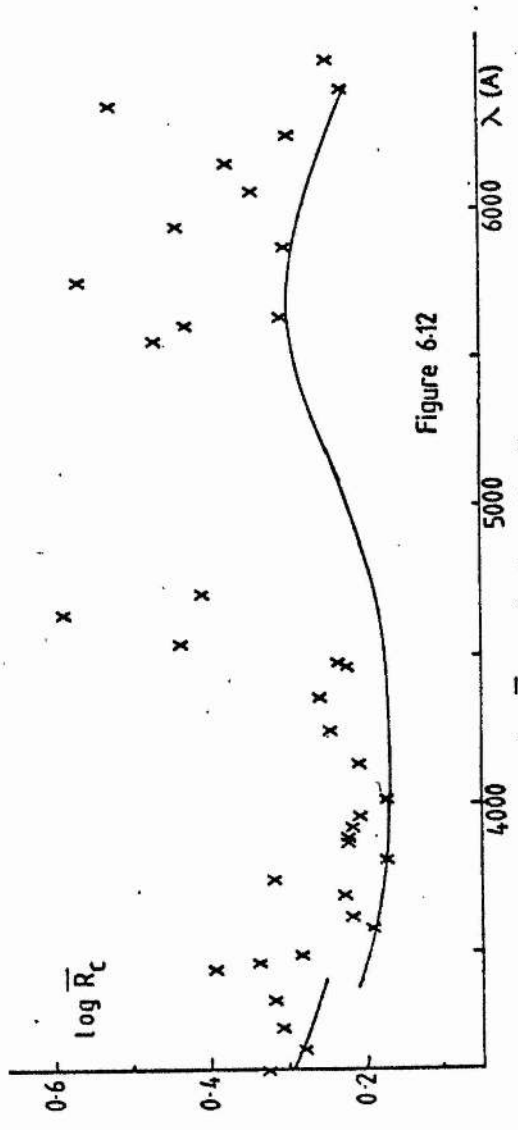

Figure 6·12
log $\overline{R}_c$ against wavelength

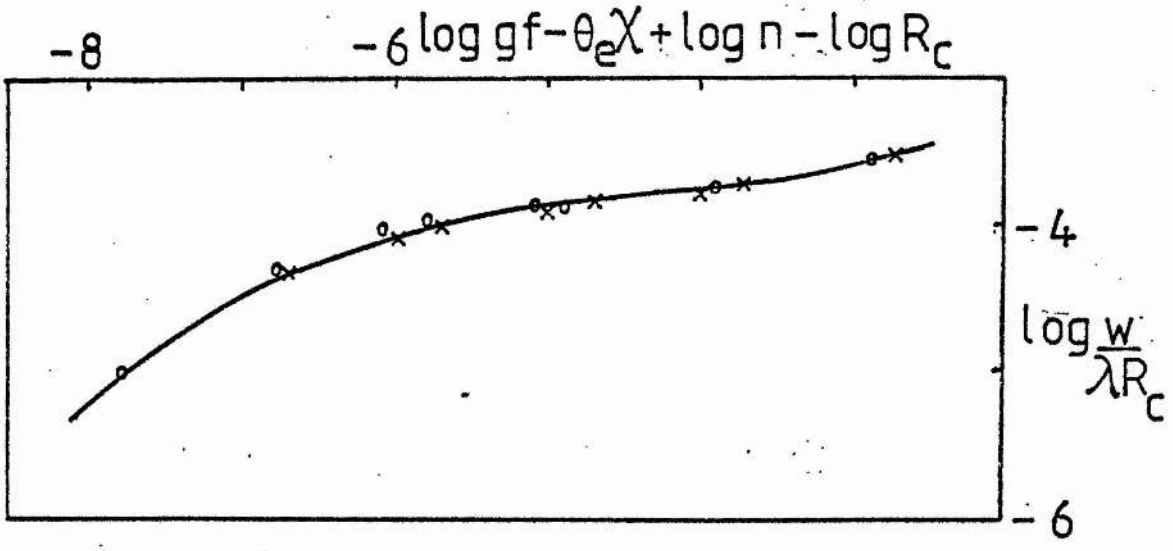

Figure 6·13 Modified curve of growth for Ti II

comments as for figure 6.10

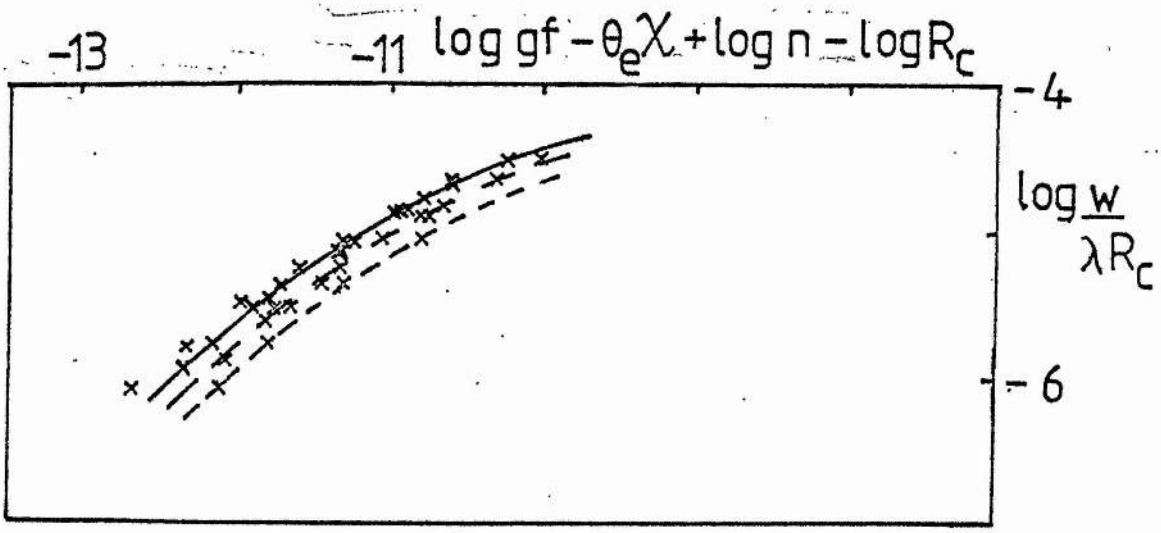

Figure 6·14 Modified curve of growth for S III

comments as for figure 6.11

7 DISCUSSION AND CONCLUSIONS

7.1 Variability

In chapter 2 it was found that HD 168476 was variable in magnitude and probably in colours, with the variation noticable over a few days. The differential 'b' magnitudes and the normality of the variances, shown by Bartlett's statistic, indicated there was no variability on a time-scale of a few hours. The radial velocities in chapter 3 again suggested that there was variation on a time-scale of days, as well as variation over a longer period. Figure 7.1 shows the mean W magnitude and mean radial velocity (both with standard deviation) for those years with measurements made of both quantities. Also included, with no error bars, are the photometric measurements in other years. Shown in figure 7.2 are the measurements made in one year, 1976. Over many years no real correlation can be seen between the radial velocity and the photometric magnitude variation. There does appear to be a trend for the photometric magnitudes and radial velocities to follow each other over a few days. However, this must be checked with more data to ascertain if this is generally the case.

Lucy (1976) in his study of the radial velocity of α Cygni used a formula

$$P_L = \frac{4\pi c_s}{\gamma g}$$

where c_s is the velocity of sound

γ is the ratio of specific heats

g is the gravitational acceleration

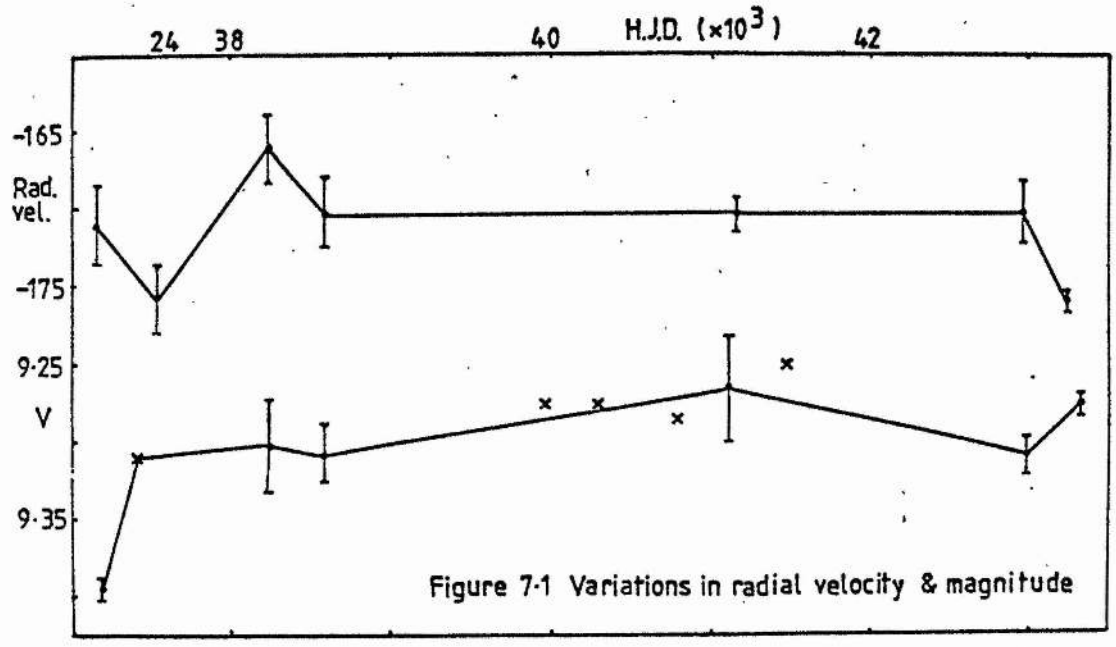

Figure 7·1 Variations in radial velocity & magnitude

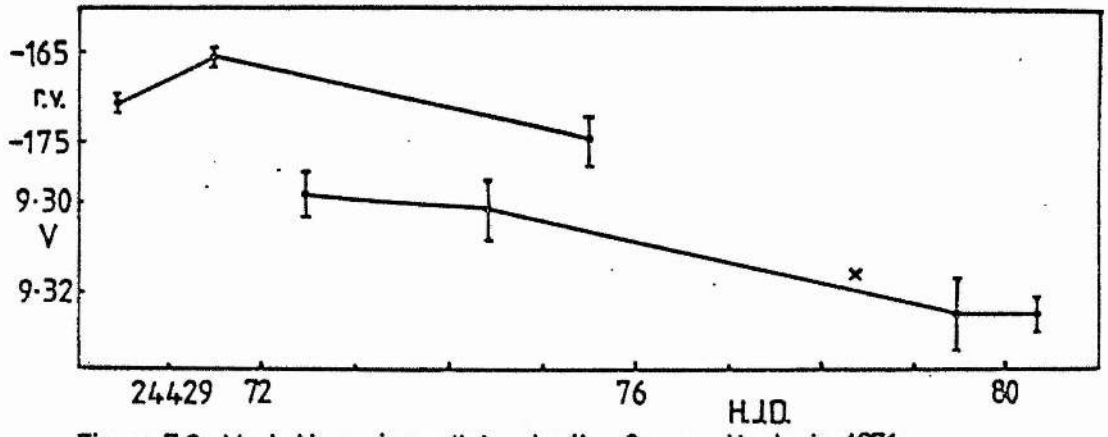

Figure 7·2 Variations in radial velocity & magnitude in 1976

for the critical period (Lamb, 1945) below which standing atmospheric oscillations are impossible in an isothermal atmosphere.

However, $$c_s = \sqrt{\frac{\gamma A T}{4}}$$

where A is a constant

$\gamma = 5/3$ (Carson, 1976)

For HD 168476 $T_e = 14000^{\circ}K$, $\log g = 1.5$

$P_L = 1.69$ days

By comparison for BD+13°3224 an estimate of the temperature and gravity was provided by Kilkenny (1979) from four-colour photometry.

For BD+13°3224 $T_e \sim 33000^{\circ}K$, $\log g \sim 3.3$ $P_L = 1.0$ hours

The critical period for BD+13°3224 is less than the actual period found, $2\frac{1}{2}$ hours, although the temperature and surface gravity must be treated with suspicion. Lucy makes an interesting note that any oscillation less than the critical period would not be a standing oscillation but a travelling wave, which would not affect the radial velocity, but would be detected as microturbulence. The microturbulent velocity for HD 168476, as noted in chapter 6, is high at 10 km/s.

HD 168476, shares several properties with the β Cephei-type variables (see Cox, 1974). It has small amplitude light variation, radial velocity variation, multiple periods and small rotational velocity as do the β Cephei stars. Stothers & Simon (1969) explain the variability by enriching the outer layers of the β Cephei star with helium by mass transfer from a binary component,

which helps to cause nuclear-energised pulsational instability. The enrichment of helium is extreme, models with the mass fraction of hydrogen in the layer equal to zero are computed. Although the extreme helium-rich stars are cooler and less massive than β Cephei stars, theories which explain the β Cephei type of variability may be useful for extreme helium-rich stars. As mentioned in chapter 1, Wood (1976) made linear adiabatic and non-adiabatic radial pulsation calculations. The model produced for HD 168476 (see chapter 6) shows that the star will be just inside the boundaries for stable pulsation in the fundamental and overtone mode. Wood also did some non-linear calculations which resulted in M_{Bol} varying by one magnitude and the radial velocity by 20 km/s. In HD 168476 the variation in magnitude is less extreme than that.

Of the known extreme helium-rich stars, it has been established that seven of them (including MV Sgr. and V348 Sgr.) are variable in some way. Only for BD+13°3224 has a period been found, and that is very short, i.e. 0.1 days (Landolt, 1975). It appears certain (Walker & Kilkenny, 1979) that HD 168476 and HD 160641 (also Landolt, 1973) are variable in a complex way. HD 124448 is probably variable (e.g. Walker & Kilkenny, 1979) and also BD+10°2179 (Landolt, 1973). The variety in the type of variation in the extreme helium-rich stars does suggest that there may not be a group-characteristic variability, but that the variability is a characteristic of the individual star or the precise position in its evolution. Eventually it may be that the spectrum lines themselves (e.g. figure 5.13) will give the most information about the nature of the variability, and the spectrum as well as the magnitude should be closely studied to see if any periodicity

is displayed.

7.2 Distance and space motion

Schönberner (1977) shows that the extreme helium-rich stars have masses between $0.7M_\odot$ and $1.0M_\odot$, with log $L/L_\odot$ from 4.1 to 4.6. Figure 7.3 shows the position of HD 168476 on the log T_e - log g diagram. Using formulae and data from Lang (1974) :-

$$\log L/L_\odot = 0.4\,(M_{B_\odot} - M_B)$$

$$M_{B_\odot} = 4.72$$

for HD 168476 $\log L/L_\odot = 4.1$, $M = 0.7M_\odot$ is used

$$M_B = -5.5, \quad M_V \simeq -4.5$$

Also $5\log r = m - M + 5 - R \times E(B-V)$

taking $R = \dfrac{A_V}{E(B-V)} = 3.2$ (Schmidt-Kaler, 1967)

for HD 168476 $E(B-V) = 0.15$ (see table 7.1)

$$r = 4.6 \text{ kpc}$$

$$\frac{L}{L_\odot} = \frac{R^2}{R_\odot^2} \times \frac{T_e^4}{T_{e_\odot}^4}$$

$$T_{e_\odot} = 5784^\circ K$$

for HD 168476 $T_e = 14000^\circ K$

$$R = 19R_\odot$$

Lynas-Gray, Walker & Hill (1979) obtained a value of $37R_\odot$ for the radius of HD 168476 using values of T_e and log g by Schönberner & Wolf (1974) and $M = 1M_\odot$.

Table 7.1 shows the summary of data for HD 168476 determined from this thesis and from other sources noted in the table.

Table 7.1 Data for HD 168476

Also called SAO 245 434
CPD-56°8755

Spectral type B5p

$m_V = 9.30 \pm 0.02$	$M_V = -4.5$
$\alpha = 18^h\ 21^m\ 07^s.25$ [a]	$\mu_\alpha = -0^s.0004 \pm 0.0005$ [a]
$\delta = -56^\circ\ 38'\ 34''.0$ [a]	$\mu_\delta = 0''.008 \pm 0.007$ [a]
$l = 338^\circ$	r.v. $= -170.9 \pm 0.7$ (s.e.)
$b = -19^\circ$	
$(U-B) = -0.69 \pm 0.02$ [b]	$(U-B)_o = -0.77$ [c]
$(B-V) = -0.01 \pm 0.01$ [b]	$(B-V)_o = -0.16$ [c]
	B.C. $= -1.01$ [c]
$(u-b) = 0.396 \pm 0.010$	$(u-b)_o = 0.335$ [c]
$(b-y) = 0.043 \pm 0.010$	$(b-y)_o = -0.048$ [c]
$c_1 = 0.188$	$c_o = 0.250$ [c]
$m_1 = 0.061$	$m_o = 0.091$ [c]
$T_e = 14000^\circ K \pm 300$	$n_{He} = 0.99$
$\log g = 1.5 \pm 0.2$	$n_C = 0.01\ ^{+0.007}_{-0.005}$
$v_t = 10$ km/s ± 5	$v_{rot} = 20$ km/s ± 20
$M \sim 0.7\ M_o$	$\log L/L_o \sim 4.1$
$R \sim 19\ R_o$	$r \sim 4.6$ kpc

Notes :-

a SAO Star Catalog (1966)

b Hill (1969a)

c Schönberner (1979)

The space motion of HD 168476 was found using a program written by Kilkenny (1973). This corrected the radial velocity for the solar motion relative to the local standard of rest and differential galactic rotation. The program used the Schmidt-Kaler (1967) modification of the Feast & Shuttleworth (1965) rotation curve, with R = 3.2. Lang (1974) gives the correction to the radial velocity for the solar motion relative to the local standard of rest as :-

$$V_{r_\odot} = 19.5(\cos\alpha_0 \cos\delta_0 \cos\alpha \cos\delta + \sin\alpha_0 \cos\delta_0 \sin\alpha \cos\delta + \sin\delta_0 \sin\delta) \text{ km/s}$$

where α_0, δ_0 are the co-ordinates for the solar apex. The proper motions were converted to km/s using (see for example Lang, 1974)

$$T = 4.74 \mu r \quad \text{km/s}$$

The values of T_α , T_δ , V_r were converted to u, v, w using the right ascension and declination of the star, the co-ordinates of the north galactic pole and the ascending node of the galactic plane on the celestial equator (see Hill, 1969b). The program also calculated the galactic co-ordinates (l,b) and the galactocentric distance.

Galactocentric distance = 6.2 kpc

with rad. vel. V_r = -170.9 km/s (see table 3.7)

μ_α = -0".006 ± 0".008
μ_δ = 0".008 ± 0".007
} (SAO Star Catalog, 1966)

M_V = -4.5

u = +14 km/s, v = +160 km/s, w = +230 km/s

space motion = 281 km/s

Since the proper motions are very uncertain the program also calculated the space motion with zero proper motions.

If μ_α = 0".0, μ_δ = 0".0

u = -104 km/s, v = +42 km/s, w = +39 km/s

space motion =118 km/s

If the proper motions can be regarded as negligible the space motion of the star is not exceptional. The calculations of Perek (1958) assumed the star was at a maximum distance of 2 kpc, and this now seems to be an underestimate, so that it is more likely that the star is in a closed galactic orbit.

7.3 Evolution

The abundances determined for HD 168476 are compared (in table 7.2) with those of other extreme helium-rich stars, R CrB stars and normal B stars. The abundances for the R CrB stars are taken from Schönberner (1975), the B stars from Scholz (1972) and the transition element abundances for the sun from Biémont (1978). HD 124448 and BD+10°2179 have abundances noted in Schönberner & Wolf (1974), BD-9°4395 in Kaufmann & Schönberner (1977) and HD 160641 from Hill (1965), the latter being a coarse analysis. For BD+10°2179 the temperature quoted is taken from Schönberner & Hunger (1978). HD 168476 is seen to belong to the main group of extreme helium-rich stars with overabundance in carbon and nitrogen, and underabundance in oxygen. HD 168476, in common with HD 160641

Table 7.2 Abundances for extreme helium-rich stars and related objects

	HD 168476	HD 124448	BD-9°4395	BD+10°2179	HD 160641	R CrB stars	B stars	Sun
H	<7.8	<7.5	8.7	8.15		7.6	12.00	
He	11.50	11.53	11.54	11.51	11.53	11.51	11.00	
C	9.5	9.46	9.30	10.0	8.58	10.00	8.6	
N	9.0	8.83	8.0	8.8	8.69		7.9	
O	8.3	8.5	8.24	<8.2	8.83	8.5	8.9	
Ne	9.4::				9.34		6.5	
Mg	7.6	8.2	(7.4)	8.0	7.53	7.5	7.3	
Al	7.3::	6.2	6.25	7.2	7.53		6.3	
Si	7.6	7.51	7.8	7.7			7.5	
P	6.4:	5.6	6.8	6.9			5.5	
S	7.1	7.20	7.6	7.4			7.2	
A		6.6		7.3			6.8	
Ca	7.0	6.9		7.2			6.4	
Sc	4.3::							3.08
Ti	5.7	5.1				5.2	4.5	4.99
V	4.4::							4.14
Cr	6.2						5.5	5.88
Mn	6.2							5.4
Fe	7.6	7.8	(6.8)	8.0		7.3	7.6	7.65
Ni	6.5						5.1	6.25
T_{eff}	14000	16000	25000	17500	31500			
log g	1.5	2.2	2.6	2.3				

Note Single colon and double colon indicate uncertainty in the abundance derived in HD 168476 due to either lack of lines or large standard deviation (see table 6.5)

appears to be overabundant in neon, although the latter star has a normal oxygen abundance, and so may not be typical of the group. BD+10°2179 appears (from visual spectra) to be exceptionally overabundant in carbon. In the ultraviolet (Schönberner & Hunger, 1978), a model with $n_C = 0.01$ was used for the C II profile at 1335A, a value used in fine analyses of other extreme helium-rich stars. That paper showed the log T_e - log g diagram reproduced in figure 7.3, which includes the position of HD 168476. For interest, the position of BD+13°3224 is shown, using the values of temperature and surface gravity quoted in section 7.1. The position of HD 168476 on the log T_e - log g diagram is entirely consistent with the theory of Schönberner (1977). The star appears to occupy a position between the hotter helium-rich stars and the R CrB stars, but the abundances determined (especially carbon) show that it is solely a member of the extreme helium-rich stars.

As can be seen from table 7.2 the R CrB stars are more abundant in carbon than the extreme helium-rich stars, suggesting that the R CrB stars will lose this excess before or while becoming extreme helium-rich stars. Warner (1967) among others comments upon the ejection of carbon from the atmospheres of R CrB stars. The short lifetimes mentioned, of around a thousand years (Dinger, 1972; Schönberner, 1977), would explain why so few extreme helium-rich stars are seen. Schönberner (1977) calculated the changes in colour and magnitude to be expected from this quick evolution, but they are not large enough to explain the observed variability. It may be that any instabilities developing in the star could trigger the observed variability and help the enhancement of carbon, nitrogen and neon by mixing material from

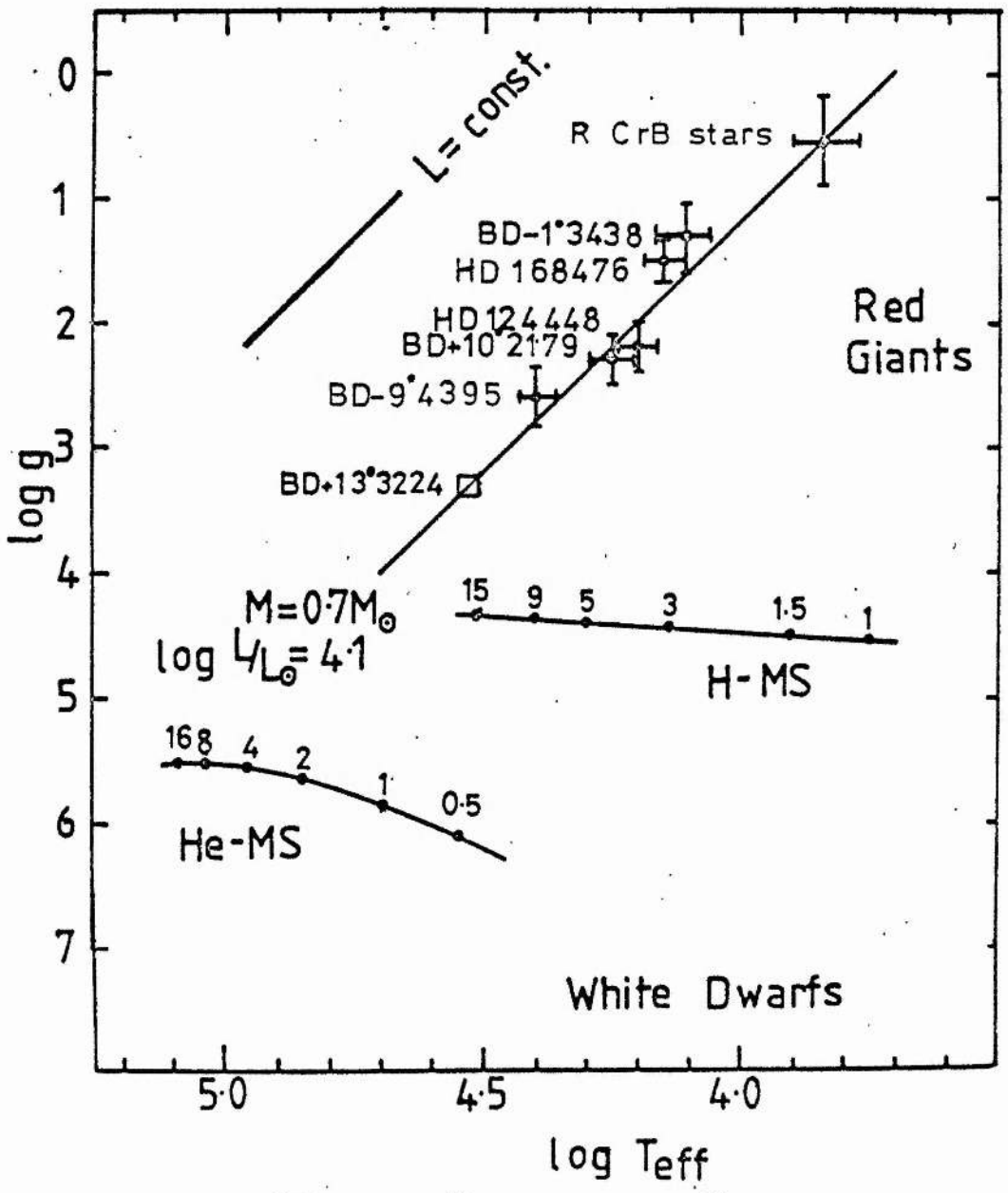

Figure 7·3 Log T_{eff} - log g diagram

different levels in the atmosphere.

Since Drilling (1973,1978,1979) has added four stars to the list of extreme helium-rich stars, the space density and birth-rate of extreme helium-rich stars were recalculated following Hunger (1975) and Schönberner (1977). A luminosity of $\log L/L_{\odot} = 4.1$ was used for all stars, and this gave much larger distances for the stars, reducing the space density.

Taking $M_B = -5.5$

$5\log r = m - M + 5 - 3.2 \times E(B-V)$ as before

$z = r \times \sin b$

$N = 12$ $\langle z \rangle = 2.3$ kpc

$\langle r \rangle = 6.4$ kpc

$\langle b \rangle = 25^{\circ}$

$$n = \frac{N}{\pi (\langle r \rangle \cos \langle b \rangle)^2 2 \langle z \rangle}$$ (see Hunger, 1975)

$= 8.5 \times 10^{-11}$ pc^{-3}

Birth-rate $= 3.4 \times 10^{-14}$ pc^{-3} yr^{-1}

As can be seen the larger value for $\langle r \rangle$ results in a birth-rate much lower than that of 6×10^{-13} pc^{-3} yr^{-1} for DB white dwarfs, quoted by Schönberner (1977). There will be large errors in this figure since M_V is rather uncertain and has a large effect on the space density. Bearing in mind that other types of stars such as Wolf-Rayet stars are rich in helium (Smith, 1973), it may not be suprising to find that extreme helium-rich stars were not the only source of helium-rich white dwarfs.

The large radius of the star suggests that it may have a cool

outer shell (less than about 700°K, Feast & Glass, 1973), as indicated from the ultraviolet lines due to neutral atoms. The ultraviolet lines might be expected to show evidence of mass loss or mass motion if there is any present, but no line shifts or asymmetries were noted. Lynas-Gray, Walker & Hill (1979) reported an upper limit to the mass loss rate of around 10^{-10} $M_\odot$ yr^{-1}. This is in agreement with Schönberner & Hunger (1978) who found that BD-9°4395 and BD+10°2179 showed no evidence of mass loss in their ultraviolet spectra. For HD 168476 Lynas-Gray et al. (1979a) used Mg II and C II resonance lines in the calculations which may have strong photospheric contributions since Mg II and C II are strong in the visible spectrum, so that they may not be reliable mass loss indicators.

The observed interstellar abundances derived from the ultraviolet spectrum (see chapter 4) may be evidence of mass loss in the fairly recent past. It may be that any mass loss or mass motion is linked with the star's variability and so that only at certain phases will any mass 'leak' from the star. This may perhaps show as the variable line profiles seen in the visible spectrum. The exposure time for the ultraviolet spectrum of HD 168476 is much too long for that type of variability to be seen. The variability noted may be the residue of an instability in the star that caused it originally to lose its hydrogen envelope, or started massive convection currents that thoroughly mixed the hydrogen in the stellar atmosphere to the region where it would be converted to helium.

As mentioned in chapter 1 Schönberner & Hunger (1978) suggest that an extreme helium-rich star could be the remainder of a binary system in which one component blew up as a supernova. This

they noted, would explain the high radial velocity seen in several of the extreme helium-rich stars. The supernova would also explain the loss of the hydrogen envelope which would be blown away in the explosion leaving a helium core behind.

7.4 Suggestions for future work

The ultraviolet spectrum of HD 168476 and the other extreme helium-rich stars is most important. The study of HD 168476 has shown that stellar and interstellar components of lines can be resolved in the case of high-velocity extreme helium-rich stars, so that it will be possible to find accurate interstellar abundances and stellar abundances. It may be possible to examine the hydrogen abundance and search for a cool shell near HD 168476 using the 21cm line. The lack of interstellar hydrogen enrichment might suggest that the supernova theory was correct, with all the hydrogen being processed to heavier elements and removed from the vicinity of the remaining star. If the hydrogen was lost from the envelope of the helium-rich star in a non-violent manner, it should enrich the interstellar medium near the stars. When larger telescopes are put into space it may be possible to search for short period variations in the ultraviolet spectra of extreme helium-rich stars indicating mass loss from the system or mass motion in the atmosphere at certain phases. Space telescopes, such as the planned astrometric telescope, may also provide better proper motions for the stars so that their movements in space can be better determined.

New techniques are now available for the study of variability in stars. The University of Cape Town high-speed photometer will be a most useful tool for the investigation of rapid variations

(flickering) in extreme helium-rich stars. The radial velocity can be more accurately studied using Dr. L. Balona's 'speedometer', in which a mask is made of the stellar spectrum and used to determine small changes in the radial velocity. If there were instruments of the accuracy and reliability of the Radcliffe two-prism spectrograph available on larger telescopes it would be possible to obtain a complete study of the radial velocities of the extreme helium-rich stars. Even with the present techniques, used in this thesis, more data will yield more results.

Further observations of HD 168476 may clarify the problem of variability in the star. It is important to discover whether the photmetric changes are in phase with the radial velocity variations, and how they relate to the observed spectral line changes. However, the other extreme helium-rich stars must also be carefully investigated. Several of the extreme helium-rich stars have not yet been investigated for variability (e.g. BD-1°3438) and it must be established if all the extreme helium-rich stars are variable and in what manner, as this may give a clue to their evolution. The observations of HD 168476 confirm Wood's (1976) theory that the star should be variable. It is important to look at other extreme helium-rich stars, especially those cooler than HD 168476 to see if they show any evidence of variation in the fundamental mode.

One of the most important objects is possibly MV Sgr., a hot R CrB star, also classed as an extreme helium-rich star. This will give us much valuable information about both groups of stars and possibly clarify the relationship between them. There may be evidence here to clarify the problem of the loss of the hydrogen envelope, and the loss of carbon by the R CrB stars.

Also important are the two new A stars discovered by Drilling (1979), LSIV-14°109 and BD+1°4381. These stars may be very close to the R CrB region of the log T_e - log g diagram, and the HdC stars described by Warner (1967). They may be found to be close binaries like ν Sgr. and HD 30353.

Future analyses may improve on the results obtained in this thesis. Table 7.1 and the formulae for reddening shown in section 2.6 show that there is not complete agreement between observed and calculated reddening in the 'uvby' photometry in all cases, most noticably in c_1. It is now increasingly possible to include non-LTE calculations in model calculations. This will mean that stars such as HD 160641 and BD+13°3224 can be completely analysed. Although non-LTE effects will not be a serious problem in the cooler members, such as HD 168476, it would be interesting to know if any non-LTE effect was observable. Mihalas et al. (1974, 1975) have produced an improved broadening theory, for the strong He I lines at 4471A (with its forbidden component at 4469A), and for 4922A, which will hopefully soon be in general use in model programs.

REFERENCES

AAT Observers Guide, 1976. Anglo-Australian Observatory.

Alexander, J.B., Andrews, P.J., Catchpole, R.M., Feast, M.W., Lloyd-Evans, T., Menzies, J.W., Wisse, P.N.J. & Wisse, M., 1972. Mon. Not. R. astr. Soc., 158, 305.

Aller, L.H., 1954. Liege Collection in 8vo XV no. 357, 353.

Avrett, E.H. & Loesser, R., 1963. J. quant. Spectr. rad. Trans., 3, 201.

Barnard, A.J., Cooper, J. & Sharney, L.J., 1969. Astr. Astrophys., 1, 28.

Barnard, A.J., Cooper, J. & Sharney, L.J., 1969. Private comm. to D. Schönberner.

Baschek, B., 1973. Astr. Astrophys., 25, 333.

Bidelman, W.P., 1952. Astrophys. J., 116, 227.

Biémont, E., 1978. Mon. Not. R. astr. Soc., 184, 683.

Boggess, A. et al., 1978a. Nature, 275, 372.

Boggess, A. et al., 1978b. Nature, 275, 377.

Böhm, K.H. & Deinzer, W., 1965. Z. Astrophys., 61, 1.

Bues, I., 1970. Astr. Astrophys., 7, 91.

Burgess, A. & Seaton, M.J., 1960. Mon. Not. R. astr. Soc., 120, 121.

Carson, T.R., 1976. Private comm..

Conover, W.J., 1971. Practical Nonparametric Statistics, Wiley, New York.

Cox, J.P., 1974. Rep. Prog. Phys., 37, 563.

Crawford, D.L., 1973. I.A.U. Symp., 50, Spectral Classification and Multicolour Photometry p. 186, eds Fehrenbach, C. & Westerlund, B.E., D. Reidel, Dordrecht-Holland.

Crawford, D.L. & Barnes, J.V., 1970. Astr. J., 75, 978.

Crawford, D.L., Barnes, J.V. & Golson, J.C., 1970. Astr. J., 75, 624.

Detz, A., 1977. Astr. Astrophys. Suppl., 28, 403.

Dinger, A., 1972. Mon. Not. R. astr. Soc., 158, 383.

Drilling, J.S., 1973. Astrophys. J., 179, L31.

" 1978. Astrophys. J., 223, L29.

" 1979. Astrophys. J., 228, 491.

Evans, D.S., Menzie, A. & Stoy, R.H., 1959. Mon. Not. R. astr. Soc., 119, 638.

Feast, M.W. & Glass, I.S., 1973. Mon. Not. R. astr. Soc., 161, 293.

Feast, M.W. & Shuttleworth, M., 1965. Mon. Not. R. astr. Soc., 130, 245.

Feast, M.W., Thackeray, A.D. & Wesselink, A.J., 1954. Mem. R. astr. Soc., 67, 51.

Feast, M.W., Thackeray, A.D. & Wesselink, A.J., 1957. Mem. R. astr. Soc., 68, 1.

Fisher, R.A. & Yates, F., 1945. Statistical Tables for Biological, Agricultural & Medical Students, 2nd. edn., Oliver & Boyd Ltd., Edinburgh.

Fowler, A., 1922. Report on Series in Line Spectra, Phys. Soc., London.

Garrison, R.F. & Hiltner, W.A., 1973. Astrophys. J., 179, L117.

Gingerlich, O., 1964. 1st Harvard-Smithsonian conference on stellar atmospheres, Smithsonian Astrophys. Obs. Special Rep. 167.

Golay, M., 1974. Introduction to astronomical photometry, Astrophys. & Space Science library 41, D. Reidel, Dordrecht-Holland.

Gould, N.L., Herbig G.H. & Morgan, W.W., 1957. Publ. astr. Soc. Pacific, 69, 242.

Gray, D.F., 1976. Observation and analysis of stellar photospheres,

Wiley, New York.

Green, L.C., Johnson, N.C. & Kolchin, E.K., 1966. Astrophys. J., 144, 369.

Greenstein, J.L. & Wallerstein, G., 1958. Astrophys. J., 127, 239.

Hack, M., 1967. Modern Astrophysics, Gauthier-Villars, Paris.

Hack, M. & Job, F., 1965. Z. Astrophys., 62, 303.

Harrison, G., 1969. M.I.T. Wavelength Tables, M.I.T. Press, Cambridge, Massachusetts.

Higginbotham, N.A. & Lee, P., 1974. Astr. Astrophys., 33, 277.

Hill, P.W., 1962. Thesis, University of Cambridge.

" 1964. Mon. Not. R. astr. Soc., 127, 113.

" 1965. Mon. Not. R. astr. Soc., 129, 137.

" 1969a. I.A.U. Inf. Bull. on Variable stars no. 357.

" 1969b. Mon. Not. astr. Soc. Southern Africa, 28, 45.

" 1970. Obs., 90, 10.

" 1978. Private comm..

Hobbs, L.M., 1974. Astrophys. J., 191, 381.

Hoffleit, D.L., 1959. Astr. J., 64, 241.

Houk, N., 1978. Michigan Spectral Catalogue Vol. 2, Ann Arbor, Michigan.

Hunger, K., 1975. Problems in Stellar Atmospheres and Envelopes p. 57, eds Baschek, B., Kegel, W.H. & Traving, G., Springer, Berlin.

Hunger, K. & Van Blerkom, D., 1967. Z. Astrophys., 66, 185.

Hunger, K. & Kaufmann, J.P., 1973. Astr. Astrophys., 25, 261.

Hunger, K. & Klinglesmith, D.A., 1969. Astrophys. J., 157, 721.

IPCS Operating Notes, 1977. Royal Greenwich Observatory.

Jackson, J., 1951. Nature, 167, 169.

Jaschek, M. & Jaschek, C., 1959. Publ. astr. Soc. Pacific, 71, 1465.

Jenkins, E.B., Drake, J.F., Morton, D.C., Rogerson, J.B., Spitzer, L. & York, D.G., 1973. Astrophys. J., 181, L122.

John, T.L., 1968. Mon. Not. R. astr. Soc., 138, 137.

Johnson, H.L. & Morgan, W.W., 1953. Astrophys. J., 117, 313.

Jones, W.W., Benett, S.M. & Griem, H.R., 1971. Technical report 71 - 128, University of Maryland.

Kaufmann, J.P. & Hunger, K., 1975. Astr. Astrophys., 38, 351.

Kaufmann, J.P. & Schönberner, D., 1974. Astr. Astrophys., 36, 201.

Kaufmann, J.P. & Schönberner, D., 1977, Astr. Astrophys., 57, 169.

Kilkenny, D., 1973. Thesis, University of St. Andrews.

" 1977. Mon. Not. R. astr. Soc., 181, 611.

" 1978. Mon. Not. R. astr. Soc., 182, 629.

" 1979. Private comm..

Kilkenny, D. & Hill, P.W., 1975. Mon. Not. R. astr. Soc., 173, 625.

Klemola, A.R., 1961. Astrophys. J., 134, 130.

Klinglesmith, D.A., Hunger, K., Bless, R.C. & Millis, R.L., 1970. Astrophys. J., 159, 513.

Kodaira, K., Greenstein, J.L. & Oke, J.B., 1970. Astrophys. J., 159, 485.

Kurtz, D., 1977. Publ. astr. Soc. Pacific, 89, 939, 941.

Kurucz, R.L. & Peytremann, E., 1975. A table of semi-empirical gf values, parts 2, 3, Smithsonian Astrophys. Obs. Spec. Rep. 362.

Lamb, H., 1945. Hydrodynamics, Dover, New York.

Landolt, A.U., 1973. Publ. astr. Soc. Pacific, 85, 661.

" 1975. Astrophys. J., 196, 789.

Lang, K.R., 1974. Astrophysical formulae, Springer, Berlin.

Lee, P. & O'Brien, A., 1977. Astr. Astrophys., 60, 259.

Lester, J.B., 1972. Astrophys. J., 178, 743.

Lindemann, E. & Hauck, B., 1973. Astr. Astrophys. Suppl., 11, 119.

Lucy, L.B., 1964. 1st Harvard-Smithsonian conference on stellar atmospheres, Smithsonian Astrophys. Obs. Special Rep. 167.

Lucy, L.B., 1976. Astrophys. J., 206, 499.

Lynas-Gray, A.E., 1979. Private comm..

Lynas-Gray, A.E., Walker, H.J. & Hill, P.W., 1979a. In preparation.

Lynas-Gray, A.E., Walker, H.J., Hill, P.W. & Kaufmann, J.P., 1979b. In preparation.

MacConnell, D.J., Frye, R.L. & Bidelman, W.P., 1972. Publ. astr. Soc. Pacific, 84, 388.

Mees, C.E.K., 1954. The theory of the photographic process, revised edn., McMillan & Co., New York.

Menzel, D.H. & Pekeris, C.L., 1935. Mon. Not. R. astr. Soc., 96, 77.

Mihalas, D., 1965. Astrophys. J. Suppl., 9, 321.

Mihalas, D., Barnard, A.J., Cooper, J. & Smith, E.W., 1974. Astrophys. J., 190, 315.

Mihalas, D., Barnard, A.J., Cooper, J. & Smith, E.W., 1975. Astrophys. J., 197, 139.

Moore, C.E., 1945. Revised multiplet table, Cont. Princeton University Obs. 20.

Moore, C.E., 1950. An ultraviolet multiplet table, NBS no. 488 sections 1 to 5, Washington.

Moore, C.E., 1965. Selected tables of atomic spectra, NSRDS-NBS3 section 1, Washington.

Moore, C.E., 1967. Selected tables of atomic spectra, NSRDS-NBS3 section 2, Washington.

Moore, C.E., 1970. Selected tables of atomic spectra, NSRDS-NBS3 section 3, Washington.

Moore, C.E., 1975. Selected tables of atomic spectra, NSRDS-NBS3

section 5, Washington.

Morbey, C.L., 1973. Publ. Dominion Astrophys. Obs., 14, 185.

Morton, D.C., 1967. Astrophys. J., 150, 535.

" 1975. Astrophys. J., 197, 85.

" 1979. In press.

Murdin, P.G., 1978. Private comm..

Nariai, K., 1973. Publ. astr. Soc. Japan, 15, 449.

Nassau, J.J. & Stephenson, C.B., 1963. Luminous Stars in the Northern Milky Way vol. 4, Hamburger Sternewarte and Warner & Swasey Obs..

Osmer, P.S. & Peterson, D.M., 1974. Astrophys. J., 187, 117.

Peach, G., 1970. Mem. R. astr. Soc., 73, 1.

Pearce, J.A., 1955. Trans. I.A.U., IX, 442.

Pedersen, H., 1978. Astr. Astrophys. Suppl., 35, 313.

Pedersen, H. & Thomsen, B., 1977. Astr. Astrophys. Suppl., 30, 11.

Perek, L., 1957. Bull. astr. Insts. Czech., 8, 177.

Perek, L., 1958. Bull. astr. Insts. Czech., 9, 117.

Peterson, A.V., 1970. Thesis, Caltech..

Petrie, R.M., 1953. Publ. Dominion Astrophys. Obs., 9, 297.

Philip, A.G.D. & Newell, B., 1975. Dudley Obs. Rep., 9, 161.

Plaskett, J.S., 1927. Mon. Not. R. astr. Soc., 87, 31.

Plaskett, J.S., Adams, W.S. & Frost, E.B., 1932. Trans. I.A.U., IV, 189.

Popper, D.M., 1942. Publ. astr. Soc. Pacific, 54, 160.

" 1946. Publ. astr. Soc. Pacific, 58, 370.

" 1947. Publ. astr. Soc. Pacific, 59, 320.

Ralston, A. & Wilf, H.S., 1960. Mathematical methods for digital computers, Wiley, New York.

Richter, D., 1971. Astr. Astrophys., 14, 415.

Roberts, J.R., Andersen, T. & Sørensen, G., 1973. Astrophys. J., 181, 567.

Rosendhal, J.D. & Schmidt, E.G., 1973. Publ. astr. Soc. Pacific, 85, 396.

SAAO Facilities Manual, 1977. South African Astronomical Observatory.

SAO Star Catalog, 1966. Smithsonian Astrophys. Obs., part 4.

Schlesinger, F., 1899. Astrophys. J., 9, 159.

Schmidt-Kaler, Th., 1967. I.A.U. Symp. 31, Radio astronomy and the galactic system p. 161, ed. Van Woerden, H., Academic Press, London.

Scholz, M., 1972. Vistas Astr., 14, 53.

Schönberner, D., 1973. Astr. Astrophys., 28, 433.

" 1975. Astr. Astrophys., 44, 383.

" 1977. Astr. Astrophys., 57, 437.

" 1978. Mitt. Astr. Ges., 43, 266.

" 1979. Private comm..

Schönberner, D. & Hunger, K., 1978. Astr. Astrophys., 70, L57.

Schönberner, D. & Wolf, R.E.A., 1974. Astr. Astrophys., 37, 87.

Schulz-Gulde, E., 1969. J. quant. Spectr. rad. Trans., 9, 13.

Selby, S.M., 1971. Standard mathematics tables, Chemical Rubber Co..

Slettebak, A., Wright, R.R. & Graham, J.A., 1968. Astr. J., 73, 152.

Smith, L.F., 1973. I.A.U. Symp. 49, Wolf-Rayet and high temperature stars p. 15, ed. Bappu, M.K.V. & Sahade, J., D. Reidel, Dordrecht-Holland.

Snow, T.P., 1976. Astrophys. J., 204, L127.

Snow, T.P. & Linsky, J.L., 1979. Phys. Astrophys. Spacelab (in press).

Stephenson, C.B., 1967. Astrophys. J., 149, 35.

Stephenson, C.B. & Sanduleak, N., 1971. Luminous Stars in the Southern Milky Way, 1, 1, Warner & Swasey Obs..

Stibbs, D.W.N., 1979. Private comm..

Stobie, R.S., 1978. Private comm..

Stock, J., Nassau, J.J. & Stephenson, C.B., 1960. Luminous Stars in the Northern Milky Way vol. 2, Hamburger Sternewarte and Warner & Swasey Obs..

Stothers, R.C. & Simon, N.R., 1969. Astrophys. J., 157, 673.

Strömgren, B., 1948. Astrophys. J., 108, 242.

Strömgren, B., 1963. Basic Astronomical Data, Stars & Stellar systems III, ed, Strand, K.A., University of Chicago Press, Chicago.

Strömgren, B., 1966. A. Rev. Astr. Astrophys., 4, 433.

Thackeray, A.D., 1954. Mon. Not. R. astr. Soc., 114, 93.

Thackeray, A.D. & Wesselink, A.J., 1952. Obs., 72, 248.

Tomley, L., 1970. Astrophys. J., 162, 239.

Trimble, V., 1972. Mon. Not. R. astr. Soc., 156, 411.

Trumpler, R.J. & Weaver, H.F., 1953. Statistical Astronomy, University of California Press.

Ueno, S., Saito, S. & Jugaku, J., 1954. Cont. Inst. Astrophys. Kyoto, 43.

Unsöld, A., 1955. Physik der Sternatmosphären 2nd edn., Springer, Berlin.

de Vaucouleurs, G., 1968. Appl. Opt., 7, 1513.

Walker, H.J. & Kilkenny, D., 1979. Submitted to Mon. Not. R. astr. Soc.

Warner, B., 1967. Mon. Not. R. astr. Soc., 137, 119.

Wayman, P.A., 1961. R. Obs. Bull., 48, Appendix E393.

Weidemann, V., 1975. Problems in Stellar Atmospheres and Envelopes, eds Baschek, B., Kegel, W.H. & Traving, G., Springer, Berlin.

Wiese, W.L., Smith, M.W. & Glennon, B.M., 1966. Atomic transition probabilities, NSRDS-NBS4 vol. I, Washington.

Wiese, W.L., Smith, M.W. & Miles, B.M., 1966. Atomic transition probabilities, NSRDS-NBS22 vol. II, Washington.

Wilson, R.E., 1953. General catalogue of stellar radial velocities, Carnegie Institution, Washington.

Wolf, R.E.A., 1973. Astr. Astrophys., 26, 127.

Wolff, S.C., Pilachowski, C.A. & Wolstencroft, R.D., 1974. Astrophys. J., 194, L83.

Wolnik, S.J. & Berthel, R.O., 1973. Astrophys. J., 179, 665.

Wood, P.R., 1976. Mon. Not. R. astr. Soc., 174, 531.

Errata

Page 9	line 11	Pedersen not Pederen
Page 91	line 19	focussed not focused
Page 100		w(A) not (cm)
Page 138	line 10	determination not detrmination
Page 141	line 15	Stefan not Steffan
Page 144	line 1	Gingerich not Gingerlich
Page 150	line 21	noticeable not noticable
Page 171	line 4	noticeable not noticable
Page 185	line 12	photometric not photmetric